2012-04-04

On the Source of Peptides for Major Histocompatibility Class I Antigen Presentation: A Dissertation

Diego José Farfán Arribas
University of Massachusetts Medical School

ON THE SOURCE OF

PEPTIDES FOR MAJOR HISTOCOMPATIBILITY CLASS I

ANTIGEN PRESENTATION

A Dissertation Presented

By

Diego José Farfán Arribas

Submitted to the Faculty of the

University of Massachusetts Graduate School of Biomedical Sciences, Worcester

in partial fulfillment of the requirements for the degree of

DOCTOR OF PHILOSOPHY

April 4th, 2012

Immunology and Virology Program

ON THE SOURCE OF PEPTIDES FOR MAJOR HISTOCOMPATIBILITY CLASS I ANTIGEN PRESENTATION

A Dissertation Presented

By

Diego José Farfán Arribas

The signatures of the Dissertation Defense Committee signify completion and approval as to style and content of the Dissertation

---

Kenneth L. Rock, M.D., Thesis Advisor

Leslie J. Berg, Ph.D., Member of Committee

Liisa K. Selin, M.D., Ph.D., Member of Committee

Fumihiko Urano, M.D., Ph.D., Member of Committee

Ian A. York, D.V.M., Ph.D., Member of Committee

The signature of the Chair of the Committee signifies that the written dissertation meets the requirements of the Dissertation Committee

---

Lawrence J. Stern, Ph.D., Chair of Committee

The signature of the Dean of the Graduate School of Biomedical Sciences signifies that the student has met all graduation requirements of the School

---

Anthony Carruthers, Ph.D.,
Dean of the Graduate School of Biomedical Sciences

Immunology and Virology Program

April 4th, 2012

"Desafortunadamente, la naturaleza parece no percibir nuestra necesidad intelectual de conveniencia y unidad, y muy seguido se deleita en la complicación y la diversidad"

(Unfortunately, nature seems unaware of our intellectual need for convenience and unity, and very often takes delight in complication and diversity)

—Santiago Ramón y Cajal (1852 –1934)
Pathologist, histologist, neuroscientist, and Nobel laureate

ACKNOWLEDGEMENTS

The work described in this dissertation would not have been possible without my advisor's support. I want to thank Dr. Kenneth Rock for his mentorship throughout these years. He has given me the opportunity to tackle different questions in the field of antigen presentation and has greatly contributed to my education. Ken is an old-school mentor: he has provided guidance while giving me the freedom to explore my own approaches and suggest new paths, and he has afforded me a chance to learn from my mistakes. It has been a long time in the Rock lab, and although other projects I have participated in have not yielded a complete story, the time has not gone to waste. I have enjoyed exposure to many techniques and gone through the process of experimental design and analysis, both of which have contributed to my scientific growth. It might have not been a quick and easy thesis work, but I can leave with the reassurance that it has been a valuable learning experience and an endurance test. Past and present members of the Rock lab have also provided a rich source of knowledge and learning; to them, my gratitude. Very constructive suggestions have been made by the members of my Thesis Research Advisory Committee. I would like to acknowledge them as well, especially Dr. Lawrence Stern for taking the time to share his expertise in quantitative biochemistry with me.

I would also like to acknowledge the following persons for providing valuable reagents in an altruistic manner:

Freidrich Cruz (University of Massachusetts Medical School, Worcester, MA)

Henry Paulus (Boston Biomedical Research Institute, Watertown, MA)

Stephanie Pöggeler (Georg-August-Universität, Göttingen, Germany)

Elaine Raines (University of Washington, Seattle, WA)

Raymond Welsh (University of Massachusetts Medical School, Worcester, MA)

David Woodland (Trudeau Institute, Saranac Lake, NY)

ABSTRACT

Peptides generated from cellular protein degradation via the ubiquitin-proteasome pathway are presented on MHC class I as a means for the immune system to monitor polypeptides being synthesized by cells. For $CD8^+$ T cells to prevent the spread of an incipient infection, it appears essential they should be able to sense foreign polypeptides being synthesized as soon as possible. A prompt detection of viral proteins is of great importance for the success of an adaptive immune response. Defective ribosomal products (DRiPs) have been postulated as a preferential source which would allow for a rapid presentation of peptides derived from the degradation of all newly synthesized proteins. Although this hypothesis is intellectually appealing there is lack of experimental data supporting a mechanism that would prioritize presentation from DRiPs. In this dissertation I describe a series of experiments that probe the DRiPs hypothesis by assessing the contribution to class I presentation of model epitopes derived from DRiPs or from functional proteins. The results show that even at the early stages after mRNA synthesis DRiPs do not account for a significant fraction of the class I presented peptides. These observations suggest that the currently widespread model whereby a mechanism exists which selectively allows for DRiPs to preferentially contribute to class I antigen presentation, is incorrect. Rather, properly folded functional proteins can significantly contribute to class I antigen presentation as they are normally turned over by the ubiquitin-proteasome pathway.

TABLE OF CONTENTS

ACKNOWLEDGEMENTS ..... **iv**

ABSTRACT ..... **vi**

LIST OF TABLES ..... **xii**

LIST OF FIGURES ..... **xiii**

ABBREVIATIONS ..... **xvi**

CHAPTER I: INTRODUCTION **1**

1.1 The Identification of the Cytolytic T cell Ligands **1**

1.2 Peptide Transport and Peptide-MHC class I Complex Formation **3**

1.3 The MHC Class I peptide ligands **4**

1.4 MHC class I Presented Peptides as Products of Proteolysis **5**

1.5 The Pepton Hypothesis **7**

1.6 The DRiPs Hypothesis **8**

1.7 Experimental Support for DRiPs **10**

1.8 Examples of DRiPs-derived Antigens 12

1.9 Cellular Protein Synthesis Shutdown 13

1.10 Mechanisms of DRiPs as a Preferential Source for Presentation 14

1.11 Post-proteasomal Processing 18

1.12 Scope of Thesis 19

1.13 Intein Catalysis 20

CHAPTER II: MATERIALS AND METHODS 26

2.1 Cell Lines, Hybridomas and T Cells 26

2.2 Molecular Cloning 28

2.3 Retrovirus and Lentivirus Packaging 39

2.4 Infection and Cell Purification 40

2.5 Mass Spectrometry 42

2.6 Radiolabeling Experiments 44

2.6.1 Pulse-chase 44

2.6.2 Continuous labeling 46

2.7 Antigen Presentation Assays 46

2.7.1 Immunofluorescent staining 47

2.7.2 Hybridoma assays 47

2.7.3 HY-specific T cell response assay 48

2.8 Clustal W Multiple Sequence Alignment 48

2.9 Mathematical Analysis 49

CHAPTER III: INTEINS CAN SPLICE IN MAMMALIAN CELLS 51

3.1 Introduction 51

3.2 Screening for Splicing 52

3.3 Extein Flanking Residues 54

3.4 Fidelity of Intein Splicing 56

3.5 Construct Description 62

3.6 Splicing Kinetics 64

3.7 Outstanding Questions and Future Applications 69

CHAPTER IV: ANTIGEN PRESENTATION OF SPLICING-DEPENDENT EPITOPES 72

CHAPTER V: PRESENTATION KINETICS 81

CHAPTER VI: MODELING PRESENTATION AT EARLY TIME POINTS AFTER TRANSLATION 86

CHAPTER VII: DISCUSSION 96

7.1 Results in the Context of the Literature 96

7.2 On the Linkage between Protein Synthesis and MHC Class I Presentation 98

7.3 Examples of DRiPs-derived Epitopes 103

7.4 DRiPs as a Preferential Source of MHC class I Ligands 104

7.5 Direct Measurements by Mass Spectrometry 107

7.6 The Pioneer Round of Translation 109

7.7 DRiPs in the Context of the Immune Response 112

7.8 Protein Degradation Kinetics and MHC Class I Presentation 117

7.9 Immune Surveillance and Cancer 120

CONCLUDING REMARKS 123

REFERENCES 125

LIST OF TABLES

Table 2.1 **Primer list 38**

Table 6.1 **MFI data from flow cytometry experiments 90**

Table 6.2 **Band densitometry data from continuous labeling experiments 92**

Table 6.3 **Parameters from KinTek explorer simulation experiments 93**

LIST OF FIGURES

Figure 1.1 **Position of the homing endonuclease and conserved residues in inteins 22**

Figure 1.2 **Diagram of the crystal structure of the *M. tuberculosis* RecA mini-intein 23**

Figure 1.3 **Clustal W alignment of the amino acid sequences of the *M. tuberculosis* and *P. chrysogenum* mini-inteins used 24**

Figure 1.4 **Enzymatic mechanisms proposed for intein catalysis 25**

Figure 3.1 **Splicing of the *Mtu* RecA mini-intein 53**

Figure 3.2 **Isoleucine in the N-terminal Splicing Junction is Detrimental for Splicing 55**

Figure 3.3 **Mass Spectrometry Digest Prediction Results 57**

Figure 3.4 **MALDI-TOF spectra of pre-spliced and intein bands 59**

Figure 3.5 **Measurement of splicing products stability 61**

Figure 3.6 **Schematic of the lentiviral constructs 63**

Figure 3.7 **The N3 mutant versions of either intein do not splice 66**

Figure 3.8 **Splicing Kinetics of the *Pch* PRP8 intein 67**

Figure 3.9 **Splicing Kinetics of the *Mtu* RecA intein 68**

Figure 4.1 **Dox titratable GFP production 73**

Figure 4.2 **Splicing dependent epitope presentation twenty-four hours after induction 76**

Figure 4.3 **Dox titratable S8L presentation 77**

Figure 4.4 **Splicing dependent epitope presentation is abrogated by proteasome inhibition 78**

Figure 4.5 **Splicing dependent epitope presentation relative to control presentation 80**

Figure 5.1 **Time course of A9M presentation from Pre-spliced, intein and splicing mutant 84**

Figure 5.2 **Time course of K9L presentation from Pre-spliced, intein and splicing mutant 85**

Figure 6.1 **Scheme depicting the model inputted into KinTek Explorer software for data fitting 88**

Figure 6.2 **Data from cells infected with GFP-NP (Pre-spliced) or GFP-PRP8-NP (Intein) encoding viruses used for model fitting in KinTek explorer 89**

Figure 6.3 **Data from cells infected with GFP-HY (Pre-spliced) or GFP-RecA-HY (Intein) encoding viruses used for model fitting in KinTek explorer 91**

Figure 6.4 **Time course and *in silico* predictions 96**

ABBREVIATIONS

3-MA	3-Methyladenine
2-ME	2-Mercaptoethanol
A9M	ASNENMETM peptide
ABC	ATP-binding Cassette
APC	Antigen Presenting Cell
ATP	Adenosine Triphosphate
BGH	Bovine Growth Hormone
Bsd^R	Blasticidin Resistance Gene
CD	Cluster of Differentiation
cDNA	Copy D Deoxyribonucleic Acid
CMV	Cytomegalovirus
CTLs	Cytolytic T Lymphocytes
DC	Dendritic Cell
DNA	Deoxyribonucleic Acid
dNTP	Deoxyribonucleoside Triphosphate
DOC	Deoxycholic Acid
Dox	Doxycycline
DRiPs	Defective Ribosomal Products
EBNA	Epstein-Barr Virus Nuclear Antigen
EDTA	Ethylenediaminetetraacetic acid
eIF	Eukaryotic Translation Initiation Factor
ER	Endoplasmic Reticulum
FACS	Fluorescence-Activated Cell Sorting
FCS	Fetal Calf Serum

G418	Geneticin
Gag	Group-specific Antigen
GAr	Glycine-Alanine Repeat
GFP	Green Fluorescent Protein (*A. victoria*)
H-2	Murine Major Histocompatibility Complex
HA tag	Hemagglutinin tag (YPYDVPDYL)
HEPES	2-[4-(2-Hydroxyethyl)-1-piperazinyl]ethanesulfonic Acid
HIV-1	Human Immunodeficiency Virus type 1
HLA	Human Leukocyte Antigen
HY	Murine Histocompatibility antigen (Y chromosome)
ICAM-1	Inter Cellular Adhesion Molecule
ICS	Intracellular Cytokine Staining
IgG	Immunoglobulin G
IN	Integrase
IRES	Internal Ribosome Entry Signal
K9L	KCSRNRQYL peptide
LB	Luria-Bertani or Lysogeny Broth
LCMV	Lymphocytic Choriomeningitis virus
LTR	Long Terminal Repeat
Luc	Firefly Luciferase
MACS	Magnetic-activated cell sorting
MFI	Mean Fluorescence Intensity
MHC	Major Histocompatibility Complex
MOPS	3-(N-morpholino)propanesulfonic acid

mRNA	Messenger Ribonucleic Acid
Mtu RecA	*Mycobacterium tuberculosis* Recombinase A
NFAT	Nuclear factor of activated T-cells
NP	Nucleoprotein
NP-40	Nonidet P-40
ORF	Open Reading Frame
PAGE	Polyacrylamide Gel Electrophoresis
pAPC	Professional Antigen Presenting Cell
PBS	Phosphate Buffered Saline
PCR	Polymerase Chain Reaction
Pol	Polymerase
PolyA	Poly-adenylation signal
Pro	Protease
Pch PRP8	*Penicillium chrysogenum* Pre-mRNA Processing factor 8
Rev	Regulator of virion expression
RFP	Red Fluorescent Protein
RLUs	Relative Light Units
RPMI	Roswell Park Memorial Institute
RT	Reverse Transcriptase
S8L	SIINFEKL peptide
SDS	Sodium Dodecyl Sulfate
SEM	Standard Error of the Mean
SILAC	Stable Isotope Labeling by Amino acids in Cell culture

TAP	Transporter Associated with Antigen Processing
Tat	Trans-activation of transcription protein
TCR	T-Cell Receptor
TNF	Tumor Necrosis Factor
tRNA	Transfer Ribonucleic Acid
Vpr	Viral protein R
VSV	Vesicular Stomatitis Virus
VSV-G	Vesicular Stomatitis Virus Protein G
WPRE	Woodchuck Hepatitis Virus Post transcriptional Regulatory Element

CHAPTER I: INTRODUCTION

1.1 The Identification of the Cytolytic T cell Ligands

The fascinating history of the antigen presentation pathway commenced with the discovery of the immune response (Ir) genes (McDevitt & Tyan 1968; Bluestein et al. 1971) and their linkage to the HLA and H-2 (Major Histocompatibility Complex [MHC] class I) loci in mice and humans (McDevitt & Tyan 1968; Levine et al. 1972). The observation that T lymphocytes were able to specifically recognize and lyse target cells that had been exposed to antigens followed, and there was an intriguing requirement for these cytolytic T lymphocytes (CTLs) and their target cells to share their genotype in the mentioned H-2 loci (Doherty & Zinkernagel 1975; Zinkernagel & Doherty 1975; Bevan 1975; Vitiello et al. 1989). The manner in which these antigens were recognized in association with target cells leading to lymphocyte mediated lysis became a subject of great interest to the scientific community.

It was hypothesized that antigens were recognized by a T-cell receptor when they were displayed on the target cell surface in the context of the products of the H-2 loci (Schrader 1979). How antigens were displayed to T-cells was still not fully understood.

Influenza proteins synthesized by cells made them targets for CTL lysis, and remarkably removing terminal fragments of the antigen sequence (Townsend et al. 1985) or removing the signal sequence that made the antigen inserted in the cell membrane did not impair lysis by CTLs (Townsend, Bastin, et al. 1986). Therefore, antigens or fragments thereof were presented at the cell membrane in association with products of the H-2 locus and they needed not be integral membrane proteins.

A crucial experiment showed how cells could be sensitized to CTL lysis by incubating them with synthetic peptides as short as fifteen amino acids corresponding to a fragment of the antigen which the CTL were specific for (Townsend, Rothbard, et al. 1986). This led to the belief that the antigens presented to CTLs may be a degradation fragment of intracellular proteins that was transported to the cell surface in association with MHC class I molecules (Townsend et al. 1985). It was assumed that these fragments would derive from enzymatic digestion of the antigenic protein, as was the case with class II presentation to helper T cells (Ziegler & Unanue 1981). The peptide association with MHC class I molecules was confirmed when the first crystal structure of a class I MHC molecule was obtained (Bjorkman et al. 1987). A groove was apparent facing the extracellular milieu on the heavy chain of HLA, comprising a bed of antiparallel beta sheets flanked by two alpha helices. The residues in this groove mapped to the regions of high polymorphism of the gene encoding the class I heavy chain (alpha 1 and 2). In the crystal, this groove harbored a then unknown protein fragment: a short peptide. Although

it was not confirmed at the time, it was already suggested that this peptide might be an antigenic epitope. Previous experiments had shown that exogenous antigens were presented as peptides, and that they bound to MHC class II molecules on macrophages (Allen et al. 1984; Babbitt et al. 1985), so the observation of a peptide associated with MHC class I contributed to solidifying the model whereby the cytolytic T cells were recognizing fragments of foreign proteins associated with self molecules on the cell surface.

1.2 Peptide Transport and Peptide-MHC class I Complex Formation

MHC class I complexes are formed in the endoplasmic reticulum (ER), yet many antigens were known to be located in the cytosol: how can these antigens access the ER to bind class I molecules? A set of experiments (Townsend et al. 1989) utilized exogenously provided viral peptides to promote class I heavy chain association with beta-2-microglobulin—the light chain of the MHC class I complex (Grey et al. 1973)—in the ER of a cell (RMA-S) with a defect in surface class I levels (Ljunggren & Kärre 1985). It was through complementation studies in RMA-S (Powis et al. 1991) and in a human cell line also defective in surface class I (Spies & DeMars 1991) that for the first time functional evidence was obtained for a peptide transporter from the cytosol to the ER,

which was also encoded in the MHC cluster (Spies et al. 1990): the transporter associated with antigen processing (encoded by *TAP1* and *TAP2),* as it would be later named. Further evidence for TAP functioning as a peptide translocator soon followed: the *TAP* homology to the ATP-binding cassette (*ABC*) family of transporters (Trowsdale et al. 1990)—of which some members transport short peptides across membranes—together with competition experiments in which MHC class I complex formation was measured after adding peptides of different lengths (Shepherd et al. 1993), led to the belief that the antigens transported into the ER by TAP were eight to sixteen amino acid long peptide fragments. Peptide transport was formally shown in vitro using microsome preparations (Lévy et al. 1991).

1.3 The MHC Class I peptide ligands

Throughout the years, the putative source of peptide ligands for MHC class I molecules has varied. First it was assumed that any protein that was degraded would contribute to class I presentation. The pepton hypothesis discussed below (Boon & Van Pel 1989) postulated the presented epitopes derived from transcription and translation of small DNA fragments. The development of proteasome inhibitors led to the current belief that the vast majority of presented peptides are dependent on proteasome degradation (Rock

et al. 1994). With some elements borrowed from the pepton hypothesis (Boon & Van Pel 1989) the DRiPs hypothesis was postulated (Yewdell et al. 1996). In the latter, defective polypeptides were introduced as a crucial source of epitopes that would solve the putative bias associated with the use of protein turnover as a supply. The use of DRiPs also accommodated the requirement for proteasomal degradation. Below I will describe in depth the features of each of the potential sources of MHC class I peptide ligands.

1.4 MHC class I Presented Peptides as Products of Proteolysis

In the quest to find a catalytic activity that may generate antigenic peptides, the ubiquitin-proteasome pathway (Ciechanover et al. 1980; Hough et al. 1986; Fagan et al. 1987) was an appealing candidate, since it was known to be the major pathway for protein degradation in cells. Proteasomes were clearly involved in the generation of the peptides presented on the MHC class I molecules (Rock et al. 1994). Post-proteasomal peptide trimming was shown to take place not only in the ER as discussed above, but also in the cytosol (Towne et al. 2005; Towne et al. 2007; Towne et al. 2008; Kawahara et al. 2009).

All in all, these findings ranging from the genetic requirements for the cellular immune response, the TCR, the MHC class I complexes, and the peptides generated through

proteolysis supported a model where the generation of epitopes for presentation to $CD8^+$ T cells started with protein degradation.

Thus presented peptides were derived from the degradation of proteins by the proteasome, and it was assumed that mature protein turnover would provide the major source of peptides, and some subsequent experiments seemed to support this concept. Initial evidence for the contribution of mature protein turnover to class I presentation came from experiments in which mature foreign proteins were introduced into the cytosol of cells and class I presentation of peptides derived from them was monitored (Okada & Rechsteiner 1982; Moore et al. 1988; Grant et al. 1995). MHC class I presentation was observed readily. Although these results could not provide quantitative data—because the amount of protein introduced might have been overwhelming—they proved that the ubiquitin-proteasome degradation of stable proteins could be a source of peptide epitopes for class I presentation.

1.5 The Pepton Hypothesis

As an alternative for the proteolytic origin of peptides bound to MHC class I molecules—the pepton hypothesis—was postulated whereby the source of peptides for presentation would be transcription and translation of short DNA sequences within any given gene (Boon & Van Pel 1989). This hypothesis arose from the puzzling observation that cells became sensitized to lysis by CTLs when transfected with small fragments of unspliced genes (Lurquin et al. 1989; Szikora et al. 1990). If presented peptides were the product of protein proteolysis it would have been very unlikely that these cells became sensitized, since the gene fragment introduced did not have a promoter and it was severely truncated. The authors pointed at the possibility that a DNA dependent RNA polymerase specialized for antigen presentation had the ability to transcribe short stretches of DNA autonomously, i.e. without the need of a promoter sequence. One advantage of this scenario is that all genes could be sampled whether or not their products were expressed. Another benefit derived from using peptons as opposed to protein degradation would be uniform sampling across the genome. The proponents of the pepton hypothesis believed that if protein degradation were the main source of peptides from presentation, the epitopes on the cell surface would be heavily biased towards the most abundant proteins, leaving little or no representation for epitopes corresponding to less abundant proteins. On the other hand, that potential biased would be eliminated by using peptons as the source for MHC class I presented peptides. This hypothesis did receive attention but

greatly lost impetus as experimental data started pointing at the proteasome as a major player in the generation of presented peptides.

1.6 The DRiPs Hypothesis

It was in the context of an acute viral infection that some (Yewdell et al. 1996) saw a paradox emerge from the findings discussed above. From the teleological point of view, a search-and-destroy system that would efficiently prevent the spread of infection would want to eliminate the virus producing cells early, before the factories are in full swing, and thereby prevent a large number of virions from being produced. A delay in detection would certainly be detrimental in controlling the infection, since the greater the number of virions produced by an infected cell before its destruction, the more likely it will be for neighboring cells to become infected. Interestingly they noted, major epitopes identified as important for the lysis of infected cells by T cells were often derived from long-lived viral proteins. Since the generation of MHC class I-presented epitopes was thought to occur as a result of protein turnover, it was assumed that long-lived viral proteins would require relatively longer times in order to be degraded, and hence sufficient peptide epitopes would not be obtained immediately upon infection; instead there would be a delay in presentation which would correlate with the epitope's source-protein half-life.

This delay seemed to conflict with the observation that T cell induced lysis takes place shortly after infection of target cells, and therefore alternative sources of degradation products other than turnover of native proteins were sought after. One such potential source was envisioned and termed Defective Ribosomal Products or DRiPs. These would encompass aberrant protein species originating during—or very shortly after—mRNA translation by ribosomes. Quality control checkpoints are in place that detect and shunt defective ribosomal products into the ubiquitin-proteasome degradation pathway. Thus, DRiPs were deemed a fitting candidate for the source of MHC class I presented epitopes, since they would provide a peptide source readily after protein synthesis begins and their abundance would be independent of the half-life of the properly folded, functional proteins they failed to become. This purported suitability of DRiPs as opposed to functional protein turnover at a later stage, led to a quest to identify and quantify DRiPs, and to correlate their availability with the levels of MHC class I antigen presentation. Moreover, it was later postulated as a corollary, that there should be some kind of cellular machinery or compartment involved in the production of DRiPs that would enable a preferential usage of DRiPs- high levels of mRNA were already derived peptides over proper protein turnover derived peptides for loading onto MHC class I complexes.

The way in which DRiPs would dominate class I presentation has also evolved. First it was postulated that DRiPs could provide only a small percentage of the presented

epitopes, the rest being provided by native protein degradation, and—under special circumstances such as viral infection—the levels of DRiPs could be up-regulated (Yewdell et al. 1996). Later the fraction of DRiPs was quantified at over thirty percent of all synthesized polypeptides

1.7 Experimental Support for DRiPs

The initial experiments aimed at identifying and characterizing DRiPs revealed a large short-lived protein pool which labeled after [^{35}S]-Methionine pulse in cells that had been starved and pre-treated with proteasome inhibitors (Schubert et al. 2000). However, in a later report (Vabulas & Hartl 2005) the magnitude of this pool was ascribed to an artifact: the observed increase in radiolabel in cells treated with proteasome inhibitors was not due to the presence of a short-lived protein pool being protected from degradation by the inhibitors, but rather to an increase in the relative incorporation of the radiolabeled amino acid—i.e. the specific activity—into those proteins. As it turns out, when cells are grown in an amino acid deficient medium, they can sense a deficit in charged tRNAs, and they respond by inhibiting translation; even more so when they have been pre-treated with proteasome inhibitors. In a radiolabeling experiment, this general reduction in translation results in an overall lower protein production, but the specific activity is enhanced. What

was estimated by Schubert et al. to be a DRiP fraction of one third of the total synthesized protein, Vabulas and Hartl reduced to a few percent at most in their experiments, when a comparison of specific activity was made between samples with or without amino acid deficient medium pre-treatment.

The empirical support for DRiPs as a major source of peptides for antigen presentation was eloquently summarized in a publication title "Tight Linkage between Translation and MHC Class I Peptide Ligand Generation Implies Specialized Antigen Processing for Defective Ribosomal Products" (Qian, Reits, et al. 2006). Indeed, the addition of protein synthesis inhibitors resulted in a nearly complete stall in antigen presentation, despite the continued presence of mature protein in the cells. In other words, this finding was consistent with the source of presented peptides being newly synthesized proteins rather the pool of older proteins. Nevertheless, there was the question of whether protein synthesis inhibition could have global effects, affecting processes other than the generation of peptides.

Another study used an innovative technique to measure the rate of peptide supply to the loading complex in the ER (Reits et al. 2000). A subunit of TAP (TAP1) was fused to GFP and its mobility along the ER membrane was measured. A diffusion coefficient was obtained by bleaching a spot on the ER with a laser and imaging the recovery of GFP fluorescence following bleaching using confocal microscopy. TAP mobility was found

to be inversely proportional to the rate of peptide transport. Using this methodology, the peptide transport rate was compared in the presence or absence of protein synthesis inhibitors. The conclusion was that the majority of the TAP substrates were derived from newly synthesized proteins, which is in accordance with the DRiPs hypothesis.

1.8 Examples of DRiPs-derived Antigens

There are a number of reports where the generation of individual epitopes is shown to be linked to the source protein's translation. Of the seven known class I epitopes derived from the lymphocytic choriomeningitis virus (LCMV) nucleoprotein (NP) in the mouse, only one has been examined and found to be linked to protein neosynthesis (Khan et al. 2001). Two class I epitopes from Epstein-Barr virus nuclear antigen (EBNA) were shown to be readily presented in the early phase of antigen expression, but their presentation declined after protein synthesis ceased (Mackay et al. 2009). In another study (Voo et al. 2004), response by $CD8^+$ T cell clones to 293T cells transfected with EBNA1 was blocked by protein synthesis inhibitors. Therefore, although few, there are examples of viral epitopes whose presentation is linked to the synthesis of its source protein.

1.9 Cellular Protein Synthesis Shutdown

As described in the previous sections, the DRiPs model is greatly supported by data establishing a link between mRNA translation and MHC class I antigen presentation. This link was established through experiments using protein synthesis inhibitors. It is worth mentioning that upon viral infection and in response to signals such as the presence of double stranded RNA (Leaman et al. 1998), cells can respond by shutting off protein synthesis as a way of preventing viral spread. The presence of interferon also leads to cellular shutoff or to apoptosis (Stark et al. 1998).

The virus-mediated inhibition of protein synthesis cannot be complete, since the virus is an obligate parasite, but there are mechanisms that lead to a partial cellular protein synthesis shutoff while allowing virally encoded proteins to continue being synthesized. This partial shutoff of cellular protein synthesis is advantageous for the virus, since it diverts the synthesis machinery to its own proteins while keeping the host cell alive. Viruses can adopt countermeasures to gain access to the cellular protein synthesis machinery and divert translation to their own mRNAs: for example, adenoviruses (Huang & Schneider 1990) and influenza virus (Feigenblum & Schneider 1993) can promote dephosphorylation of eIF4E, thus preventing cap-mediated translation initiation, which is essential for cellular transcripts but not for viral protein synthesis (Dolph et al. 1990).

In situations where cells are infected with viruses that direct translation towards their own mRNAs, most of the cellular DRiPs would rapidly wane, leaving chiefly viral DRiPs available for processing and presentation.

1.10 Mechanisms of DRiPs as a Preferential Source for Presentation

The neo-synthesis data that was used to support DRiPs as the major source of presented peptides suggested that mature proteins were excluded from the presentation pathway or were presented very inefficiently: this is counterintuitive, since mature proteins are still degraded by the ubiquitin-proteasome pathway. Why would they not be presented? They should be, especially since cytosolic peptides from loaded exogenous proteins or synthesized from minigenes are readily presented. For this preference for DRiPs to operate, additional mechanisms had to be postulated. If DRiPs are to be preferentially utilized as a source, there must be some kind of compartmentalization at the translation level. Once more, like in the DRiPs hypothesis paper (Yewdell et al. 1996), another review (Yewdell & Nicchitta 2006) pointed out the future experiments that will, in the authors' opinion, support their pre-conceived idea that DRiPs are the major source of class I presented peptides. Several possibilities are described: 1) "immunoribosomes"

that have the ability to translate recently synthesized mRNAs (marked by different cap and polyA-binding protein) and are more error-prone than conventional ribosomes 2) ER-associated ribosomes 3) mRNAs degraded after the pioneer round of translation in the nucleus in the context of nonsense-mediated decay. HLA-encoded tRNAs that might be more prone to charging the wrong amino acid was also proposed to contribute to deliberate DRiP generation for immune surveillance purposes. As of today there is very little evidence for immunoribosomes, and none for rough ER ribosomes being more error-prone. Below are the details of the published attempts made to identify possible elements of this postulated compartmentalization.

A modulation of the accuracy of translation could represent a mechanism of DRiP induction by augmenting DRiP production in infected cells. It is hard to envision a way of compartmentalizing translation accuracy so that the fidelity would be as good as possible for regular translation and more error-prone for DRiP translation. A global decrease in fidelity in infected cells might allow for an increase in DRiPs, and although the side effects would be detrimental for the cell's health, it would not be a problem since it is destined to die after alerting the immune system to the infection. To examine this possibility tRNAs isolated from cells infected with different viruses were compared with those from uninfected cells (Netzer et al. 2009). The effects of viral infection on Met-tRNA misacylation were rather small—in most cases there was an increase from <0.1% to 0.1-0.4% of tRNAs wrongly charged with methionine (the fold-increase cannot be

determined since the data are given as a range). The authors claim that this increase would lead to a significantly greater DRiP rate by virtue of a higher likelihood of misfolding shortly after protein synthesis due to amino acid misincorporation, thus contributing to an increase in class I antigen presentation.

With regards to the aforementioned "immunoribosomes", a possible candidate took the spotlight: a set of ribosomes that specifically scans for alternative translation initiation sites. Shastri and colleagues found a mechanism that could explain the observation of cryptic reading frame epitopes (Malarkannan et al. 1999), whereby translation initiation occurred from codons other than AUG, i.e. not encoding methionine (Schwab et al. 2004). They used T-cell hybridomas as a readout for peptides initiated at CUG (encoding leucine as the N-terminal amino acid). They observed that translation could start at CUG and it was not hindered by the presence of AUG sites upstream and out of frame. This phenomenon was interpreted as the existence of a subpopulation of ribosomes that specifically scans for CUG instead of AUG. Interestingly, CUG initiation was enhanced when the eukaryotic initiation factor 2α (eIF2α) was phosphorylated, which occurs as a result of many types of viral infections (Sonenberg 2000, chap.31–35) and of cellular stress (Sonenberg 2000, chap.15). This would support the idea that upon infection or during situations of cellular stress, aberrant translation products resulting from incorrect initiation events would become more abundant, thus leading to a greater amount of

DRiPs. In addition non-AUG initiation has been observed in retroviruses, such as human T-cell lymphotropic virus, in which it allows for in-frame expression of regulatory proteins (Corcelette et al. 2000).

Support for compartmentalization of preferential substrates for MHC class I presentation came from the observation that peptides encoded as ubiquitin fusions—which are liberated in the cytosol by ubiquitin hydrolase activity, rather than by degradation of the source protein by the ubiquitin-proteasome pathway—did not compete for MHC class I binding with peptides encoded as NP fusions, which are liberated by the proteasome (Lev et al. 2010).

An enticing compartmentalized source of DRiPs is the nucleus. Inhibiting viral mRNA transport from the nucleus to the cytosol led to a lower than expected reduction in antigen presentation, suggesting nuclear translation was an important contributor to MHC class I presented epitopes (Dolan et al. 2010). The inhibition of viral mRNA transport to the cytosol led to a substantial decrease in viral protein levels, as expected. However the magnitude of the decrease in protein expression was not matched by the reduction in antigen presentation. This was taken to imply that the contribution of viral proteins synthesized in the nucleus was greater than the contribution by the products of cytosolic translation. Nevertheless, this initial observation led to an interest in nuclear translation, in particular, in the non-sense mediated decay of RNA pathway. This is a quality control

mechanism whereby a pioneer round of translation takes place from the pre-mRNA still associated with splicing machinery components in the nucleus. If protein synthesis terminates upstream of the 3' splice junction, a cascade is triggered that leads to the degradation of the pre-mRNA before it can mature and exit the nucleus. In order to test whether the products of this pioneer round of translation contribute to class I antigen presentation, a model epitope was encoded upstream of a cDNA encoding a termination codon 5' of a splice junction (Apcher et al. 2011). Indeed the model epitope was presented in transfected cells, and the levels of presentation were close to those in cells transfected with control constructs.

1.11 Post-proteasomal Processing

Peptides were recovered from ternary complexes with MHC class I heavy chain and beta-2-microglobulin, and their sequence matched that of full-length cellular (Wallny & Rammensee 1990) or non-self (Townsend et al. 1985) proteins. However, the length of the isolated peptides ranged mostly from eight to ten amino acids (Van Bleek & Nathenson 1990; Falk et al. 1991). TAP could transport peptides this size, but longer peptides were transported as well. These longer precursor peptides were soon shown to be trimmed in the ER after being transported by TAP in order to fit the class I heavy

chain peptide binding motif (Roelse et al. 1994). It would take longer, though, until the identification and characterization of the enzymatic activities responsible for this trimming process in the ER (Serwold et al. 2002; York et al. 2002; Saveanu et al. 2005; Georgiadou et al. 2010).

1.12 Scope of Thesis

The work described in this dissertation is aimed at assessing the contribution of different sources of peptides to MHC class I antigen presentation. DRiPs have been postulated as a dominant or exclusive contributor to this pathway. Since the evidence for the DRiPs model was far from conclusive, it became apparent that the key to elucidating which, if any, of the two sources of peptides—DRiPs or mature proteins—was the major contributor to MHC class I presentation was a direct comparison between substrates which could specifically yield peptides from one or the other source. The experiments presented in this dissertation will compare the contribution of a model substrate which can yield epitopes from both folded and misfolded species, relative to that of another model substrate which can yield epitopes exclusively from properly folded species by virtue of a post-translational self-catalytic process which requires an appropriate tertiary structure: protein splicing.

1.13 Intein Catalysis

An intein is a domain within a polypeptide that can splice, leaving re-ligated flanking domains, known as exteins. This occurs by a self-catalytic process that does not require any other proteins (Figure 1.4). There are many examples of inteins in nature, mostly in single cell organisms (prokaryotes and eukaryotes) (Perler 2002). Inteins are believed to have originated as "selfish genetic elements", since they possess homing endonuclease activity (Dujon et al. 1986; Bremer et al. 1992). They are encoded by mobile genetic elements that are transmitted to the progeny at rates higher than expected from Mendelian inheritance, as they insert via duplicative transposition. Homing endonucleases are selected so they do not interfere with coding sequences in the host genome. They can be found in intergenic sequences, introns, and when they intervene coding sequences, they are associated with inteins, so the gene product they intervene is still produced normally after translation and intein splicing. A mini-intein is an intein in which the homing endonuclease coding sequence has been removed and the minimal elements required for splicing are retained (Figure 1.1).

Two amino acids—threonine and histidine—in the conserved N3 domain, also known as "Motif B" of inteins are crucial for splicing (Ghosh et al. 2001). Remarkably, this domain is far from the splicing ends in the primary structure, and these amino acids only come close together with the splicing sites when the intein attains its native three-

dimensional structure (Klabunde et al. 1998). Enzymatic mechanisms have been proposed (Klabunde et al. 1998; Ding et al. 2003) where the histidine in the N3 domain is involved in the N-S acyl shift that takes place as the first step in intein catalysis as shown in Figure 1.4. Both the histidine in the N3 domain and a threonine residue N-terminal of it (positions 73 and 51 in the *Synechocystis* sp. DnaB sequence) contribute to stabilizing the intermediate during the N-S acyl shift step (Ding et al. 2003) The full length RecA intein from *Mycobacterium tuberculosis* (*Mtu* RecA) crystal structure (Van Roey et al. 2007) also predicts a close arrangement between the splicing sites and the histidine in the N3 domain (Figure 1.2), in spite of these amino acids being far apart in the primary sequence (Figure 1.3).

Therefore, the requirement to attain tertiary structure in order for splicing to occur makes inteins an excellent tool to distinguish folded, functional protein species from those that are misfolded or that have not yet acquired their native structure.

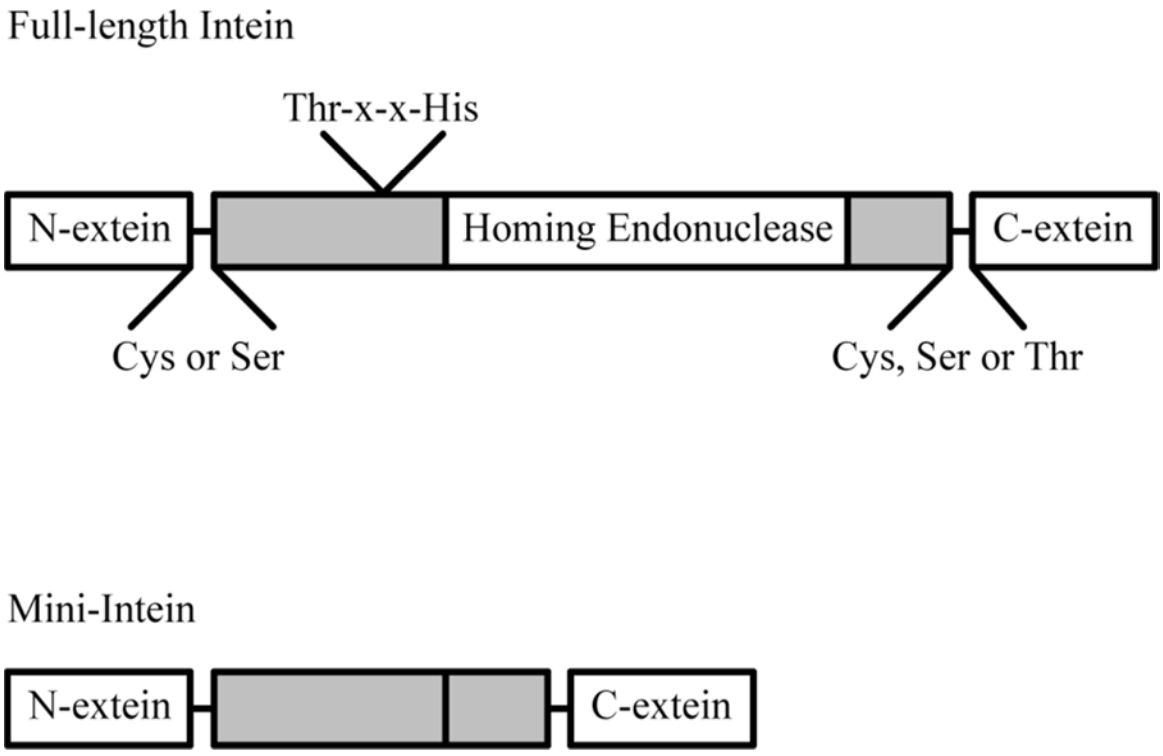

Figure 1.1 Position of the homing endonuclease and conserved residues in inteins. Summarized diagram of a typical intein showing the residue requirement at the intein-extein junction and at the N3 domain. In a mini intein (bottom) the homing endonuclease activity is removed and the residues involved directly or indirectly in the splicing catalysis remain. Modified from (Perler 2002)

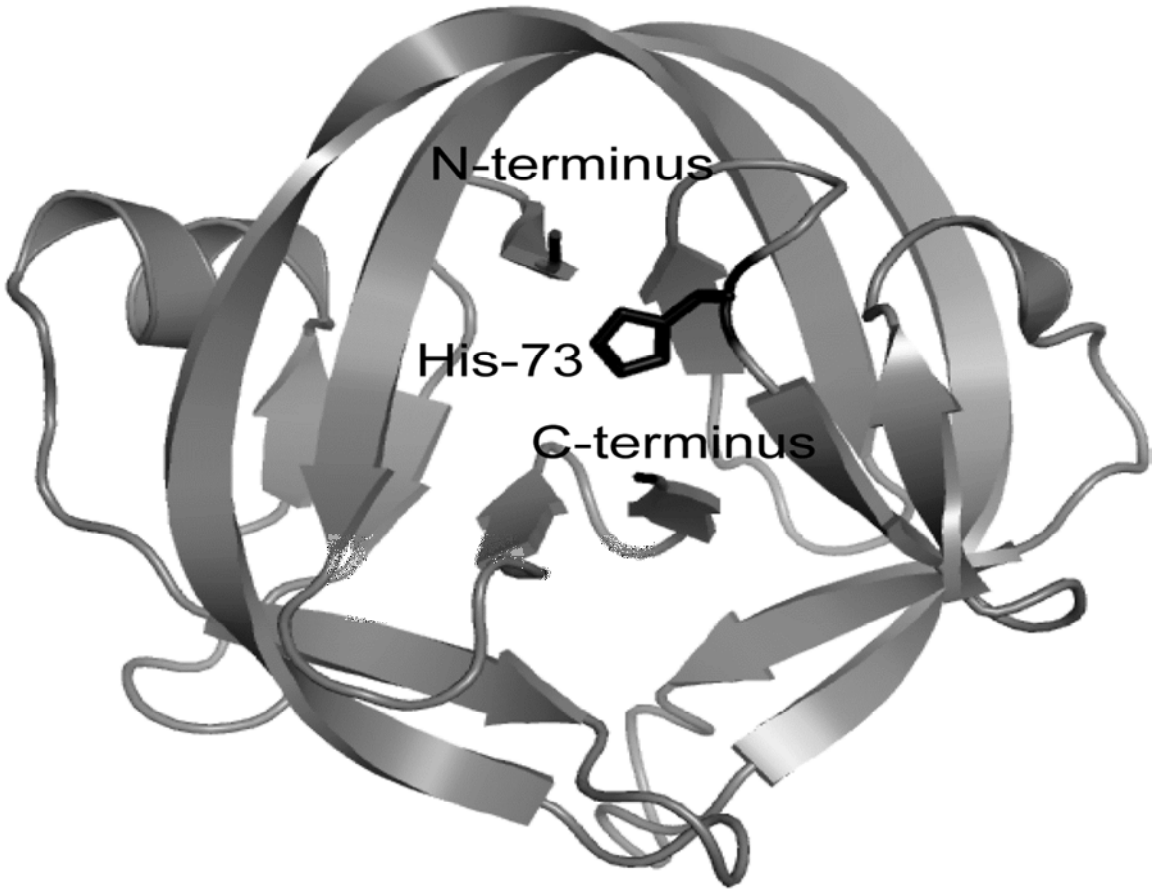

Figure 1.2 Diagram of the crystal structure of the *M. tuberculosis* RecA mini-intein (Van Roey et al. 2007). Highlighted in black are the terminal residues and the histidine side chain in the N3 block, all of which are involved in catalysis. Made with PyMol software (Delano Scientific, Palo Alto, CA) using the data deposited in the Protein Data Bank, ID 2imz (Van Roey et al. 2007).

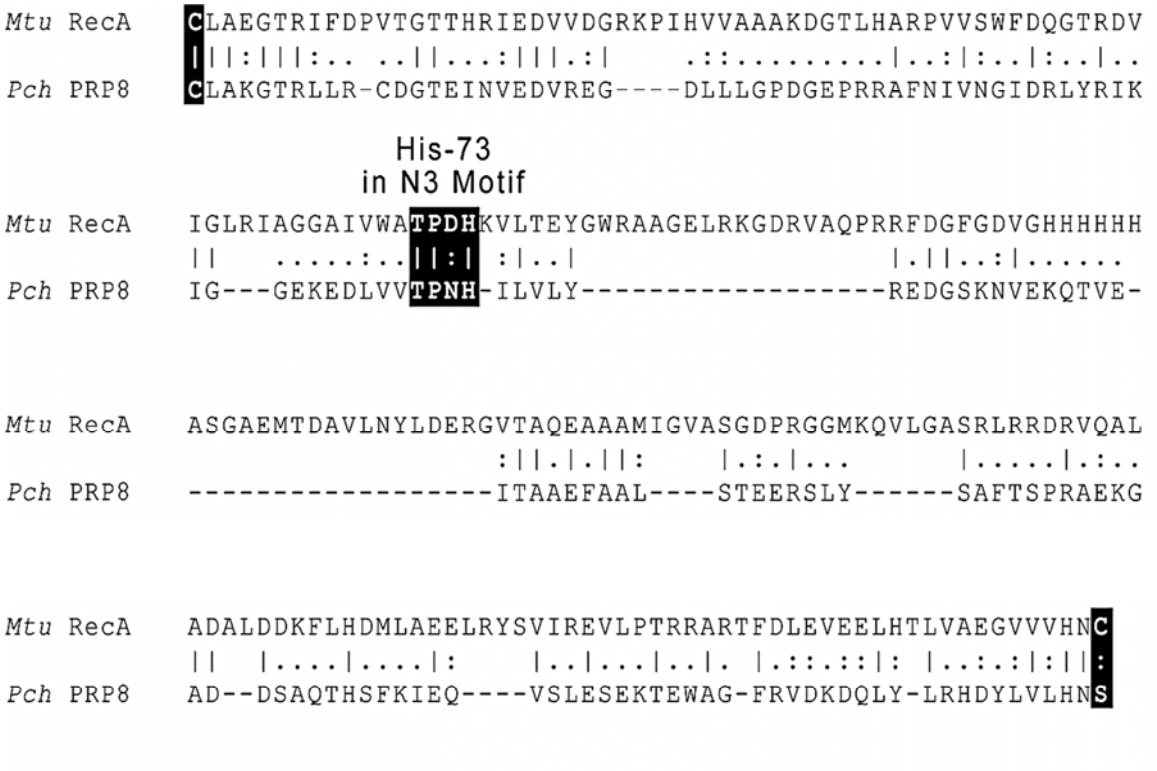

Figure 1.3 Clustal W (Thompson et al. 1994) **alignment of the amino acid sequences of the *M. tuberculosis* and *P. chrysogenum* mini-inteins used**. The regions involved in the splicing catalysis are highlighted in black.

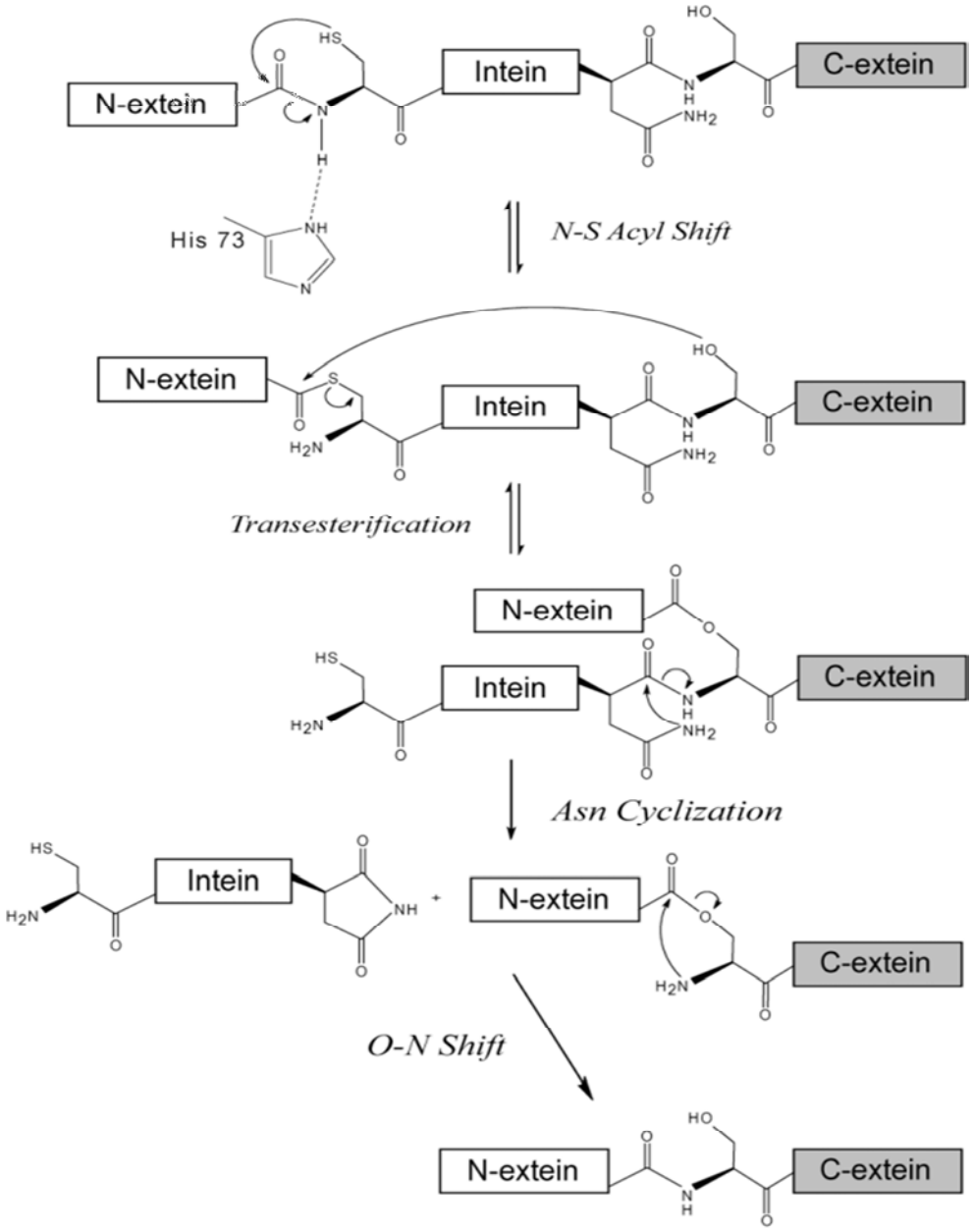

Figure 1.4 Enzymatic mechanisms proposed for intein catalysis Modified from (Klabunde et al. 1998; Ding et al. 2003). The histidine in the N3 block appears hydrogen bonded to the amino group on the N-splicing site. The different steps proposed for catalysis are shown: N-S acyl shift, transesterification, asparagine cyclization and O-N shift.

CHAPTER II: MATERIALS AND METHODS

2.1 Cell Lines, Hybridomas and T Cells

All cell lines were grown in a tissue culture humidified incubator at 37 °C and 5% CO_2 in RPMI-1640 supplemented with 10% FCS, 100 μM Non-essential amino acids, 1 mM sodium pyruvate, 2 mM L-glutamine, 0.25 μg/ml Amphotericin B, 50 U/ml Penicillin G, 50 μg/ml Streptomycin Sulfate, 55 μM 2-ME, 10 mM HEPES

E36 cells were selected as the target cells for antigen expression. E36 cells are an established cell line derived from Chinese hamster lung carcinoma (Gillin et al. 1972). Murine H-2D^b and ICAM1 were previously transfected into E36 cells and stable transfectants were selected (E36.17.3 or E36/D^b) (Mo et al. 1999). These cells were infected with a lentivirus encoding H-2K^b to yield E36/K^{b}D^b (hereafter E36).

The AN9-D^b-specific 12.64 hybridoma was provided by Dr. David Woodland (Trudeau Institute, Saranac Lake, NY). This hybridoma has been shown to recognize ASNENMETM and not CSNENMETM as its cognate peptide in the context of H-2D^b (Sigal & Wylie 1996). This is important, since detection of CSNENMETM would defeat

the purpose of recognizing exclusively peptides derived from spliced species, as the degradation of an unspliced intein-containing protein could generate CSNENMETM. 12.64 cells were transduced first with a retrovirus encoding the mouse CD8-alpha chain (Lyt-2a) cDNA downstream of an IRES (Levkau et al. 2001). The retrovirus was packaged using the plasmid pBMN-IRES-Lyt-2a, a generous gift from Dr. Elaine Raines (University of Washington, Seattle, WA). After selection, the resulting line was infected with a lentivirus encoding the mouse CD8-beta chain in the pTRIPZ plasmid vector (Open Biosystems, Lafayette, CO). After selection, yet another round of lentiviral transduction was performed, this time the vector encoded a minimal promoter containing NFAT binding sites upstream of a luciferase ORF (NFAT-Luc cassette). The final line is 12.64-CD8αβ-Luc (hereafter 12.64).

The NFAT-Luc cassette lentivirus was generated by Freidrich Cruz, UMass Medical School, Department of Pathology. It was subcloned from pGL3-NFAT32 (Addgene, Cambridge, MA) along with the bsd^R ORF driven by the SV40 promoter from pCDNA6 (Invitrogen, Carlsbad, CA), into the lentiviral vector pCDH1 (Systems Biosciences), replacing the CMV promoter. The resulting plasmid, pCDH1-NFAT-Luc-Bsd was transcribed in 293T cells and packaged into VSV-G pseudotyped lentivirus.

The SL8-K^b-specific RF33-Luc (hereafter RF33) was derived from the RF33 T cell hybridoma which recognizes SIINFEKL in the context of H-2 K^b (Rock et al. 1990).

These cells were also transduced with the NFAT-Luc cassette described above. This cell line was generated by Kenneth Rock and Freidrich Cruz, UMass Medical School, Department of Pathology.

Spleens from female HY (*Jarid1d*, also called *Smcy)* TCR transgenic mice (Kisielow et al. 1988) in the C57BL/6 background (a kind gift of Dr. Raymond Welsh, UMass Medical School Department of Pathology) were used as a source of HY-D^b-specific $CD8^+$ T cells.

2.2 Molecular Cloning

See a schematic diagram of the constructs used in the experiments on Figure 3.6. All constructs were analyzed for correct insertion and sequenced. Restriction enzyme and Calf Intestinal Phosphatase treatment was performed according to the manufacturer's instructions (New England Biolabs, Ipswich, MA). RNA extraction, plasmid purification, PCR cleanup, and purification from agarose gel electrophoresis were performed using Qiagen's (Valencia, CA) nucleic acid purification kits. PCR for cloning was performed with the Platinum Pfu polymerase kit (Invitrogen, Carlsbad, CA); and for *E. coli* colony screening, with the Taq polymerase kit (Invitrogen, Carlsbad, CA). DNA

ligations were performed at different insert to vector ratios using T4 DNA ligase (Invitrogen, Carlsbad, CA). For cloning into pCDNA (Invitrogen, Carlsbad, CA), DH5α subcloning efficiency competent *E. coli* were used for transformation of ligated products (Invitrogen, Carlsbad, CA), and cells were plated on LB-Miller broth agar petri dishes with 100 µg/mL ampicillin (Sigma, Saint Louis, MO). For cloning into pTRIPZ (Open Biosystems, Lafayette, CO), XL-10 gold ultracompetent *E. coli* were used for transformation of ligated products (Stratagene, Agilent Technologies, Santa Clara, CA), and cells were plated on LB-Lennox broth (NaCl 5 g/L) agar petri dishes with 100 µg/mL ampicillin (Sigma, Saint Louis, MO) and 25 µg/mL.

The PCR routine used was as follows:

94°C	2 min	
94°C	30 s	x 30 cycles
50-55°C	30 s	
72°C	1 min/kilobase pair	
72°C	5 min	
4°C	∞	

Construct No. 1 (a & b): pCDNA-GFP-Int-A9M. Precursor of GFP-PRP8-A9M

Sequence: (*GFP*)-SIINFEKL-A-(*Pch PRP8*)-SNENMETM-DS-(*HA tag*)

PCR 1.1

Template: pGPch-1, encoding the *Pch* PRP8 intein (Stephanie Pöggeler)

Forward Primer: S8L PRP8 Fwd

Reverse Primer: TP Rev

PCR 1.2

Template: pGPch-1 (Stephanie Pöggeler)

Forward Primer: TPNH Fwd for wild-type (a) or tpnl Fwd for N3 mutant (b)

Reverse Primer: PRP NP Rev

PCR 1.3 (a, wild-type; b, N3 mutant)

Template: Ligation of PCRs 1.1a or b, and PCR 1.2, both after *Spe*I digestion

Forward Primer: S8L PRP8 Fwd

Reverse Primer: NP HA Xba Rev

Construct No. 2 (a & b): pCDNA-GFP-PRP-A9M: same as above, but inserting a short peptide from natural N-extein (GSFWEK) to enhance splicing efficiency.

Sequence: (*GFP*)-SIINFEKL-GSFWEK-A-(*Pch PRP8*)-SNENMETM-DS-(*HA tag*)

PCR 2.1 (a, wild-type; b, N3 mutant)

Template: precursor construct No. 1 PCR 1.3 a or b (see above)

Forward Primer: S8L PRP 2 Fwd

Reverse Primer: NP HA Xba Rev

PCR 2.2

Template: pEGFP-C1 (Clontech, Mountain View, CA)

Forward Primer: GFP Kpn Fwd

Reverse Primer: GFP S8L H3 Rev

PCR product 2.1 was digested with *Hind*III and *Xba*I

PCR product 2.2 was digested with *Kpn*I and *Hind*III

Vector: pCDNA 3.1 Hygro (Invitrogen, Carlsbad, CA) was digested with *Kpn*I and *Xba*I and treated with calf intestinal phosphatase (New England Biolabs, Ipswich, MA).

Digested PCR products 2.1 and 2.2 were ligated with digested vector to generate pCDNA-GFP-PRP-A9M wild-type or N3 mutant.

Construct No. 3: GFP-NP: pre-spliced (no intein) version of construct No. 2

Sequence: *(GFP)*-SIINFEKL-GSFWEK-ASNENMETM-DS-(*HA tag*)

PCR 3.1

Template: PCR 2.1

Forward Primer: Fus NP Fwd 3

Reverse Primer: NP HA Rev

PCR product 2.1 was digested with *Hind*III and *Xba*I

Vector: pCDNA 3.1 Hygro (Invitrogen, Carlsbad, CA) was digested with *Kpn*I and *Xba*I and treated with calf intestinal phosphatase (New England Biolabs, Ipswich, MA).

Digested PCR products 3.1 and 2.2 were ligated with digested vector to generate pCDNA-GFP-A9M.

Construct No. 4: pCDNA-GFP-Int-K9L. Precursor of GFP-Rec-K9L.

Sequence: (*GFP*)-(*Mtu RecA*)-CSRNRQYL-(*HA tag*)

PCR 4.1

Template: pEGFP-C1 (Clontech, Mountain View, CA)

Forward Primer: GFP Kpn Fwd

Reverse Primer: gint Rev

PCR 4.2

Template: pGFPmU, encoding the *Mtu* RecA intein (Henry Paulus)

Forward Primer: Gint Fwd

Reverse Primer: Int SMCY Rev

PCR 4.3

Template: 0.1 μL of PCRs 4.1 and 4.2

Forward Primer: GFP Kpn Fwd

Reverse Primer: Int SMCY Rev

PCR 4.4

Template: PCR 4.3

Forward Primer: GFP Kpn Fwd

Reverse Primer: SMCY HA Rev

PCR product 4.4 was digested with *Kpn*I and *Xba*I.

Vector: pCDNA 3.1 Hygro (Invitrogen, Carlsbad, CA) was digested with *Kpn*I and *Xba*I and treated with calf intestinal phosphatase (New England Biolabs, Ipswich, MA).

Digested PCR product 4.3 was ligated with digested vector to generate pCDNA-GFP-Int-K9L.

Construct No. 5: pCDNA-GFP-Rec-K9L.

Sequence: (*GFP*)-SIINFEKL-DEY-K-(*Mtu RecA*)-CSRNRQYL-(*HA tag*)

PCR 5.1

Template: pGFP-SICNFEKL (Made before)

Forward Primer: CMV Fwd

Reverse Primer: GFP S8L H3 Rev

PCR 5.2

Template: pCDNA-GFP-Int-K9L

Forward Primer: S8L H3 Fwd

Reverse Primer: SMCY HA Rev

PCR 5.3

0.1 µL of PCRs 5.1 and 5.2

Forward Primer: GFP Kpn Fwd

Reverse Primer: SMCY HA Rev

Vector: pCDNA 3.1 Hygro (Invitrogen, Carlsbad, CA) was digested with *Kpn*I and *Xba*I and treated with calf intestinal phosphatase (New England Biolabs, Ipswich, MA).

Digested PCR product 4.3 was ligated with digested vector to generate pCDNA-GFP-Rec-K9L.

Construct No. 6: pCDNA-GFP-Rec-K9L N3 mutant version (does not splice).

Sequence: (*GFP*)-SIINFEKL-DEY-K-(N3 mutant *Mtu RecA*)-CSRNRQYL-(*HA tag*)

PCR 6.1

Template: Construct No. 5, pCDNA-GFP-Rec-K9L.

Forward Primer: CMV Fwd

Reverse Primer: N3 RecA mut Rev

PCR 6.2

Template: Construct No. 5, pCDNA-GFP-Rec-K9L.

Forward Primer: N3 RecA mut Fwd

Reverse Primer: SMCY HA Rev

PCR 6.3

Template: 0.1 μL of PCRs 6.1 and 6.2

Forward Primer: CMV Fwd

Reverse Primer: Int SMCY Rev

Vector: pCDNA 3.1 Hygro (Invitrogen, Carlsbad, CA) was digested with *Kpn*I and *Xba*I and treated with calf intestinal phosphatase (New England Biolabs, Ipswich, MA).

Digested PCR product 4.3 was ligated with digested vector to generate pCDNA-GFP-Rec-K9L N3 mutant

Construct No. 7: pCDNA-GFP-K9L. Pre-spliced version of construct No 5.

Sequence: (*GFP*)-SIINFEKL-DEY-KCSRNRQYL-(*HA tag*)

PCR 7.1

Template: Construct No. 5, pCDNA-GFP-Rec-K9L.

Forward Primer: CMV Fwd

Reverse Primer: Fus HY Rev

PCR 7.2

Template: PCR 7.1

Forward Primer: CMV Fwd

Reverse Primer: Int SMCY Rev

Vector: pCDNA 3.1 Hygro (Invitrogen, Carlsbad, CA) was digested with *Kpn*I and *Xba*I and treated with calf intestinal phosphatase (New England Biolabs, Ipswich, MA).

Digested PCR product 4.3 was ligated with digested vector to generate pCDNA-GFP-K9L.

pTRIPZ lentiviral vector (Open Biosystems, Lafayette, CO): This vector provides a lentiviral backbone along with two expression cassettes: one for the reverse tetracycline transactivator, and another one for RFP (red fluorescent protein) and micro RNA expression driven by a doxycycline-inducible CMV minimal promoter. The RFP and micro RNA regions in pTRIPZ were removed by digesting with *Age*I and *Mlu*I restriction enzymes and purifying the vector fragment from an agarose gel. Constructs No. 2 a & b, 3, 5, 6, and 7 were used as templates for PCR reactions to introduce *Age*I and *Mlu*I restriction sites. Primers were GFP Age Fwd and BGH Mlu Rev. The ORFs contained the construct and a BGH poly(A) signal from pCDNA 3.1. These PCR products were

digested with *Age*I and *Mlu*I restriction enzymes and ligated to the digested vector treated with calf intestinal phosphatase (New England Biolabs, Ipswich, MA). The resulting plasmids were sequenced using the GFP Age Fwd and BGH Mlu Rev primers, and the correct clones were selected and plasmid DNA was amplified and purified.

The *Mtu* RecA mini-intein encoding plasmid (pGFPmU) was a generous gift from Dr. Henry Paulus (Boston Biomedical Research Institute, Watertown, MA) (Gangopadhyay et al. 2003). The *Pch* PRP8 mini-intein encoding plasmid (pGPch-1) was kindly provided by Dr. Stephanie Pöggeler (Georg-August-Universität Göttingen, Göttingen, Germany) (Elleuche et al. 2008). The GFP encoding sequence was amplified from pEGFP-C1 (Clontech, Mountain View, CA), which encodes a modified *Aquoera victoria* GFP. The pCDH lentivirus expression vector (System Biosciences, Mountain View, CA) encoding H-2K^{b} was provided by Freidrich Cruz (UMass Medical School, Worcester, MA).

Table 2.1: Primer list

Primer Name	5' to 3' Sequence
BGH Mlu Rev	GGCACGCGTAGCCCACCGCATCCCCAGC
CMV Fwd	CGCAAATGGGCGGTAGGCGTG
Fus HY Rev	TAAGTACTGTCGATTCCTTGAACACTTGTACTCGTCAAGCTTCTCAAAGTTGATGATACTC
Fus NP Fwd 3	GGCGAAGCTTGGATCCTTCTGGGAGAAAGCGAGTAACGAAAACATGGAAACTATG
GFP Age Fwd	CGGACCGGTCGCCACCATGGTGAGCAAGGGCG
GFP Kpn Fwd	GAGCGGTACCGCCACCATGGTGAGCAAGGGCGAGGAGC
GFP S8L H3 Rev	GCTCTAGATTAAAGCTTCTCAAAGTTGATGATACTC
Gint Fwd	CTGTACAAGTGCCTCGCAGAGGGCACCCGAATC
gint Rev	CTCTGCGAGGCACTTGTACAGCTCGTCCATGCC
Int SMCY rev	AACGTAAGTACTGTCGATTCCTTGAACAGTTGTGCACGACAACCCCTTC
N3 RecA mut Fwd	TGTGGGCGACACCCGATCTTAAGGTGCT
N3 RecA mut Rev	AAGATCGGGTGTCGCCCACAC
NP HA Xba Rev	GCTCTAGATTAAGCGTAATCTGGAACGTCATATGGATAGCTGTCCATAGTTTCCATGTT
PRP NP rev	CATAGTTTCCATGTTTTCGTTACTGTTGTGCAGGACAAGGTAGTC
S8L H3 Fwd	GAGAAGCTTGACGAGTACAAGTGCCTCGCAG
S8L PRP 2 Fwd	CCCCAAGCTTGGATCCTTCTGGGAGAAAGCGTGTCTCGCCAAGGGGACC
S8L PRP8 Fwd	CCCCAAGCTTGCGTGTCTCGCCAAGGGGACC
SMCY HA rev	GCTCTAGATTAAGCGTAATCTGGAACGTCATATGGATAACGTAAGTACTGTCGATTCCTTGAAC
TP Rev	GGGGACTAGTTCCTCTTTCTCACCGCCGATC
TPNH Fwd	GGGGGAACTAGTGGTGACGCCGAACCATATTC
tpnl fwd	GGGGGAACTAGTGGTGACGCCGAACCTGATTC

Table 2.1: Primer list. DNA primers used for molecular cloning and sequencing (alphabetically listed).

2.3 Retrovirus and Lentivirus Packaging

VSV-G pseudotyped lentivirus particles were generated by co-transfecting the lentiviral vector with a lentivirus packaging mix (Open Biosystems, Lafayette, CO) into LentiX 293T cells (Clontech, Mountain View, CA). The packaging mix contains seven HIV-1 genes (gag, pro, vpr, rt, in, tat, rev) in three different plasmids (pTLA1-Pak, pTLA-1-Enz, pTLA1-Tat/Rev). The HIV-1 envelope gene is substituted by the VSV-G encoding gene, therefore the resulting virions were pseudotyped, which conferred them a much broader tropism than that of HIV-1 (Gilden et al. 1981). Seventy-two hours after transfection supernatants were collected and concentrated by 20,000 x*g* ultracentrifugation in an SW28 rotor (Beckman Coulter, Indianapolis, IN). Pellets were resuspended in 0.5 mL PBS. In order to calculate the virus titer, RNA copy number in supernatants was obtained using quantitative PCR. RNA extraction was performed from 50 µL of resuspended pellets using the QIAamp Viral RNA Mini Kit purification kit (Qiagen, Valencia, CA). RNA was reverse-transcribed into single strand DNA using the iSCRIPT kit with random hexamer primers (Bio-Rad, Hercules, CA). Copy number was determined using a TaqMan® assay with primers and fluorescein labeled probes specific for the enhanced GFP gene ("EGFP All", Applied Biosystems, Foster City, CA). Serial dilutions of GFP containing plasmid DNA were used as a standard.

The PCR routine was as follows:

95°C	10 min	
95°C	15 s	x 40 cycles
60°C	1 min	

VSV-G pseudotyped retrovirus particles were generated by transfecting pBMN-IRES-Lyt2a (Levkau et al. 2001) into Phoenix GP cells, which expresses only murine leukemia virus gag-pol and VSV-G. Seventy-two hours after transfection supernatants were collected and concentrated by 20,000 x*g* ultracentrifugation in an SW28 rotor (Beckman Coulter, Indianapolis, IN). Pellets were resuspended in 0.5 mL PBS.

2.4 Infection and Cell Purification

E36 cells were cultured overnight in RPMI-1640 10% FCS in 12 well plates so they will be in logarithmic growth phase the next morning. Infection with retrovirus or lentivirus was performed in the presence of polybrene (SIGMA, St Louis, MO) at 10 μg/mL. The inoculum varied depending on the titer. Although not always possible, the preferred multiplicity of infection was five to ten. Titers were estimated or calculated as shown above. Seventy-two hours later infected cells were purified to at least 90% purity by

positive selection after overnight induction with 1 μg/mL doxycycline. For positive selection cells were detached with trypsin EDTA, neutralized and washed, and stained with either 25-D1.16 antibody (Porgador et al. 1997) or biotin-conjugated anti-mouse CD8α (clone 53-6.7, BD biosciences, San José, CA) in PBS containing 2% FCS and 2 mM EDTA followed by a wash step and binding to 5 μm Dynal beads (Invitrogen, Carlsbad, CA) conjugated to goat anti-mouse IgG or to streptavidin according to the manufacturer's instructions (Dynabeads Pan mouse IgG or Dynabeads M-280 Streptavidin, Invitrogen, Carlsbad, CA). Cells were washed twice using a Dynamag magnet according to the manufacturer's instructions (Invitrogen, Carlsbad, CA) and returned to culture. The purified E36 cells were maintained in G418 and monitored for H-2K^b, H-2D^b, and ICAM-1 expression by flow cytometric staining. The monoclonal antibodies used for staining were AF6-88.5, KH-95 (both from BD biosciences, San José, CA), and YN/1.7 (Takei 1985) respectively. When necessary, E36 cells were sorted for high uniform expression of all the transfected genes (FACS sort was performed by the University of Massachusetts Medical School Flow cytometry core personnel).

2.5 Mass Spectrometry

All the mass spectrometry experiments were performed by the staff of the mass spectrometry core at the University of Massachusetts Medical School.

Polyacrylamide gel bands were excised from silver stained gels for mass spectrometry. Cos-7 cells were collected after twenty-four hours transient transfection, centrifuged at 300 x*g* and pellets lysed in chilled Tris buffered saline 0.5% DOC 1% NP-40 with a protease inhibitor cocktail (Complete mini, Roche, Indianapolis, IN). Cold lysates obtained were centrifuged at 15,000 rpm in a tabletop microfuge and supernatants were passed through a 0.22 μm column (SpinX, Corning, Corning, NY). Filtrates were subject to immunoprecipitation overnight at 4°C with 20 μL Sepharose protein A (GE Healthcare, Piscataway, NJ), which had been previously bound to purified anti-GFP rabbit polyclonal antibody (300 ng/sample, Invitrogen, Carlsbad, CA). Beads were washed three times with the lysis buffer described above, resuspended in Laemmli loading buffer (New England Biolabs, Ipswich, MA), and ran on 10 % SDS-PAGE with Tris-Glycine running buffer (Ornstein 1964). Silver staining was performed following manufacturer's instructions (Bio-Rad, Hercules, CA).

The bands excised corresponded to the putative spliced size (lower band) in cells transfected with a construct encoding GFP-SI-RecA mini-intein-CNFEKL-HAtag, or the pre-spliced version: GFP-SICNFEKL-HAtag. Samples were first reduced and alkylated with Iodoacetamide to protect Cysteines. After a cyanogen bromide digestion (CNBr) it should yield the C-terminal DELYKSICNFEKLYPYDVPDYA peptide, which encompasses the splice junction and therefore is appropriate to ascertain splicing fidelity.

Peptides were analyzed on an Axima CFR instrument (Shimadzu, Columbia, MD) in reflectron mode, a Matrix-assisted laser desorption/ionization (MALDI) quadrupole ion trap (QIT) time-of-flight (TOF) analyzer. The resulting spectra were amplified to find the peak corresponding to the C-terminal DELYKSICNFEKLYPYDVPDYA peptide which has an expected m/z of approximately 2742.26 Thomson, as predicted using the MS-Digest in ProteinProspector 4.0.6 software (University of California).

2.6 Radiolabeling Experiments

2.6.1 Pulse-chase

E36 cells were cultured overnight with 2 μg/mL doxycycline in RPMI-1640 10% FCS in 150 mm^2 flasks. Cells were trypsinized, washed with PBS and resuspended in RPMI-1640 without L-Methionine or L-Cysteine (SIGMA, St Louis, MO). Cells were starved in this medium for 20 minutes and [^{35}S]-L-Met/Cys mix was added (100 μCi/million cells, EasyTag, Perkin Elmer, Waltham, MA) for 3 minutes. Cells were transferred to an ice bath and centrifuged at 300 x*g* for 5 min at 4 C, labeled media was removed and cells were resuspended in chase media (RPMI-1640 10% FCS with excess L-Methionine and L-Cysteine). Aliquots were collected at the indicated times, centrifuged at 300 x*g* and pellets lysed in chilled Tris buffered saline 0.5% DOC 1% NP-40 with a protease inhibitor cocktail (Complete mini, Roche, Indianapolis, IN). Cold lysates were centrifuged at 15,000 rpm in a tabletop microfuge and supernatants were passed through a 0.22 μm column (SpinX, Corning, Corning, NY). Filtrates were subject to immunoprecipitation overnight at 4°C with 15 μL Dynabeads protein G (Invitrogen, Carlsbad, CA), which had been previously bound to HA-7 monoclonal anti-HA tag antibody (300 ng/sample, SIGMA, St Louis, MO). Beads were washed three times with the lysis buffer described above, resuspended in loading buffer (XT buffer with reducing

agent, Bio-Rad, Hercules, CA), and ran on 10 % bis-tris SDS-PAGE with MOPS running buffer (50 mM MOPS 50 mM Tris 1 mM EDTA 0.1% SDS, 5 mM sodium bisulfite). Gels were dried and exposed to a phosphor storage screen (GE Healthcare, Piscataway, NJ). Screens were scanned using a Typhoon trio imager (GE Healthcare, Piscataway, NJ), and bands were analyzed with ImageJ software (NIH, USA). Pre-spliced and spliced bands contained fewer methionine and cysteine residues than the full length intein bands, hence their density measurements were adjusted accordingly. For the GFP-RecA-HY constructs the pre-spliced or spliced species contained three cysteines and five methionines; whereas the unspliced intein had four cysteines and nine methionines, therefore the adjustment factor was sixty-two percent, and it was applied to the unspliced intein band intensity value obtained from Image J. In the case of the GFP-PRP-NP constructs the pre-spliced or spliced species contained no cysteines and seven methionines; whereas the unspliced intein had two cysteines and seven methionines, therefore the adjustment factor was seventy-eight percent.

2.6.2 Continuous labeling

Uninduced E36 cells were starved as described above, and grown in the presence of label (25 μCi/million cells [^{35}S]-L-Met/Cys mix, EasyTag, Perkin Elmer, Waltham, MA) and doxycycline. Aliquots were collected at the indicated times and transferred to tubes containing excess methionine and cysteine in an ice bath. Samples were processed as described above.

2.7 Antigen Presentation Assays

Expression of the lentivirally transduced antigen constructs in E36 cells was induced at different times by adding serially diluted doxycycline to cells growing in 96 well plates at 10^5 cells/well in triplicate to final concentrations ranging from 1,000 ng/mL to 8 ng/mL. Antigen presentation was stopped by transferring cells to an ice bath for FACS staining or—for hybridoma assays—by adding brefeldin A to 1 μg/mL (GolgiPlug, BD biosciences, San José, CA).

2.7.1 Immunofluorescent staining

Cells were trypsinized and stained with 300 ng 25-D1.16 in 30 μL PBS containing 2% FCS and 0.01% sodium azide (flow cytometry buffer) on ice followed by a wash step and staining with 150 ng Alexa Fluor 647 goat anti-mouse IgG (Invitrogen, Carlsbad, CA). Cells were analyzed on a FACSCalibur (BD biosciences, San José, CA) flow cytometer. The results were analyzed with FlowJo software (Tree Star, Ashland, OR).

2.7.2 Hybridoma assays

10^5 hybridoma cells/well were added to opaque white, clear bottom 96 well plates containing E36 cells induced for different times in triplicates. Cells were co-cultured in the presence of brefeldin A for sixteen hours. After centrifugation in an Allegra tabletop centrifuge (Beckman Coulter, Indianapolis, IN), dry pellets were lysed with 20 μL passive lysis 5X buffer (Promega, Madison, WI), and luciferase activity was measured with the Luciferase Assay System (Promega, Madison, WI) on a POLARstar OPTIMA luminometer (BMG Labtech, Ortenberg, Germany). 100 μL luciferase substrate were injected per well and readings were taken for 12 seconds on a well by well basis.

2.7.3 HY-specific T cell response assay

Cell surface presentation of K9L-D^b complexes was quantified by co-culturing female HY TCR-transgenic splenocytes with E36 cells induced for different lengths of time in the presence of brefeldin A and then quantifying TNFα production by intracellular cytokine staining assays (Murali-Krishna et al. 1998). The response was measured as % $TNF\alpha^+$ gated on $CD8^+$ $T3.70^+$ cells. The anti-mouse TNF alpha antibody and the HY TCR clonotypic antibody T3.70 were from eBioscience, San Diego, CA. The anti-mouse CD8α (clone 53-6.7) was from BD biosciences, San José, CA.

2.8 Clustal W Multiple Sequence Alignment

The alignment data shown in Figure 1.3 were obtained using the ClustalW2 (Thompson et al. 1994) tool at the following server address on the World Wide Web:

http://www.ebi.ac.uk/Tools/services/web/toolform.ebi?tool=clustalw2

Alignment parameters: EBLOSUM62 matrix, gap penalty 12, extend penalty 2.

Results: 23.1% identity, 34.8% similarity.

2.9 Mathematical Analysis

GraphPad Prism (GraphPad Software, La Jolla, CA) was used to fit exponential decay curves to the densities of the gel bands from pulse-chase experiments shown in Figures 3.7 and 3.8. The splicing rate constants on Table 6.3 were derived from these fittings. KinTek Explorer (Johnson et al. 2009b; Johnson et al. 2009a) was used to model the kinetics of expression, splicing, epitope processing, and transport, using the model shown in Figure 6.1. All steps except k_5 were modeled as first order processes. k_1 and k_6 represent the translation rate for intact intein and pre-spliced constructs. Values were obtained by fitting densitometry values or GFP fluorescence values (Figures 6.2 and 6.3). A process with rate equal to k_1 replenishing the mRNA pool was included to simulate a constant mRNA supply. k_2 represents the splicing rate, determined from the pulse-chase data in Figure 3.8 or 3.9. k_3 represents the degradation rate of spliced or pre-spliced protein. The value was obtained from fitting the densitometry or GFP fluorescence data (Figures 6.2 and 6.3). k_4 represents the rate of peptide epitope generation after degrading the source protein and MHC I loading . Its value is unknown, although there are in vitro studies in the literature (Cascio 2001). We were able to vary this value over a wide range ($0.001 - 1\ h^{-1}$) with little effect on the Pre-spliced to Intein presentation ratio. k_5 represents the delay due to MHC-peptide trafficking from the endoplasmic reticulum to the cell surface, and is modeled as a fixed time delay, added to the time scale of the kinetic simulation before plotting in Figure 6.4. Varying k_5 within a range of literature

values (Table 6.3) did not significantly change the predicted presentation ratios shown in Figure 6.3. The loss of surface MHC I complexes by re-internalization was found to be around 0.02 h^{-1} by pulse-chase in a study using dendritic cells (Kukutsch et al. 2000). Varying this surface complex turnover rate (k_8 in Figure 6.1) from 1.5 to 5 h^{-1} in our model did not significantly affect the predicted Pre-spliced to Intein presentation ratios shown in Figure 6.3, and hence it was not explicitly included in the model.

CHAPTER III: INTEINS CAN SPLICE IN MAMMALIAN CELLS

3.1 Introduction

Inteins display self-splicing capabilities even *in vitro* in purified preparations. This strongly suggests that no other cellular factors are required for splicing to occur. For this reason it was believed that splicing could be achieved in mammalian cells despite the inteins originating from bacteria or fungi. There is one example in the literature (Ozawa et al. 2000) where an intein—in this case a split DnaE intein from the cyanobacterium *Synechocystis species*—had been expressed in mammalian cells and splicing had indeed taken place. It was nevertheless necessary to ascertain the splicing capability of the inteins to be used for splitting the epitopes that will be measured in antigen presentation assays.

3.2 Screening for Splicing

For this purpose, inteins were cloned into mammalian expression vectors interrupting the GFP sequence. Inteins were inserted downstream of glycine 128 and upstream of aspartate 130, removing isoleucine 129 (N-terminus…VNRIELKG-Intein-DFKEDGNIL…C-terminus). Splicing was scored by measuring fluorescence in E36 cells transfected transiently.

. It is worth noting that three inteins from different species failed to splice when tested in this fashion (*Saccharomyces cerevisiae* Vacuolar Membrane H^+ ATPase 1 [VMA1], *Cryptococcus neoformans* PRP8, and *Mycobacterium leprae* RecA).

When the *Mtu* RecA and *Pch* PRP8 mini-inteins were tested (kind gifts from Henry Paulus at the Boston Biomedical Research Institute, Watertown, MA; and Stephanie Pöggeler at Georg-August-Universität, Göttingen, Germany) GFP fluorescence was observed in the wild-type intein transfected cells, whereas cells transfected with a splicing mutant (N3 mutant, in which the N3 domain sequence TxxH was mutated to TxxL) did not show a fluorescent signal. The data for *Mtu* RecA is shown in Figure 3.1.

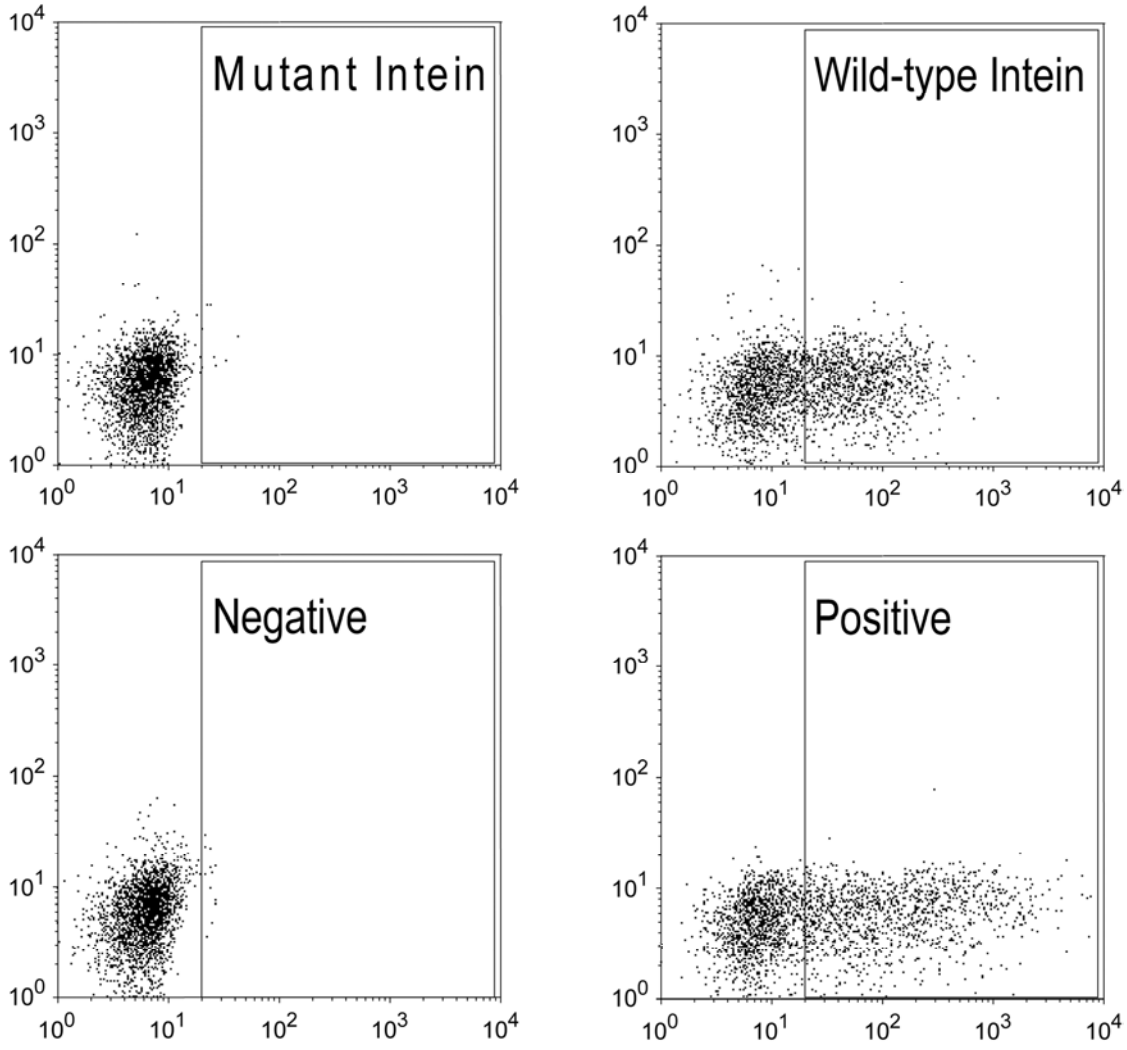

Figure 3.1 Splicing of the *Mtu* RecA mini-intein. Flow cytometry dot plots of Cos-7 cells transiently transfected for twenty-four hours with plasmids encoding GFP split by the mini-intein sequence. The mini-intein was inserted downstream of glycine 128 of GFP and upstream of aspartate 130, removing isoleucine 129 (N-terminus…VNRIELKG-Intein-DFKEDGNIL…C-terminus). The wild-type intein is the *Mtu* RecA mini-intein (Gangopadhyay et al. 2003), and the mutant intein is an N3 domain mutant in which TPDH was mutated to TPDL.

Once the splicing capability had been ascertained, constructs were made in which model epitopes were intervened by the intein sequence and fused to GFP in order to monitor expression, and to S8L as a control splicing-independent epitope. An HA tag was placed at the C-terminus to facilitate immunoprecipitation.

3.3 Extein Flanking Residues

It was found through trial and error, that the presence of hydrophobic amino acids on the N-terminal splicing junction greatly hindered splicing. This was the case when S8L was placed immediately N-terminal of the intein's cysteine at the N-extein-intein junction: splicing was hampered by the C-terminal leucine in S8L. Isoleucine also caused splicing to become inefficient. As shown in Figure 3.2, most of the immunoprecipitated material was recovered in the full-length unspliced band after transient transfection of Cos-7 cells with a construct encoding GFP-SI-*Mtu* RecA mini-intein-CNFEKL-HA tag. In order to maintain splicing, a linker was introduced between S8L and the inteins: DEYK for the RecA constructs and GSFWEK for the PRP8 constructs. The pre-spliced versions also contained these linkers, but no inteins. Thus, the pre-spliced constructs were identical to their intein-containing counterparts after the splicing reaction had occurred.

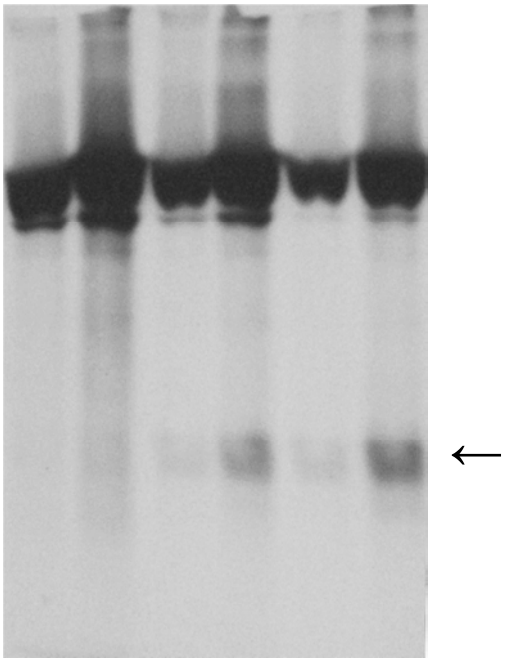

Lane: 1 2 3 4 5 6

Figure 3.2 Isoleucine in the N-terminal Splicing Junction is Detrimental for Splicing. SDS-PAGE and autoradiogram after pulse-chase and immunoprecipitation with anti-GFP antibody of lysates made from either 293T or Cos-7 cells transiently transfected with a construct encoding GFP-SI-*Mtu* RecA mini-intein-CNFEKL-HA tag. The top bands correspond to the full-length unspliced construct and the bottom bands to the spliced product (arrow). Lanes one and two: pulse; lanes three and four: one hour chase; lanes five and six: two hour chase. Odd numbered lanes: 293T cells; even numbered lanes: Cos-7 cells.

3.4 Fidelity of Intein Splicing

In order to confirm the product of the splicing reaction was identical to the pre-spliced construct, the corresponding bands were excised from silver stained gels and processed for mass spectrometry as described in the methods section. This comparison was made between a construct encoding the *Mtu* RecA mini-intein splitting a modified S8L peptide (GFP-SI-*Mtu* RecA mini-intein-CNFEKL-HA tag) and its pre-spliced counterpart (GFP-SICNFEKL-HA tag).

The online digestion software tool within Prospector (http://prospector.ucsf.edu, University of California, San Francisco) was used to generate cleavage sites by cyanogen bromide and the mass upon charge (m/z) values of the corresponding ionized peptides. Figure 3.3 shows the prediction software output. Because the cysteines were protected with iodoacetamide, the expected peptide that would verify the splicing reaction was correct—DELYKSICNFEKLYPYDVPDYA—would be carbamidomethylated (-CH_2-SH + I-CH_2-$CONH_2$ → -CH_2-S-CH_2-$CONH_2$; i.e. cysteine + Iodoacetamide → S-carbamidomethyl cysteine), and therefore the expected m/z is 2742 Thomson for the mono-ionized form.

Considered modifications: | Carbamidomethyl (C) |

Digest Used: CNBr Max. # Missed Cleavages: 1 User AA Formula 1: C2 H3 N1 O1

Minimum Digest Fragment Mass: 800 Maximum Digest Fragment Mass: 4000

Minimum Digest Fragment Length: 5

pI of Protein: 5.4 Protein MW: 28961

Amino Acid Composition: A9 C3 D20 E17 F13 G22 H9 I13 K21 L22 M6 N14 P12 Q8 R6 S11 T16 V19 W1 Y14

1 MVSKGEELFT GVVPILVELD GDVNGHKFSV SGEGEGDATY GKLTLKFICT TGKLPVPWPT

61 LVTTLTYGVQ CFSRYPDHMK QHDFFKSAMP EGYVQERTIF FKDDGNYKTR AEVKFEGDTL

121 VNRIELKGID FKEDGNILGH KLEYNYNSHN VYIMADKQKN GIKVNFKIRH NIEDGSVQLA

181 DHYQQNTPIG DGPVLLPDNH YLSTQSALSK DPNEKRDHMV LLEFVTAAGI TLGM***DELYKS***

241 ***ICNFEKLYPY DVPDYA***

m/z (mi)	m/z (av)	Modifications	Start	End	Sequence
1190.5953	1191.3399		80	89	(h)KQHDFFKSAM(Met->Hsl)(P)
1486.8516	1487.7905		220	234	(h)VLLEFVTAAGITLGM(Met->Hsl)(D)
2685.2429	2687.0156		235	256	(h)DELYKSICNFEKLYPYDVPDYA(-)
2742.2644	2744.0678	1Carbamido methyl	235	256	(h)DELYKSICNFEKLYPYDVPDYA(-)

Figure 3.3 Mass Spectrometry Digest Prediction Results. Output from the ProteinProspector version 5.10.1 Proteomics tools for mining sequence databases in conjunction with Mass Spectrometry experiments. MS-Digest tool was used to obtain m/z prediction values after inputting the expected splicing product (GFP-SICNFEKL-HA tag). The key peptide DELYKSICNFEKLYPYDVPDYA that determines a correct splicing reaction is italicized. (mi), monoionized; (av), average; m/z, mass upon charge (in Thomson [1 Thomson = 1.036426 x 10^{-8} kgC^{-1}]). Hsl, homoserine lactone.

As shown in Figure 3.4 bottom panel, there are peaks in the intein sample very close to the predicted values for the key peptide DELYKSICNFEKLYPYDVPDYA (2,742 Thomson) whose presence confirms a correct splicing reaction. The intein sample was contaminated with some detergent as reflected by the cluster series in the spectra, but the presence of the 2742 peptide was evident. This confirms both the identity of the lower band as the spliced product and the precision of the cleavage and relegation reaction. Therefore, the splicing reaction did take place as expected in mammalian cells expressing intein constructs.

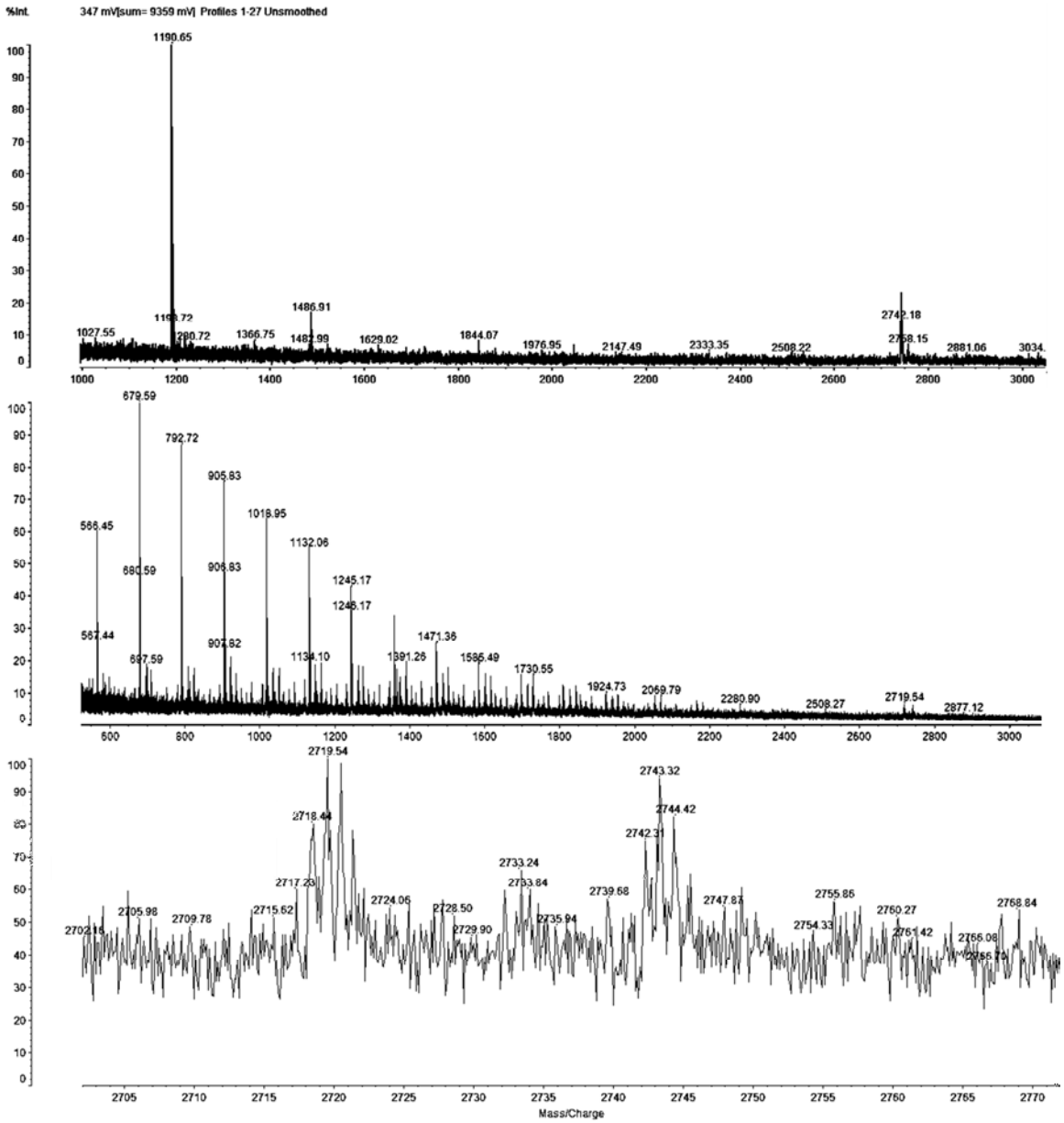

Figure 3.4 MALDI-TOF spectra of pre-spliced and intein bands. Comparison between a construct encoding the *Mtu* RecA mini-intein splitting a modified S8L peptide (GFP-SI-*Mtu* RecA mini-intein-CNFEKL-HA tag) and its pre-spliced counterpart (GFP-SICNFEKL-HA tag). Top panel: Pre-spliced, middle panel: intein, bottom panel: intein zoomed into m/z region of interest. The 2427 peak is apparent in both samples.

The splicing efficiency of the *Mtu* RecA and the *Pch*PRP8 mini-inteins was acceptable (Figure 3.1), but the intein flanking residues could be an issue (Figure 3.2), therefore it was imperative to find epitopes that could accommodate the requirements for efficient splicing, namely contain a cysteine (for RecA) or a serine (for PRP8)—which is necessary for the C-terminal splicing junction—and have no hydrophobic residues adjacent to the N-terminal splice junction. Of course, having an antigen presentation readout amenable for the epitope in question is paramount. The influenza A virus PR8 strain nucleoprotein 366-374 ASNENMETM (Cerundolo et al. 1991), and the murine male epitope SMCY 738-746 KCSRNRQYL (Markiewicz et al. 1998), both H-2D^{b}-restricted, fulfilled these requirements.

Another aspect related to the splicing fidelity is the stability of the spliced product. In order to confirm this, GFP levels in cells transiently transfected with plasmids encoding the RecA mini-intein fused to GFP (GFP-RecA-HY) construct and its pre-spliced counterpart were measured after treating them with the protein synthesis inhibitor cycloheximide at 50 mg/mL (Morimoto et al. 1967). As shown in Figure 3.5, the products of the intein splicing reaction *in vivo* were as stable as the pre-spliced protein. The approximate half-life was twelve hours in both cases.

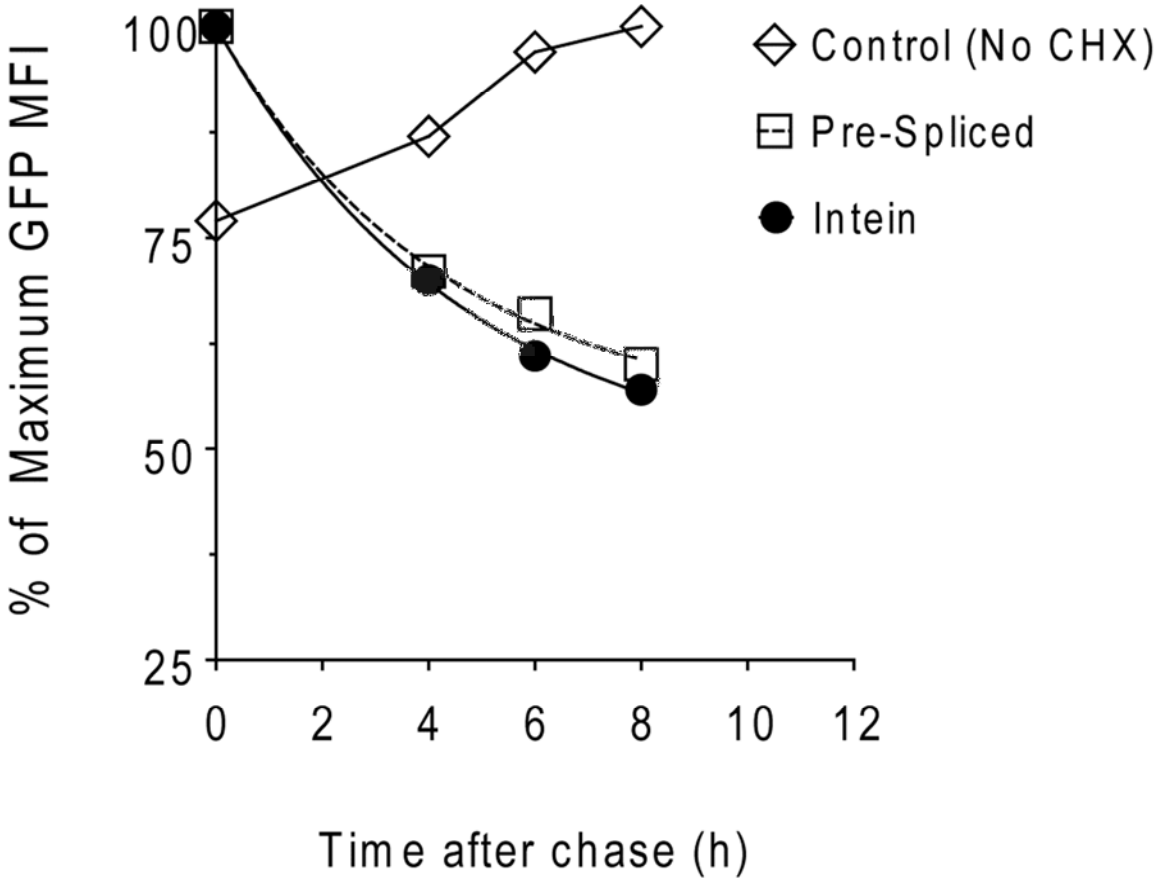

Figure 3.5 Measurement of Splicing products stability. Comparison of the stability of GFP fusions in E36 cells transiently transfected with plasmids encoding the RecA mini-intein fused to GFP (GFP-RecA-HY) construct and its pre-spliced counterpart were measured after treating them with the protein synthesis inhibitor cycloheximide at 50 mg/mL. GFP MFI fourteen hours post-transfection.

3.5 Construct Description

The final version of the constructs used from here on as shown in Figure 3.6 was subcloned into a lentivirus expression vector (a modified version of pTRIPZ, Open Biosystems, Lafayette, CO) which contained two promoters: a CMV minimal promoter followed by tetracycline operator sequences in tandem, and a ubiquitin promoter. The CMV minimal promoter drives the expression of the insert when a reverse tetracycline transactivator encoded downstream of the ubiquitin promoter is bound to the tetracycline analogue doxycycline (Gossen & Bujard 1992). Thus, once cells were transduced, a single provirus encoded both the expression cassettes described above, and upon addition of doxycycline, expression from the CMV minimal promoter commenced. The insert expression in this system proved to be very tightly controlled as no expression could be detected in the absence of doxycycline either by measuring GFP fluorescence or by anti-HA immunoprecipitation and SDS-PAGE after metabolically labeling the infected cells. In contrast with the classical repressor system, the transactivator system allowed expression to be gradually controlled by increasing amounts of doxycycline, displaying a relatively broad dynamic range (Figure 4.1).

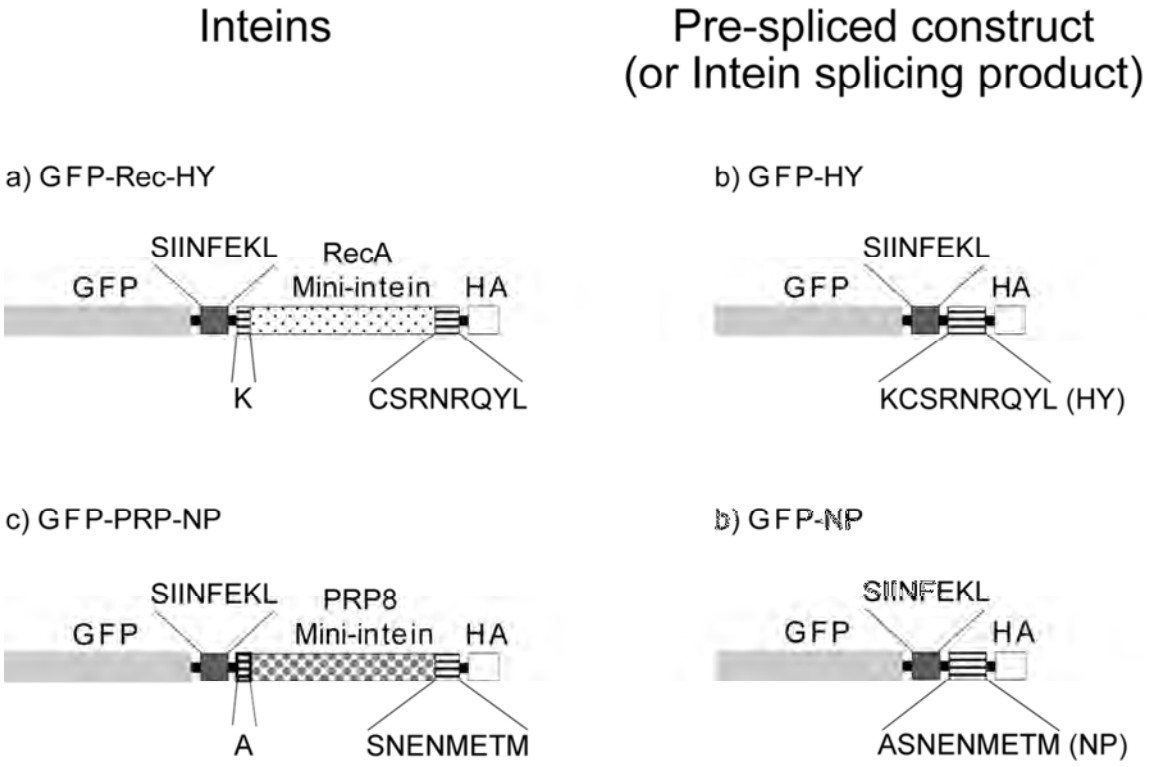

Figure 3.6 Schematic of the lentiviral constructs. Inserts used to transduce the E36 antigen presenting cells. Note that the product of the pre-spliced construct is the same as generated by intein splicing. The positions of the class I epitopes SIINFEKL (S8L), KCSRNRQYL (K9L), and ASNENMETM (A9M) are shown relative to GFP, HA tag, and the two different inteins. The black horizontal bars between boxes represent short linkers.

3.6 Splicing Kinetics

The kinetics of intein splicing *in vivo* were assessed by pulse-chase. E36 cells infected with the lentiviral constructs described in Figure 3.6 were subjected to a short metabolic labeling and the label was chased for increasing time periods. After immunoprecipitation with anti-HA or anti-GFP antibodies and SDS-PAGE two major bands were observed corresponding to the predicted molecular weights of the spliced and unspliced constructs. As expected, no splicing was observed in cells infected with the N3 mutant versions of either intein; at the latest time point all the immunoprecipitated protein co-migrated with the unspliced intein band (Figure 3.7). The splicing kinetics were substantially faster for the *Pch* PRP8 infected cells than for the *Mtu* RecA infected cells, as revealed by quantification of band densities after pulse-chase (Figures 3.8 and 3.9). In the case of *Pch* PRP8 infected cells, even when a short three minute pulse was applied, a large fraction was already in the spliced form (Figure 3.8). This was in stark contrast to the *Mtu* RecA infected cells, in which virtually no splicing took place until 20 minutes after labeling had ceased. This difference in splicing kinetics will prove useful in establishing whether presented epitopes are preferentially drawn from proteins shortly after their translation: if the contribution to presentation were mainly from species translated within a very short period from their degradation, the *Pch* PRP8 intein infected cells would show higher presentation levels compared to their pre-spliced counterpart than the *Mtu* RecA infected cells, since splicing and therefore generation of the epitope would be a

rare event in recently synthesized *Mtu* RecA intein proteins by virtue of the slower splicing kinetics.

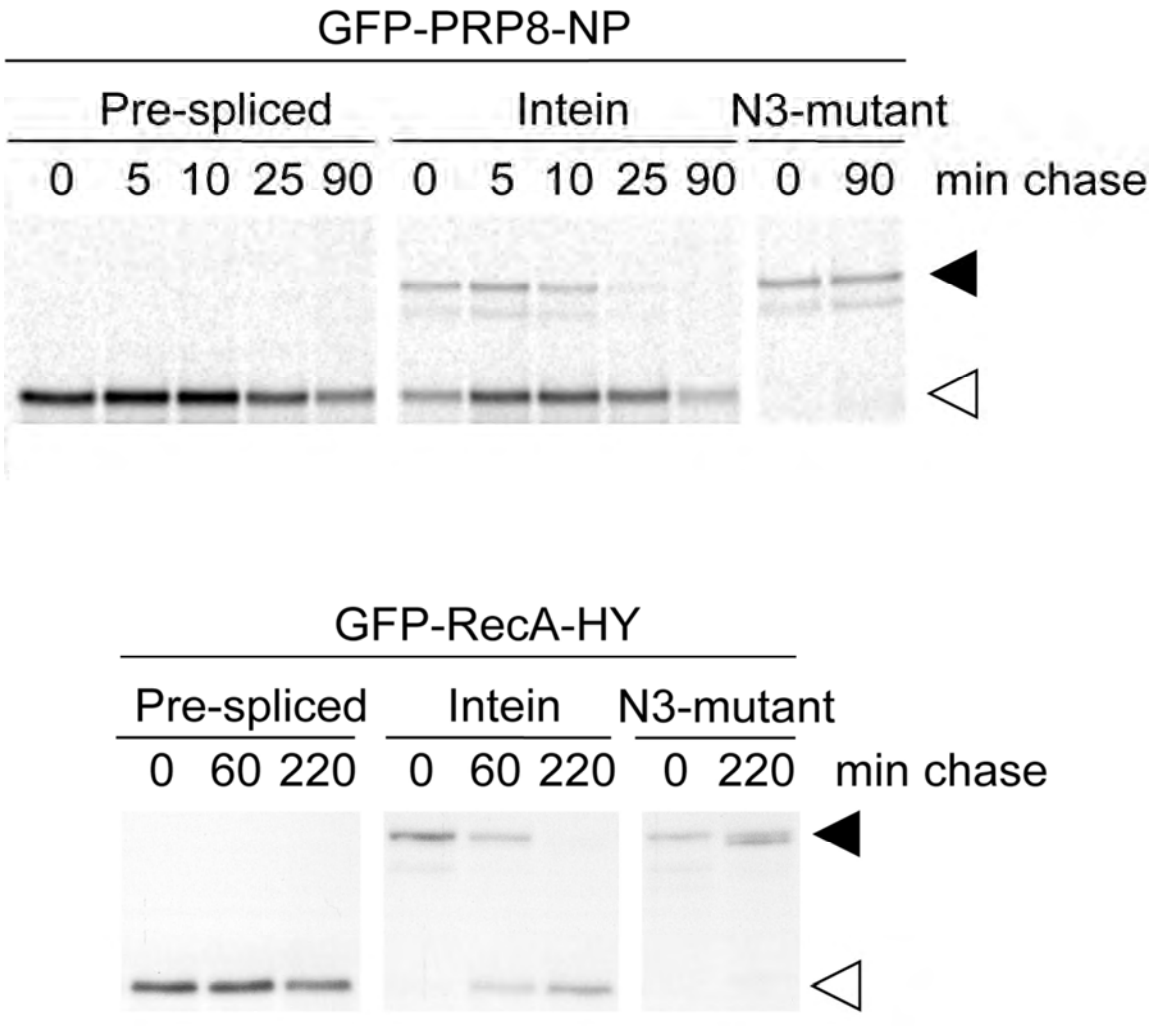

Figure 3.7 The N3 mutant versions of either intein do not splice. Autoradiogram after SDS-PAGE and anti-GFP immunoprecipitation of lysates from GFP-Rec-HY lentivirus infected E36 cells subjected to [^{35}S]-Met/Cys pulse label followed by a "cold" chase. The unspliced intein is indicated with a black arrowhead, and the spliced version with an open arrowhead.

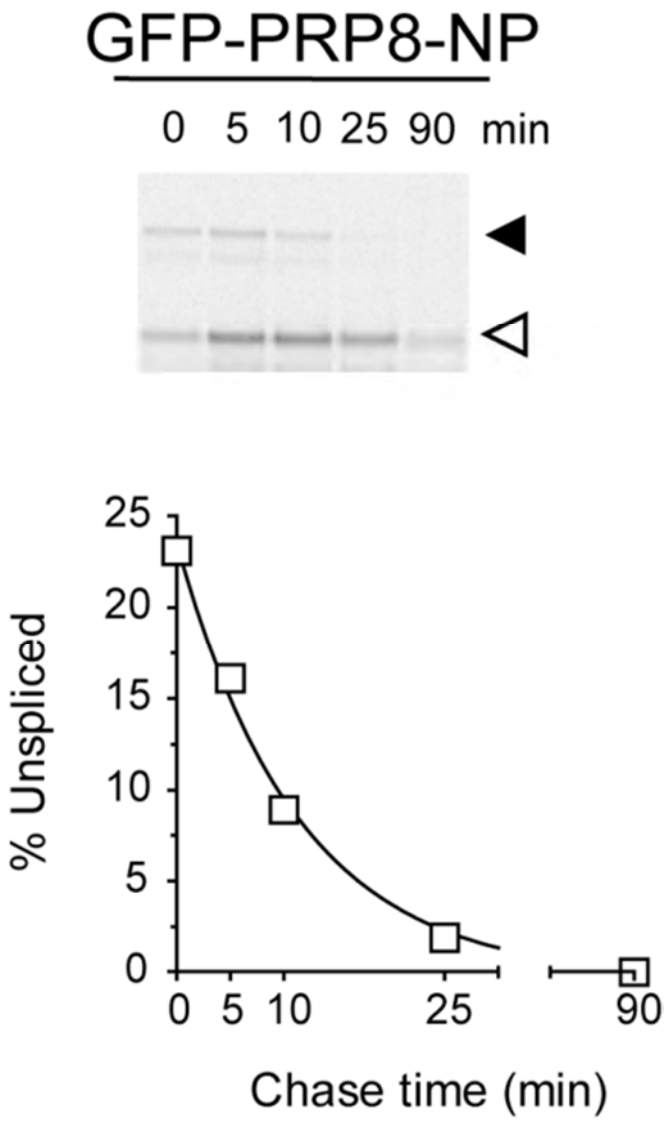

Figure 3.8 Splicing Kinetics of the *Pch* PRP8 intein. Autoradiogram after SDS-PAGE and anti-HA immunoprecipitation of lysates from GFP-PRP-NP lentivirus infected E36 cells pre-treated with epoxomicin (5 μM, 2h) and subjected to [^{35}S]-Met/Cys pulse label followed by a "cold" chase. The unspliced intein is indicated with a black arrowhead, and the spliced version with an open arrowhead. On the bottom: densitometry quantification of the bands on the autoradiogram above.

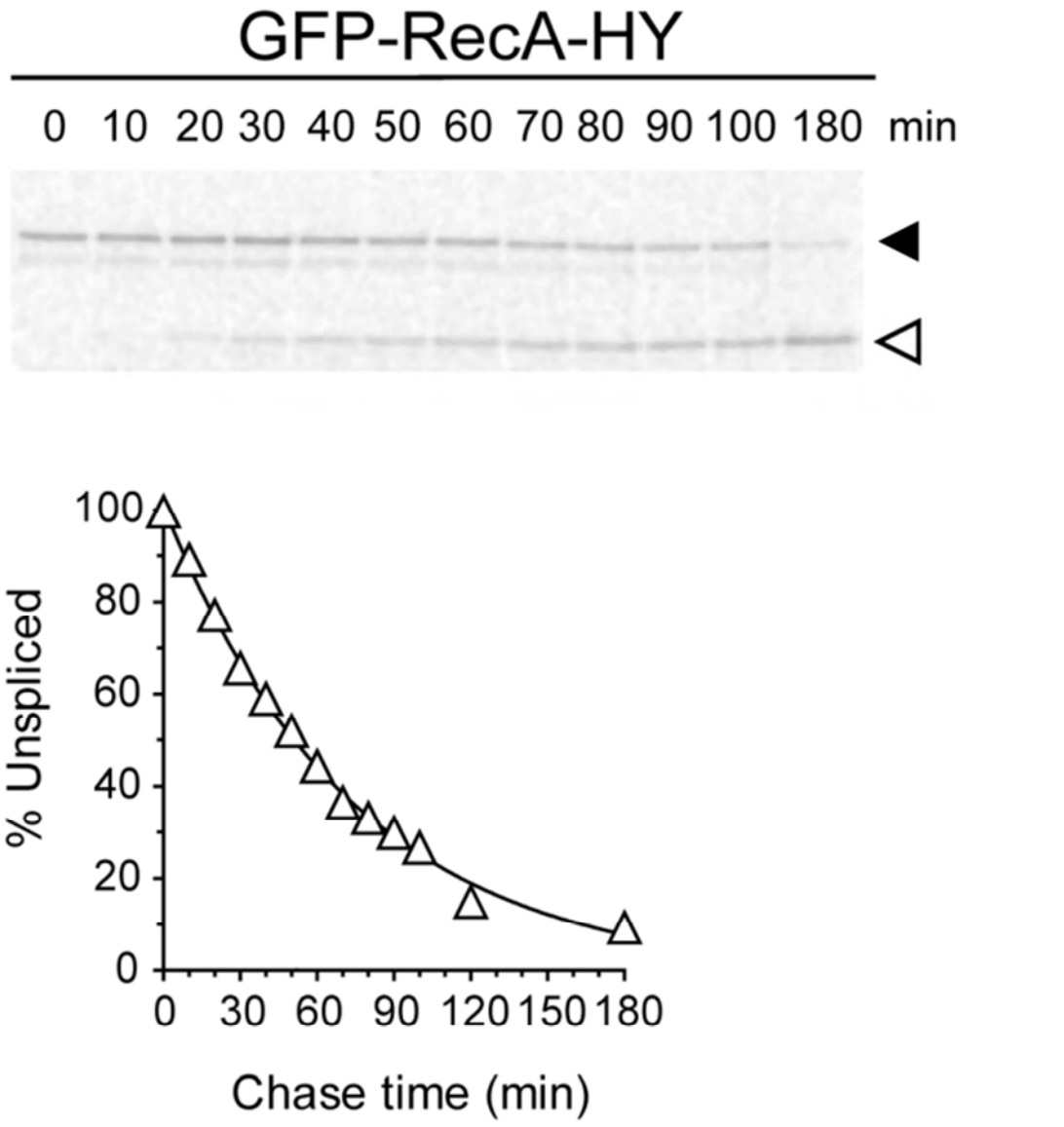

Figure 3.9 Splicing Kinetics of the *Mtu* RecA intein. Autoradiogram after SDS-PAGE and anti-HA immunoprecipitation of lysates from GFP-Rec-HY lentivirus infected E36 cells pre-treated with epoxomicin (5 μM, 2h) and subjected to [^{35}S]-Met/Cys pulse label followed by a "cold" chase. The unspliced intein is indicated with a black arrowhead, and the spliced version with an open arrowhead. On the bottom: densitometry quantification of the bands on the autoradiogram above.

Given the kinetics observed for intein splicing, it appears likely that the slowing splicing intein (RecA) will introduce a delay in the generation of the spliced product. This would be equivalent to slowing down the appearance rate of the protein substrate for epitope production. If we consider comparing epitope production from intein containing constructs to epitope production from pre-spliced constructs, this extra process should be taken into account and corrected for, since at early time points the difference in levels of pre-spliced versus spliced protein will likely be significant. In order to correct for this factor, a computer model was utilized to quantify the delay in the generation of spliced protein as time goes by. The model and the conclusions derived from it are presented in Chapter VI of this dissertation.

3.7 Outstanding Questions and Future Applications

I have shown in this chapter that inteins can in some cases splice in mammalian cells when produced from expression cassettes. The splicing has been shown to occur at different rates depending on the nature of the intein itself as well as on the flanking exteins. There are however a few outstanding questions and possible applications that could be addressed in the future.

Although only a very limited number of inteins have been tested, it is likely that other inteins will also be able to splice in mammalian cells. This prompts the question of what the kinetics of splicing of different inteins would be. It would be interesting if a set of inteins with gradually faster or slower splicing kinetics could be obtained. With such a set, a more robust correlation may be obtained between splicing rate and presentation of splice-dependent epitopes. In addition, more slowly splicing inteins could help rule out more definitely the possibility that the split epitope is generated before fusion protein acquires a completely folded and functional state.

In this dissertation mini-inteins have been used instead of full-length inteins. This is advantageous in this case because it makes the constructs considerably smaller while retaining the splicing activity of the intein. There are other situations however, in which it would be interesting to use inteins to deliver cargo. For example, the homing endonuclease coding sequence that has been deleted in the constructs shown here, could be instead replaced with a reporter gene, and the intein fused to a sequence encoding a protein of interest. Thus, after the fusion protein is synthesized the intein with the reporter protein would be excised from the protein of interest. This would be useful in situations where one wants to use the reporter gene to obtain a precise estimate of a gene of interest expression, but a fusion protein encompassing the protein of interest and the reporter protein is not functional or is not targeted to the appropriate compartment. The current systems utilized for this purpose are based on dual promoters, bicistronic mRNAs

or on the 2A peptide system. All these systems are problematic in that the stoichiometry of the two proteins encoded is not even and it may vary under different circumstances. For example, in situations of cellular-stress IRES-dependent translation can be enhanced while cap-dependent translation is inhibited (Fernandez et al. 2001; Lewis et al. 2008). Dual promoter systems use a different promoter for each of the transcripts often leading to uneven expression. The 2A peptide system (Szymczak et al. 2004) relies on short peptides derived from the *picornaviridae* family that cause ribosomal skipping and ultimately the peptide bond is not formed while translation continues 3' of the mRNA (Donnelly et al. 2001). Of these systems, the 2A peptide system is the only one where even stoichiometry of the reporter protein and protein of interest can be achieved, although some fusion proteins can be observed (Provost et al. 2007). It is not known whether the proposed intein system for tandem protein expression would be more efficient than the 2A peptide system, and therefore it remains as a possible alternative.

CHAPTER IV: ANTIGEN PRESENTATION OF SPLICING-DEPENDENT EPITOPES

Lentivirus-infected E36 cell populations were either sorted by FACS or positively selected using magnetic beads. Populations with similar GFP MFI after maximal induction were recovered. For the *Pch* PRP8 constructs, the infection efficiency was low and matched expression clones were isolated by limiting dilution. In an effort to quantify the levels of presentation in cells infected with intein encoding viruses so that they could be compared to their pre-spliced counterparts, measurements were made using either T cell hybridomas or the 25.D1-16 monoclonal antibody which recognizes the S8L epitope in the context of H-2K^b (Porgador et al. 1997). It soon became apparent that there were substantial differences in presentation even between cell clones infected with the same virus or in different experiments. This variability would be detrimental for our purpose of making accurate comparisons, and therefore appropriate controls were sought after in order to minimize it. As a first attempt to normalize the antigen presentation measurements, the GFP mean fluorescent intensities (MFI) were examined (Figures 4.1 and 4.2).

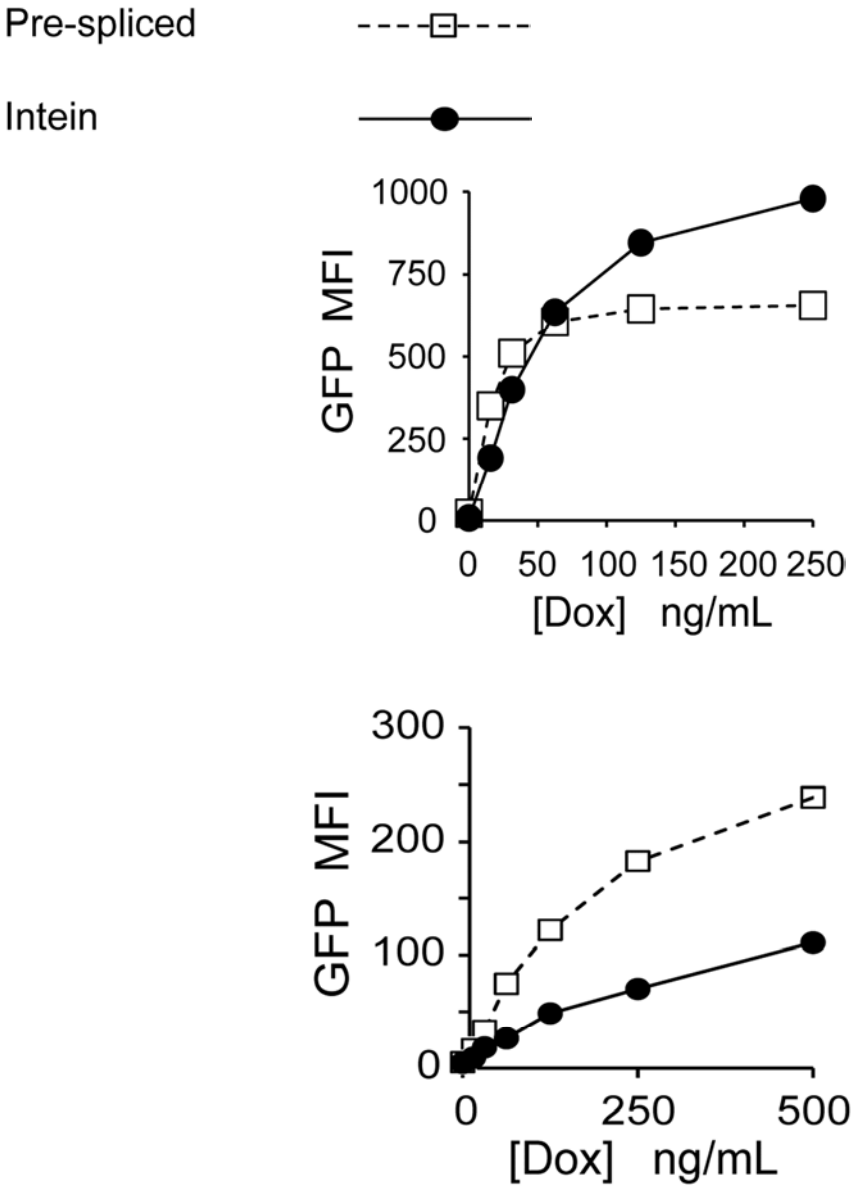

Figure 4.1 Dox titratable GFP production. GFP MFI measured by flow cytometry in cells treated with serial dilutions of doxycycline for twenty-four hours. Top: cells infected with GFP-PRP-NP or GFP-NP. Bottom: cells infected with GFP-Rec-HY or GFP-HY.

The magnitude of the GFP MFI and the kinetics of GFP accumulation were somewhat different when comparing pre-spliced to intein constructs. This can probably be attributed to clonal or population differences, since the lentiviral copy number in the genome can vary. Nevertheless, valid comparisons could be made between intein and pre-spliced expressing cells by selecting doxycycline concentrations that yielded similar GFP MFIs. In addition, an internal control was built into the antigen constructs that allowed comparisons within the same cell: measuring the splicing dependent epitopes (HY or NP) relative to a splicing-independent epitope—S8L—which controls for potential clonal variation in other processes involved in antigen presentation, such as components of the ubiquitin proteasome pathway, transporters, or MHC class I chain synthesis.

The control epitope S8L presentation however, is H-2K^b-restricted, as opposed to the H-2D^b-restricted presentation of both the intein-dependent epitopes, HY and NP, hence it was important to monitor H-2K^b and H-2D^b surface expression to ensure comparable levels in cells infected with the intein versus pre-spliced construct encoding viruses. Flow cytometry measurements were made regularly to monitor this.

Figure 4.3 shows that the presentation of S8L on H-2K^b was also titratable with varying doxycycline concentrations. A dose response pattern was observed after induction of the constructs' expression using serial dilutions of Dox for twenty-four hours followed by

surface staining with 25.D1-16 and flow cytometry, or by a hybridoma assay in the presence of brefeldin A. This experiment validated the use of S8L as a control since the range of doxycycline concentrations at which S8L presentation displayed a linear range was compatible with the doses used for NP or HY assays (Figure 4.3).

The presentation of HY, NP, and S8L epitopes was inhibited by the specific proteasome inhibitor epoxomicin (Sin et al. 1999) as shown in Figure 4.4, indicating that after splicing the resulting protein is turned over via the classical ubiquitin-proteasome pathway.

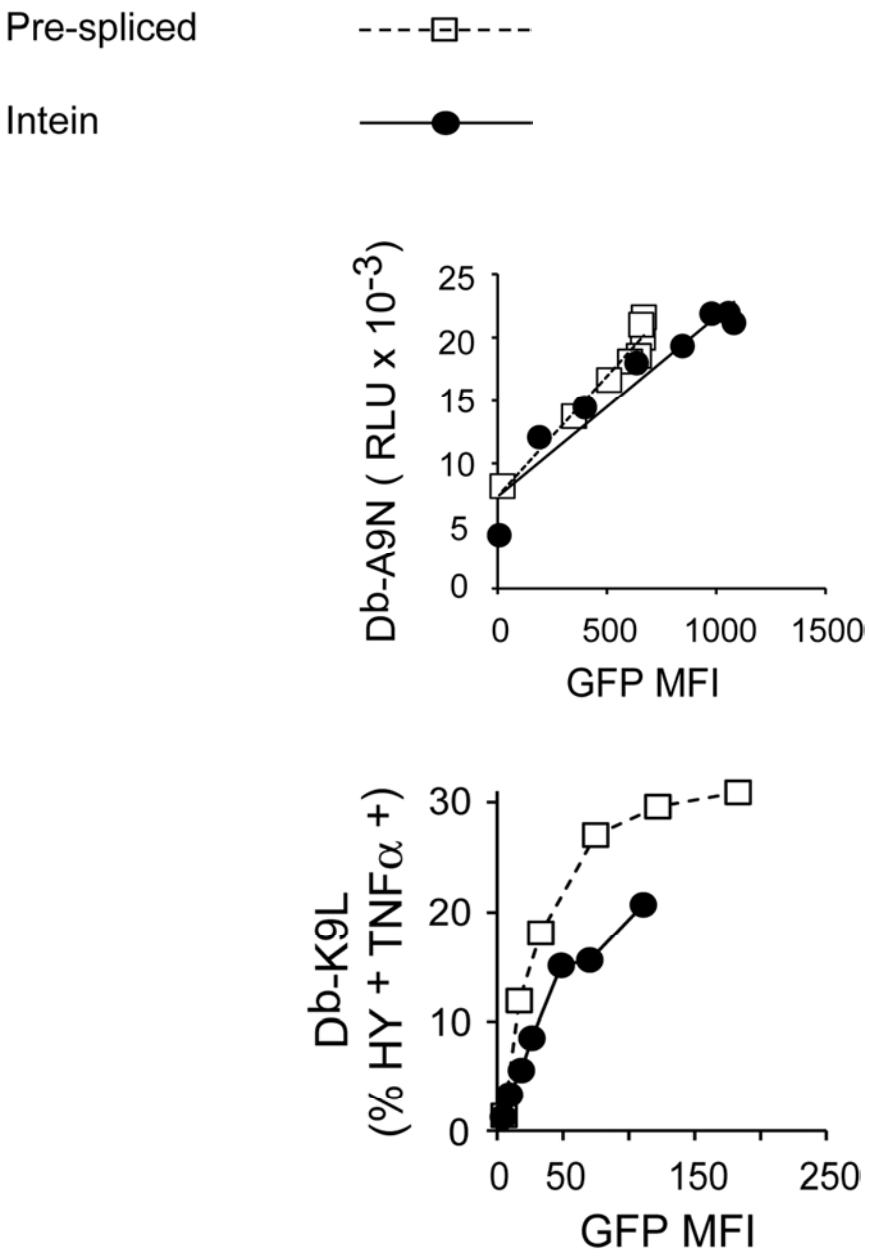

Figure 4.2 Splicing dependent epitope presentation twenty-four hours after induction. Presentation of NP epitope measured by 12.64-Luc hybridoma assay (top) in cells infected with GFP-PRP-NP or GFP-NP vs. GFP MFI, or of HY epitope (bottom) measured by TNFα ICS in cells infected with GFP-Rec-HY or GFP-HY.

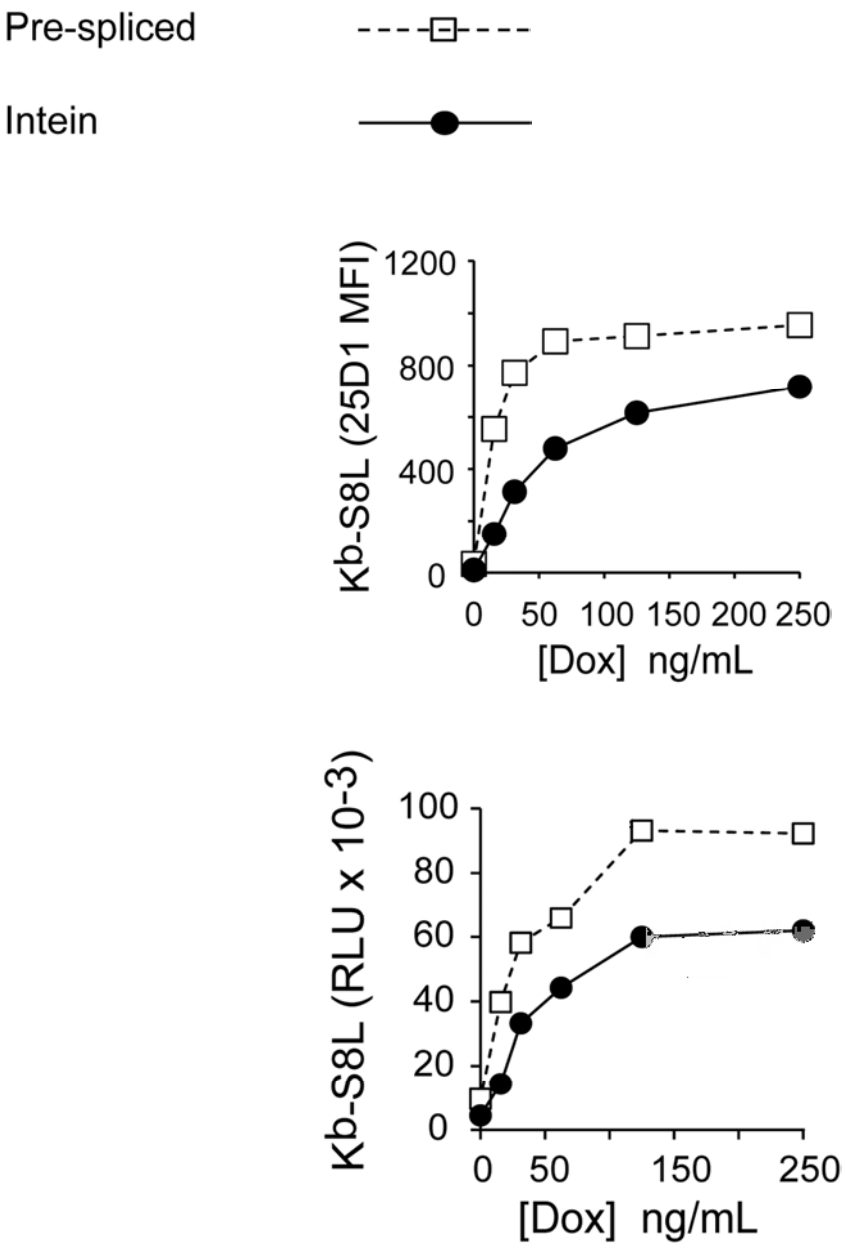

Figure 4.3 Dox titratable S8L presentation. Presentation of S8L epitope on H-2K^b twenty-four hours after induction measured by flow cytometry (top) in cells infected with GFP-PRP-NP or GFP-NP and stained with 25.D1-16, or (bottom) in cells infected with GFP-Rec-HY or GFP-HY and used as APCs for an RF33-Luc hybridoma assay.

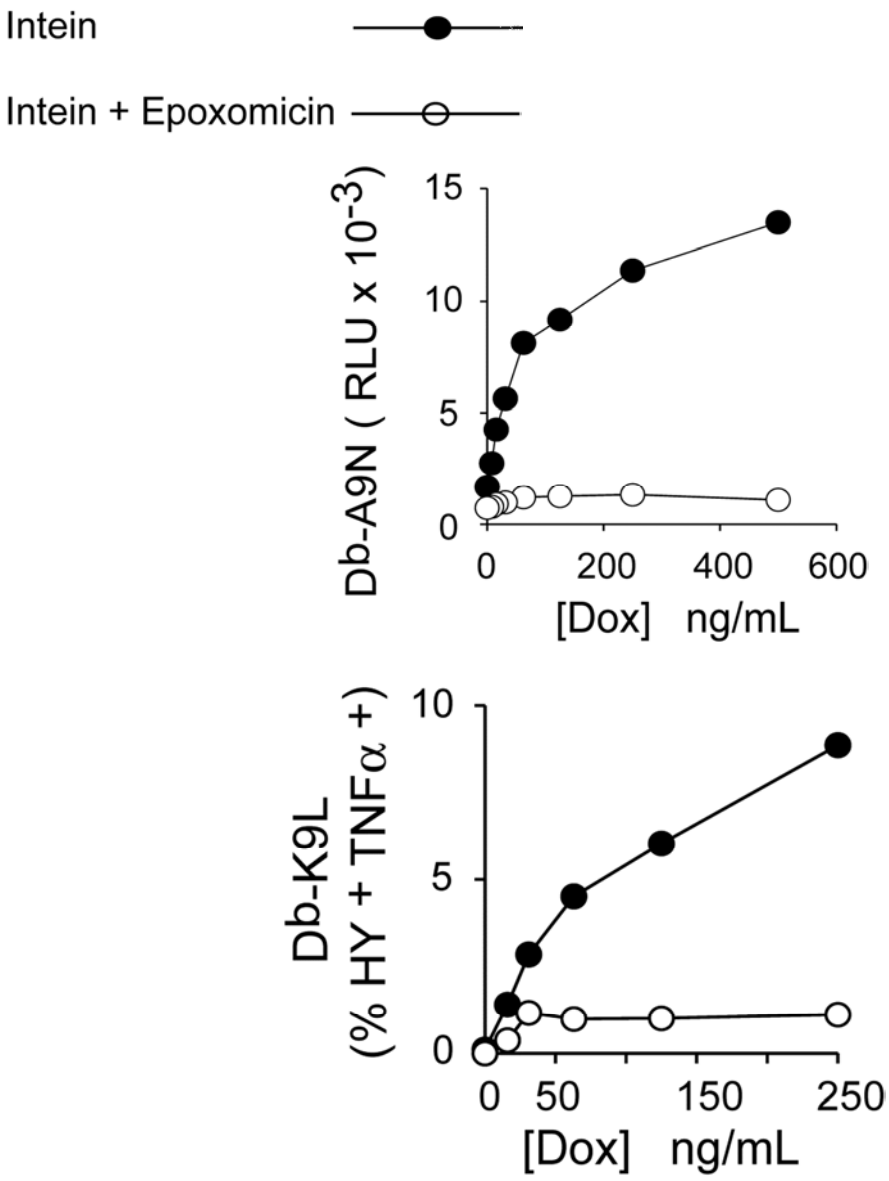

Figure 4.4 Splicing dependent epitope presentation is abrogated by proteasome inhibition. Presentation of NP epitope (top) vs. [Doxycycline] in cells infected with GFP-PRP-NP with or without 5 μM epoxomicin six hours after induction; or presentation of HY epitope (bottom) vs. [Doxycycline] in cells infected with GFP-Rec-HY or GFP-HY four hours after induction.

Representing the splicing-dependent epitope relative to S8L—as a control for expression and presentation differences—over a range of Dox concentrations yields a scatter plot that can be fitted to a straight line (Figure 4.5). The slopes of such lines represent the level of splicing-dependent epitope presentation relative to the level of control epitope presentation. The values of these slopes were used as a normalized figure reflecting the levels of presentation that can be used to compare presentation between cells transduced with intein or pre-spliced encoding viruses.

At steady state, twenty-four hours after induction, the slopes were almost identical when comparing intein versus pre-spliced both for *Pch* PRP8 and for *Mtu* RecA (Figure 4.5). In other words, the presentation of the splicing-dependent epitope was as efficient as the one that did not require splicing. Therefore, mature proteins are by no means a negligible source of MHC class I presented epitopes. This also clearly points at a minor or non-existent contribution from DRiPs to presentation at steady-state.

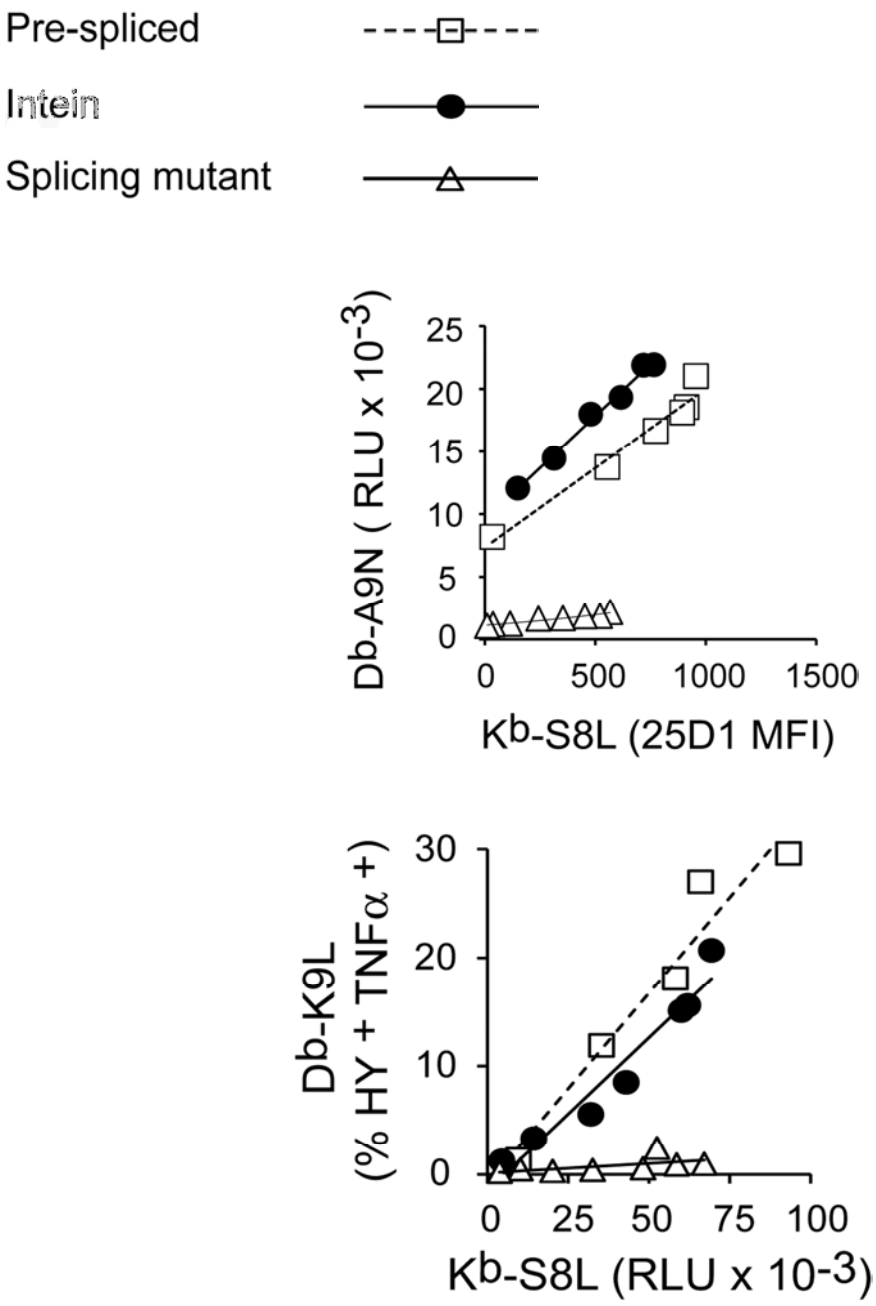

Figure 4.5 Splicing dependent epitope presentation relative to control presentation. Presentation of NP epitope (top) vs. S8L epitope in cells infected with GFP-PRP-NP or GFP-NP or presentation of HY epitope (bottom) vs. S8L epitope in cells infected with GFP-Rec-HY or GFP-HY twenty-four hours after induction**.** Regression lines are shown.

CHAPTER V: PRESENTATION KINETICS

In the previous chapter the presentation levels at steady state were shown to rely heavily on mature proteins as opposed to DRiPs. This begs the question of whether the postulated importance of DRiPs in the early phases after viral antigen expression is actually true. The presence of a Dox-inducible promoter in the viral constructs used allowed time course measurements of antigen presentation on MHC class I as described. As before, measurements of both the splicing-dependent and the control splicing-independent epitope presentation were made and the data represented as the slopes of the regression lines obtained after plotting these two parameters.

The comparison between pre-spliced and *Pch* PRP8 intein infected cells showed that even as early as two hours after induction, the difference in presentation slopes was small, and as the induction time increased the difference between intein and pre-spliced was reduced until it was negligible (Figure 5.1).

In the case of the infections with viruses encoding the *Mtu* RecA construct or the pre-spliced counterpart, the situation was slightly different: there was virtually no presentation from the cells infected with the intein construct encoding virus at the two

hour time point, and even at the four hour time point the difference with the presentation levels from the pre-spliced was substantial. It took up to twelve hours for the presentation levels from pre-spliced and intein to be equal (Figure 5.2).

The results from the cells infected with the *Mtu* RecA construct encoding virus could lead to the interpretation that DRiPs are the major contributor in the early phase of antigen expression and although turnover from mature proteins does contribute to presentation, its contribution is only appreciable long after antigen expression has commenced. However, the fact that presentation from the *Pch* PRP8 construct did occur very early on and at a substantially high level points at an alternative interpretation: there is a delay in the generation of the peptide epitope from the time of protein synthesis in the constructs that contain an intein by virtue of the fact that the splicing reaction occurs at a certain rate and the epitope is not formed until splicing is completed. Therefore the amount of substrate available for degradation and presentation at the early times after expression induction is expected to be lower for the intein containing constructs than for the pre-spliced constructs, and this will be reflected on lower presentation levels from the intein containing constructs early after protein synthesis starts. This interpretation is consistent with the fact that the differences observed in presentation levels at the early time points seem to correlate with the splicing kinetics; in other words the differences between pre-spliced and intein for the rapidly splicing intein (*Pch* PRP8) were smaller than for the intein that splices more slowly (*Mtu* RecA). In order to ascertain whether

this explanation is plausible it was necessary to estimate what the expected differences in peptide epitope availability would be for pre-spliced and intein containing constructs along time. Since the splicing kinetics have been described for these two inteins, the expected rate of appearance of the spliced product could be factored into a mathematical model to obtain a prediction of the expected difference in presentation between pre-spliced and intein containing constructs at any given time.

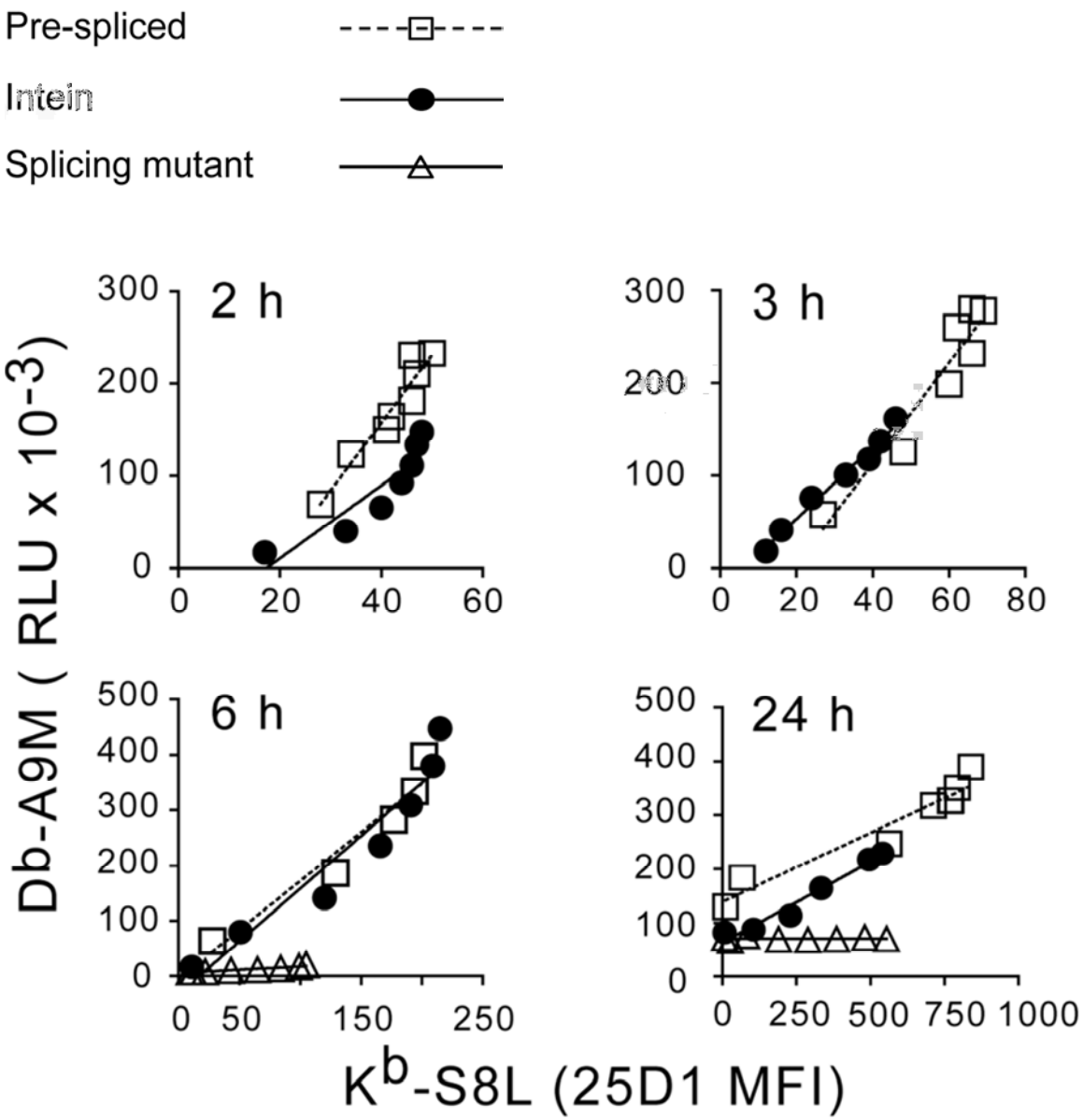

Figure 5.1 Time course of A9M presentation from Pre-spliced, intein and splicing mutant. Measurements and linear regression of surface presentation of the A9M epitope versus the S8L epitope in cells infected with GFP-PRP-NP or GFP-NP for the different times shown. A9M measured by 12.64-Luc hybridoma assay, and S8L measured by 25.D1-16 staining and flow cytometry.

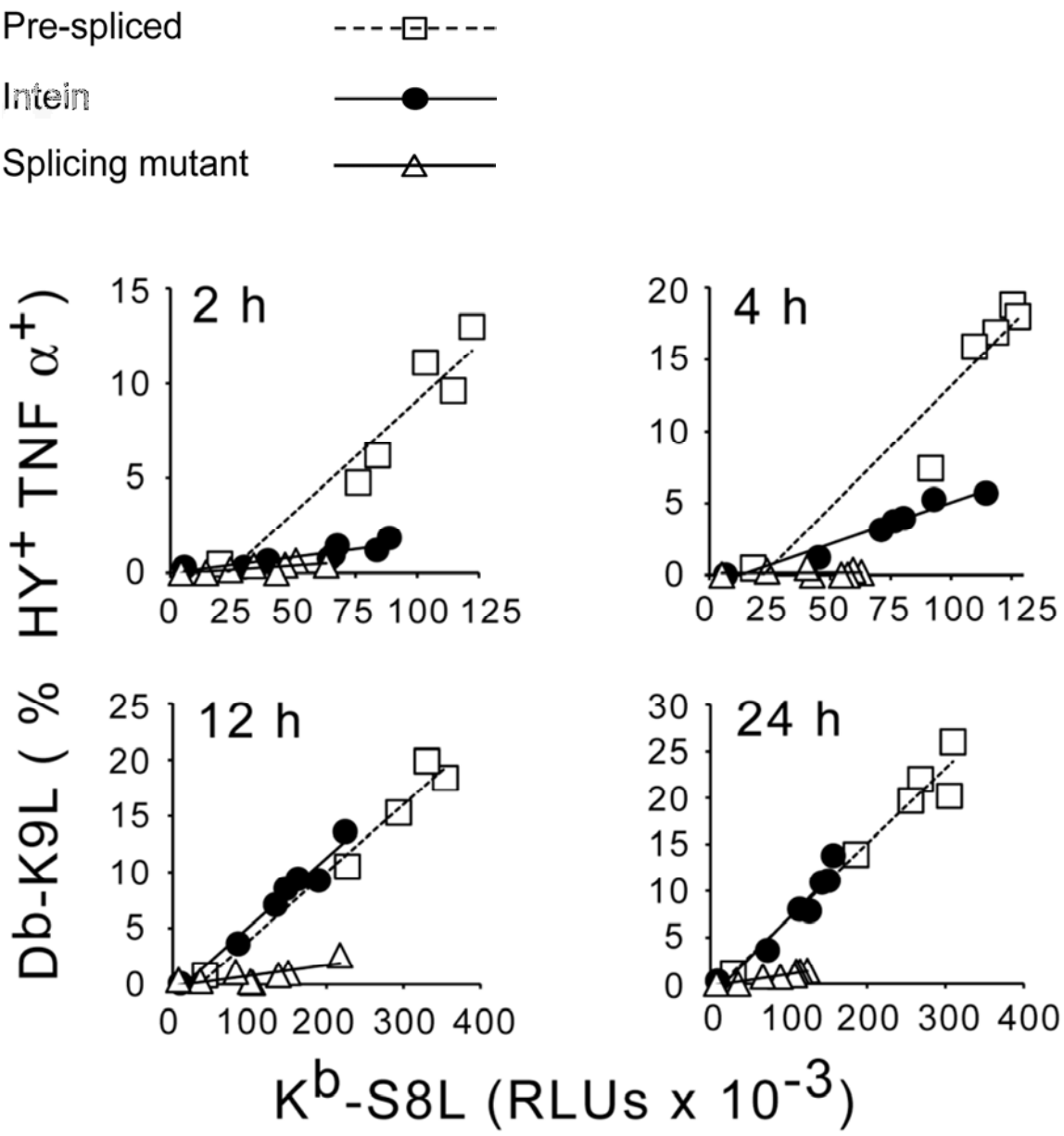

Figure 5.2 Time course of K9L presentation from Pre-spliced, intein and splicing mutant. Measurements and linear regression of surface presentation of the A9M epitope versus the S8L epitope in cells infected with GFP-Rec-HY or GFP-HY for the different times shown. K9L measured by TNFα ICS, and S8L measured by RF33-Luc hybridoma assay.

CHAPTER VI: MODELING PRESENTATION AT EARLY TIME POINTS AFTER TRANSLATION

The question of whether the differences in presentation levels observed in the previous chapter between pre-spliced and intein at the early time points can be attributed to the delay in the generation of the epitopes by splicing requires a precise prediction of what the presentation levels would be if DRiPs did not contribute to presentation when splicing rates were factored in. Mathematically modeling the processes involved in MHC class I antigen presentation could provide such predictions, and a comparison between the observed data and the predicted values would allow to determine what the contribution to MHC class I presentation of DRiPs versus mature functional proteins is. The KinTek Explorer application was used to generate the model. This software is designed to model chemical reactions after mixing the initial reagents, but the processes can be written in such a way that they mimic biological events.

Figure 6.1 shows a scheme of the processes that have been modeled to obtain the predicted values of antigen presentation. There is an initial notional pool of mRNA used to mimic translation in the cells after expression is induced, since any given mRNA molecule can be translated over and over, so it is not exhausted after a round of

translation. The rates of protein synthesis and splicing are also modeled with their values obtained from experimental data. The proteasomal degradation and peptide trimming are combined into one process to generate processing products. Finally, MHC-peptide complex formation and transport to the surface as well as removal of cell surface complexes are also included in the model. The synthesis and degradation rate values for the different species were obtained from flow cytometry experiments (Figure 6.2) or from constant metabolic labeling experiments (Figure 6.3). On Table 6.3 there is a detailed description of each of these processes and the rate values assigned to them.

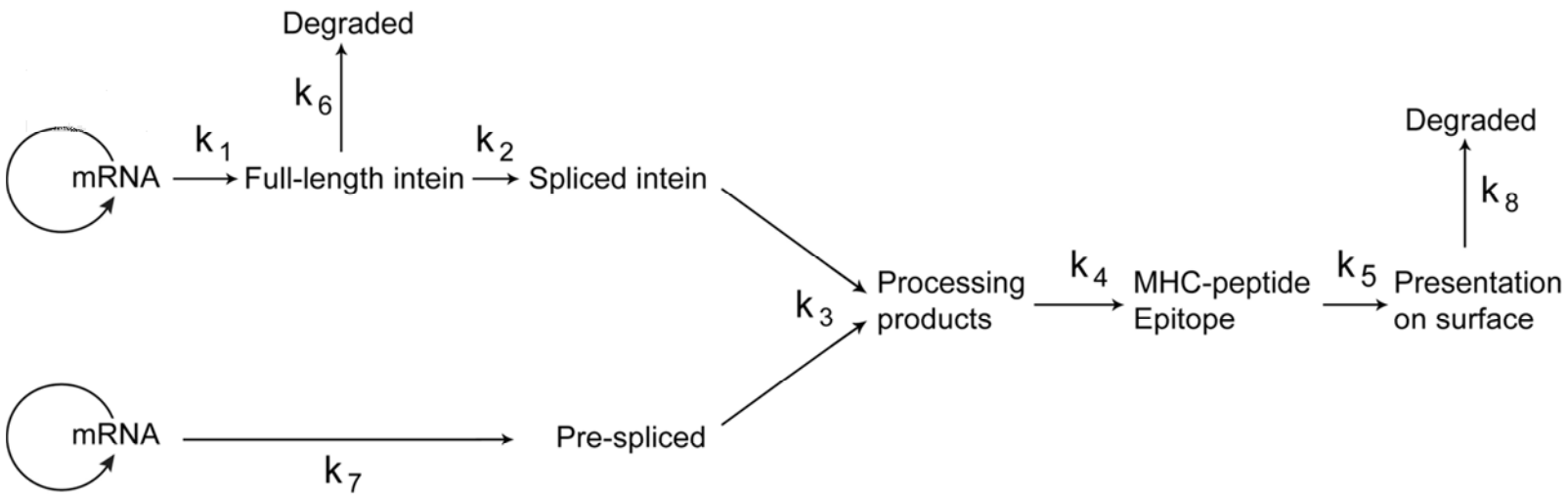

Figure 6.1 Scheme depicting the model inputted into KinTek Explorer software for data fitting. The different processes and constants are described on Table 6.3.

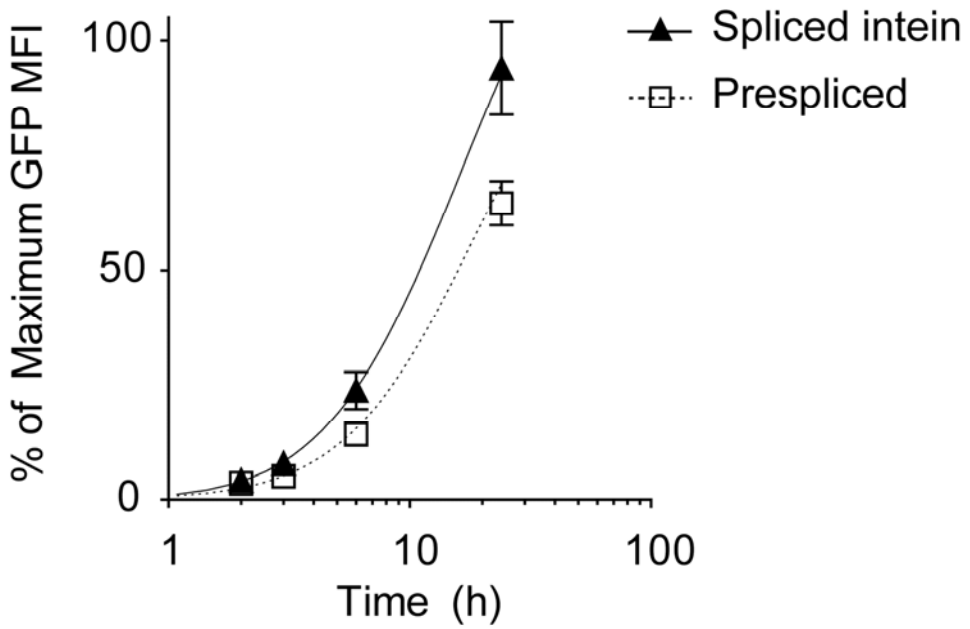

Figure 6.2 Data from cells infected with GFP-NP (Pre-spliced) or GFP-PRP8-NP (Intein) encoding viruses used for model fitting in KinTek explorer. Flow cytometry experiments measuring GFP content per cell (GFP mean fluorescence intensity). Lines are the result of fitting the KinTek explorer model to the observations (symbols). Symbols represent the mean of at least three independent experiments ± SD.

Table 6.1: MFI data from flow cytometry experiments.

Time (h)	Pre-spliced	Intein
2	3.7	4.4
3	5.3	8.2
6	15	25.2
24	68.8	100

Table 6.1 MFI data from flow cytometry experiments. % maximum GFP mean fluorescence intensity (MFI) data from E36 cells transduced with GFP-NP or GFP-PRP-NP constructs. The N3 mutant of the PRP8 construct is minimally fluorescent, thus the intein GFP MFI values were used to obtain the rates on Table 6.3. Averages of at least 3 independent experiments.

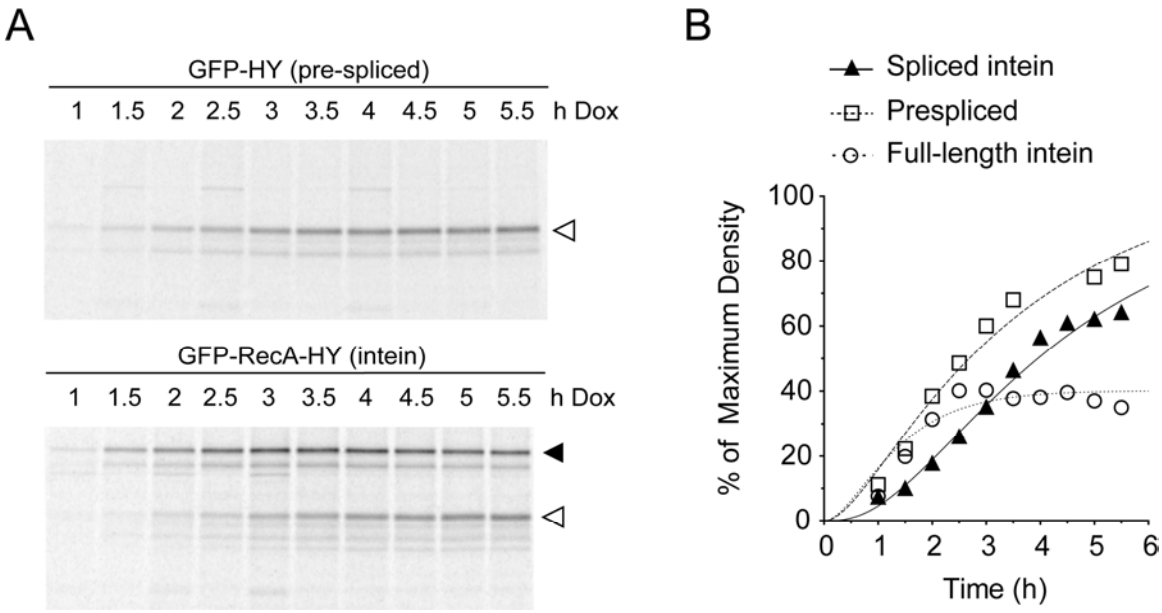

Figure 6.3 Data from cells infected with GFP-HY (Pre-spliced) or GFP-RecA-HY (Intein) encoding viruses used for model fitting in KinTek explorer. **A**, Constant metabolic labeling experiments. Autoradiograms after anti-HA immunoprecipitation at different times after expression induction and SDS-PAGE. Unspliced intein band: black arrowhead, and spliced product band or Pre-spliced band: open arrowhead. **B**, KinTek fit (curves) of the band densities in A (symbols). Symbols represent average values of three independent experiments.

Table 6.2: **Band densitometry data from continuous labeling experiments**.

Time (h)	Full-length intein	Spliced intein	Pre-spliced
1	8	8	11
1.5	20	10	22
2	31	18	38
2.5	40	26	49
3	40	35	60
3.5	38	46	68
4	38	56	66
4.5	40	61	64
5	37	62	75
5.5	35	64	79

Table 6.2 Band densitometry data from continuous labeling experiments. E36 transduced with the GFP-RecA-HY construct. Values represent % maximum band density from SDS-PAGE autoradiograms (see Methods). Averages of three independent experiments.

Table 6.3: Parameters from KinTek explorer simulation experiments.

Reaction	Constant	Value	
		RecA-HY	PRP-NP
Intein synthesis	k_1	0.91 h^{-1}[a]	0.17 h^{-1}[b]
Pre-spliced synthesis	k_7	0.69 h^{-1}[a]	0.13 h^{-1}[b]
Full-length Intein degradation	k_6	0.39 h^{-1}[a]	0.06 h^{-1}[b]
Pre-spliced degradation	k_3	0.31 h^{-1}[a]	0.07 h^{-1}[b]
Intein Splicing	k_2	0.72 h^{-1}[c]	5.42 h^{-1}[c]
Spliced product degradation	k_3	0.31 h^{-1}[a]	0.07 h^{-1}[b]
Epitope Processing	k_4	0.001 – 1 h^{-1} [d]	
MHC I complex transport	k_5	45-90 min[e]	

Table 6.3 Parameters from KinTek explorer simulation experiments. GFP-HY and GFP-RecA-HY constructs. The source of the values is detailed below.

a) KinTek fit of densitometry data from Figure 6.3 and Table 6.2

b) KinTek fit of GFP fluorescence data from Figure 6.2 and Table 6.1

c) GraphPad Prism k value from fitting exponential decay curves to pulse-chase data (Figures 3.3 and 3.4)

d) This range was obtained from KinTek's FitSpace computation (Johnson et al. 2009a). It shows there is no effect of this process on the presentation ratio over a very wide range of values.

e) A 45-90 minute delay from epitope processing to cell surface presentation was estimated. Values within this range are reported in the literature (Zhang et al. 2011; Hurtado et al. 2011). In a study using mouse fibroblasts (Zhang et al. 2011), the half time of K^b trafficking through the ER was around 30 minutes, with completion in 2 hours. Another study with human cells (Hurtado et al. 2011) showed it took 35-60 min for MHC-I complexes already in the Golgi and ER to reach the cell surface.

The model includes synthesis, splicing, processing, and presentation steps (Figure 6.1), with rates derived from the literature, our experiments (Figures 3.3, 3.4, 6.2, and 6.3), or a range of values derived from the KinTek software fit (Table 6.3). For GFP-RecA-HY the lag in presentation of the splicing-dependent epitope shortly after induction (Figure 5.2) could be entirely accounted for by the delay in post-translational generation of the epitope due to the splicing reaction (Figure 3.9). Moreover, if this interpretation is correct, a slower kinetic of early presentation would be less apparent with an intein construct that spliced more rapidly (Figure 3.8), just as it was observed (compare GFP-RecA-HY, Figure 5.2, with the faster-splicing GFP-PRP8-NP, Figure 5.1).

All in all, no evidence has been found of a substantial contribution from DRiPs to the presentation of epitopes from cells infected with viruses encoding the model constructs, even at early time points. Thus I conclude DRiPs are not a preferential source of peptides for antigen presentation.

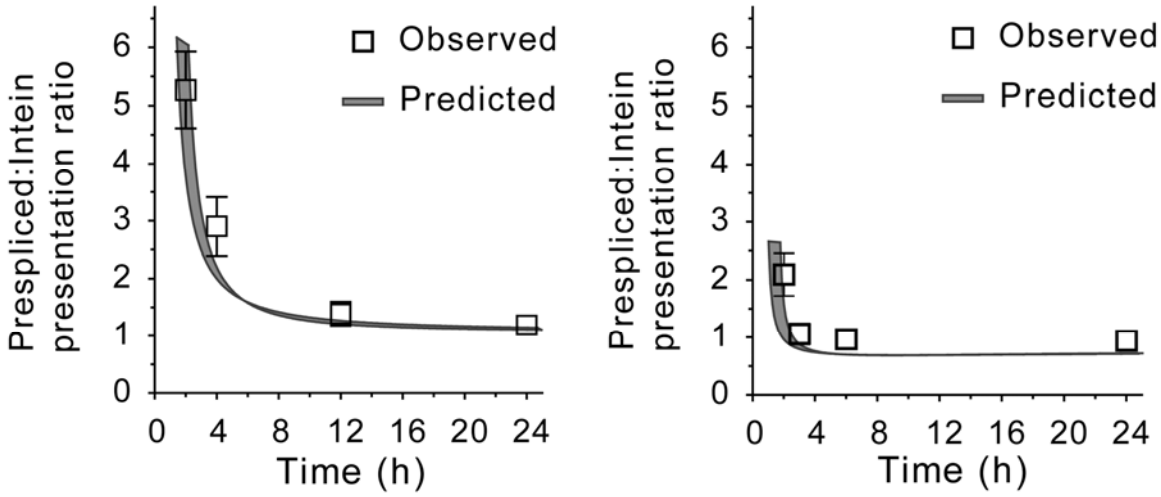

Figure 6.4 Time course and *in silico* predictions. Presentation from cells expressing the pre-spliced vs. the intein constructs (Left: GFP-RecA-HY; right: GFP-PRP-NP) as a function of Dox induction time. Observed points were calculated as the quotient of the slopes of the regression lines fitted in Figures 5.1 and 5.2**,** and plotted as mean ± SEM of at least three independent experiments. Predicted curves were obtained from the described KinTek Explorer simulation experiments.

CHAPTER VII: DISCUSSION

7.1 Results in the Context of the Literature

The results of the experiments presented in this dissertation did not confirm the outcome predicted by the DRiPs model (Yewdell et al. 1996): that the class I presentation of epitopes derived from mature functional species should have not been detected, or at least it should have been significantly smaller in magnitude to the presentation from species derived from DRiPs. Considering the properties of the model constructs described in this dissertation, the DRiPs model would predict a significantly lower presentation from the intein constructs than from the pre-spliced constructs. The steady-state data (Figure 4.2) clearly show there is indeed substantial presentation of the splicing dependent epitopes, and that the presentation levels on the cells infected with the intein-containing viruses is not different from the presentation levels on the cells infected with the pre-spliced construct viruses. Furthermore, early after antigen expression is induced the differences in presentation can be fully explained by the delay in the post-translational generation of the splicing dependent epitopes, both for a fast splicing (*Pch* PRP8) and a slow splicing (*Mtu* RecA) intein (Figure 6.4).

Most of the data supporting the DRiPs model relies on global protein synthesis inhibition. The approach described in this dissertation, on the other hand, is based on model substrates. By introducing the intein catalysis requirement for epitope formation I aimed at removing DRiPs from the equation. It is however very difficult if not impossible with today's technology to ascertain that every protein species with a spliced epitope is properly folded, since establishing protein conformation using classical means such as circular dichroism, nuclear magnetic resonance or crystallography would not be practical. Even considering this caveat and the possibility that in some instances a polypeptide with a spliced epitope could be triaged as defective and enter the DRiPs pool, the absolute lack of contribution by DRiPs observed with this system would have been unexpected if DRiPs were the exclusive or dominant source of peptides for MHC class I antigen presentation.

The results presented here however, are consistent with earlier experiments in which mature proteins loaded into the cytosol readily contributed to MHC class I antigen presentation (Okada & Rechsteiner 1982; Moore et al. 1988; Grant et al. 1995). The results in this dissertation not only confirm these previous findings, but extend them significantly by providing quantitative information about the contribution from the mature functional species of a given protein versus that from species of this same protein that are degraded before intein catalysis takes place; likely because of translation or folding mistakes. What is more, these experiments led to the quantification of the

contribution to antigen presentation from mature proteins that are synthesized by the presenting cell—as opposed to proteins supplied externally like in the earlier experiments—in a situation analogous to a viral infection. The earlier experiments with exogenous antigens could not exclude that the process was highly inefficient, nor whether the antigen that was presented came from defective molecules (e.g. denatured ones) in the inoculum. Therefore, while earlier experiments suggested that the cellular machinery has indeed the capacity to process and present mature proteins when externally provided in large amounts, this dissertation provides evidence supporting the degradation of endogenous mature proteins as a major source for MHC class I antigen presentation.

7.2 On the Linkage between Protein Synthesis and MHC Class I Presentation

The data provided in support of the DRiPs model and the data presented in this dissertation are clearly opposing. As described in the introduction chapter, much of the data supporting the DRiPs model relies on global protein synthesis inhibition. This approach is a dangerous one, since the collateral effects of stalling protein synthesis are manifold and thus control experiments must be carefully designed to ensure the effects observed after inhibition are not artificial.

In one of their experiments (Qian, Reits, et al. 2006), cells were infected with recombinant vaccinia virus (rVV) encoding a protein fused to an ovalbumin derived class I epitope (SIINFEKL), and surface MHC class I-SIINFEKL complexes were measured. When these cells were treated with the reversible proteasome inhibitor MG132 three hours post infection, and two hours later with the protein synthesis inhibitor cycloheximide while MG132 was washed off, a recovery in presentation even in the presence of cycloheximide was observed. This was ascribed to a burst in presentation from DRiPs that had accumulated during the MG132 treatment, although peptides from turnover of mature protein could have accumulated as well, but the authors assume the peptides generated from turnover in two hours would be insignificant. It is worth noting however, that it took one hundred minutes to start observing an increase in MHC-SIINFEKL and two hundred minutes to increase up to a modest level. It also took one hundred minutes from the initial rVV infection time until surface complexes are first observed, presumably because time is needed for DNA transcription, mRNA translation, peptide generation, and class I complex transport to the cell surface. Considering that cells had been under MG-132 treatment for two hours there should have been considerable DRiPs accumulation; one would expect class I presentation to have occurred much more efficiently than in the initial phase of the infection, since high levels of mRNA were already present and translated substrates (DRiPs) should have accumulated, and yet they observed only a slow and moderate increase in surface MHC-SIINFEKL complexes.

This suggests that the treatments applied may be affecting cell physiology and antigen presentation in additional ways that may confound the interpretation of the results. While cells were under cycloheximide treatment, processes other than peptide generation may be affected if they necessitate de novo protein synthesis, which would make it difficult to estimate if and how much peptide production does depend on protein synthesis. Newly synthesized class I heavy chains associate with the ER chaperone calnexin (Degen & Williams 1991), which in turn associates with TAP. The binding of beta-2 microglobulin is stabilized by peptide, and allows the complex to be released from calnexin (Rajagopalan & Brenner 1994). When beta-2-microglobulin is not present, class I heavy chains remain bound to calnexin (Rajagopalan & Brenner 1994) until they are eventually degraded, and the heavy chain-beta-2-microglobulin complex is very unstable in the absence of peptide (Sugita & Brenner 1994)

Therefore, a plausible alternative explanation for the observation that surface MHC class I complexes cease to appear after protein synthesis is inhibited could be that the complex formation requires de novo synthesis of class I heavy chain and beta-2-microglobulin molecules. After some time in the absence of new protein synthesis, the pre-existing heavy chain and beta-2-microglobulin would form class I complexes and would exit to the Golgi or be degraded (Rajagopalan & Brenner 1994); no further complexes would be formed even with a stable peptide supply from protein turnover.

This situation is reflected in the mentioned experiments (Qian, Reits, et al. 2006): upon MG132 wash and cycloheximide addition there is a small increase in MHC-SIINFEKL complexes that plateaus shortly afterwards. Moreover, the retardation observed in class I trafficking to the cell surface originally attributed to a diminished supply of peptides in the presence of protein synthesis inhibitors (Schubert et al. 2000), could in fact be accounted for by a requirement for de novo synthesis for complex formation.

Similarly, in experiments where cells were treated with ricin (Grant & Rock 1992) or cycloheximide (Donohue et al. 2006) before being exposed to exogenous native antigen (which obviously does not require synthesis by the cell), class I cross-presentation was abrogated. The main control that I have found absent from the cited experiments is aimed at ruling out the possibility that steps downstream in the pathway from peptide generation may be affected if they require protein synthesis. Data in the earlier literature pointing at such a possibility exists as described in the introduction of this dissertation, therefore it is likely that the MHC class I antigen presentation results obtained in experiments where protein synthesis inhibitors have been used are flawed and represent an artifact.

The TAP mobility study described in the introduction concluded that the majority of the TAP substrates were derived from newly synthesized proteins (Reits et al. 2000). The authors observed that in the presence of cycloheximide only thirty percent of the peptide transporting activity remained. This was attributed to an imminent reduction in peptide supply due to the decrease on the DRiP pool resulting from exposure to cycloheximide. However as discussed above, protein synthesis inhibition could also have an effect in presentation by preventing newly synthesized MHC class I molecules from being receptive to peptide. This possibility is hard to distinguish from a *bona fide* effect on peptide supply. Nevertheless the TAP mobility experiments presented a great opportunity to resolve this issue. The laboratory where these experiments were performed has shown proficiency in the synthetic antigenic peptide microinjection technique. Had they microinjected peptide at different concentrations and in the presence or absence of cycloheximide treatment, a comparison could have been made in terms of TAP mobility, thus confirming or ruling out an effect of global protein synthesis inhibition on MHC class I loading and on cell surface presentation. A similar control experiment was indeed performed but only at a single peptide concentration of 10 mM in the microinjection needle, and only in the presence of cycloheximide. This concentration is no doubt overwhelming and it should have been titrated down in order to make the experiment informative with regards to the question of whether there is an effect of global protein synthesis inhibition on MHC class I loading.

7.3 Examples of DRiPs-derived Epitopes

There are examples in the literature where the generation of individual epitopes appears to be dependent on *de novo* synthesis of their source protein. In the context of the LCMV infection (Khan et al. 2001), an epitope derived from the nucleoprotein showed a strong dependence on protein synthesis. It should be noted that there are seven known class I epitopes derived from the LCMV nucleoprotein in the mouse, and only one was linked to protein neosynthesis. It is not known whether all others were analyzed, but they could have been and most likely they were, therefore the vast majority of the epitopes derived from NP did not show a dependency on neosynthesis.

In the case of the Epstein-Barr virus, because of the special characteristics of its EBNA proteins, the possible dominance of DRiPs as a source of peptides for MHC class I presentation (Mackay et al. 2009) cannot be generalized, for the native form of this antigen may not be degraded via the ubiquitin-proteasome pathway. This is an unusual fact that could be a means of viral immune evasion. There is evidence that the degradation of the EBNA protein does not occur through the ubiquitin-proteasome pathway once the infection is established (Levitskaya et al. 1997; Sharipo et al. 1998; Heessen et al. 2002; Hoyt et al. 2006). Even mutants in which the glycine-alanine-rich domain (GAr) of EBNA-1 has been deleted (Daskalogianni et al. 2008) degradation might not proceed mainly through the ubiquitin-proteasome pathway, although this is

controversial. It has been pointed out that EBNA1 is in fact at least partly degraded in infected B cells through autophagy instead of through the usual ubiquitin-proteasome pathway (Leung et al. 2010). It is obvious that if the degradation of the mature protein by the proteasome is prevented with or without GAr, then most of the class I presentation will be forced to derive from DRiPs, therefore the apparent linkage between translation and presentation in this case is due to the special circumstances surrounding the degradation of the EBNA proteins

7.4 DRiPs as a Preferential Source of MHC class I Ligands

With regards to the mechanisms that would allow for DRiPs to be used preferentially there have been several models. In one case an increase in mis-aminoacylated tRNAs upon viral infection or exposure to interferon was reported (Netzer et al. 2009). This would lead to a significantly greater DRiP rate due to amino acid misincorporation, thus contributing to an increase in class I antigen presentation. Therefore, this mechanism would not imply that DRiPs are preferentially presented, but rather that their abundance increases with infection. It is however a noteworthy fact that in the lengthy literature concerning the identification of MHC class I epitopes, there is not a single case of amino acid misincorporation in the epitope itself, which seems inconsistent with protein species

with high rate of misincorporation being the principal source of peptides for presentation. Also, a study where proteins with mutations were assessed for their antigen presentation potential showed that in spite of the mutants' actual misfolding, their degradation was only slightly faster, and epitope production was not significantly enhanced (Golovina et al. 2005).

Because the model system described in this dissertation deals with defined epitopes in frame, it is not possible to quantify the contribution of out of reading frame peptides (Malarkannan et al. 1999) or the non-AUG initiation phenomena (Schwab et al. 2004) described in the introduction chapter. The preponderance of DRiPs may be magnified as a consequence of the effects that viral infections have on the fidelity of mRNA translation. Although I have used lentiviral vectors to express the constructs described here, the possible effects that the infection may have on the translational machinery will most likely be minimal, since the viruses used are non-replicative and they integrated in the cellular DNA well before the antigen presentation experiments were conducted. Thus, in this experimental system the contribution to MHC class I antigen presentation from alternative reading frames or non-AUG initiation cannot be established. It is possible that non-AUG initiation derived products might be an important contributor to MHC class I presentation under the circumstances discussed in the introduction chapter, namely viral infection and cellular stress. Nevertheless, this mechanism cannot explain a preferential use of peptides derived from DRiPs for MHC class I antigen presentation,

rather it might make peptides derived from DRiPs more likely to be presented by virtue of their increased abundance in a situation of viral infection or cellular stress. However, whether this increased contribution is significant is still to be determined.

Thus, a scenario where the relative contribution to MHC class I presentation from different sources is determined by the abundance of their degradation products, in contrast with a different scenario where there exists a specialized mechanism or compartment preferentially supplying peptides from defective proteins, would be in agreement with the views put forth in this dissertation.

Looking back at the results shown here, the products of the spliced inteins were relatively stable, and there was nevertheless abundant presentation of the epitopes they contained. This might seem counterintuitive at first glance, but if we consider the expression levels were high, even at a very small degradation rate, a significant supply of peptides could be contributed to the class I presentation pathway. In this regard it would be informative if we could compare constructs with different stability or a construct whose half-life could be modulated, such as the one described recently (Dolan et al. 2011).

To summarize, sixteen years after the DRiPs hypothesis was introduced, almost all of the supporting data is indirect and could be explained in alternate ways.

7.5 Direct Measurements by Mass Spectrometry

The contribution from mature proteins to the MHC class I pathway of antigen presentation was questioned in studies using SILAC where no correlation was observed in the presented epitope levels and the abundance of the corresponding source proteins in cells (Milner et al. 2006). The interpretation that this absence of correlation pointed at a predominance of DRiPs as a source for presented peptides is flawed, since it is not the abundance of the source protein but rather the turnover rate that determines the peptide availability to the pathway (Pratt et al. 2002). In other words, a very abundant protein that is very slowly turned over would generate many potentially presentable peptides per unit of time. When they did compare the turnover rate with HLA-derived peptide abundance (Milner et al. 2006) they interpreted that there was evidence for a DRiP-centric model: a biphasic pattern in the production of presented peptides was observed, and the early presentation wave was attributed to DRiPs. However, only seven peptides—three clear ones—displayed this biphasic pattern attributable to DRiPs, and most of their source proteins were part of multimeric complexes and likely the

appearance of peptides derived from them in the first phase could have been due to the degradation of the proteins before assembly into complexes even though they were not necessarily defective. This phenomenon is known to occur with members of multimeric complexes, e.g. the CD3 components (Alarcon et al. 1988). Finally and most important, although it was not pointed out in the paper, the data showed that the majority of presented peptides were labeled even ninety-six hours after the free labeled amino acids were chased from the cells. Unfortunately, in this study (Milner et al. 2006) the number of proteins for which a turnover rate could be obtained was rather low. It is expected that with newer technology this number could be increased substantially. Therefore the generation of presented peptides was not restricted to a short-lived DRiP pool but rather come from more long-lived proteins which acquired their label days before degradation.

Future experiments using SILAC technology could be performed to ascertain the contribution of DRiPs as compared to that of mature proteins to the pool of MHC class I presented peptides. By looking at mass shifts in peptides derived from proteins labeled with stable isotopes, it is possible to establish the proteome turnover rate. Proteins can be labeled by culturing cells for sufficient time in the presence of amino acids containing a heavy isotope, followed by culture with unlabeled amino acids. By sampling at intervals during the chase and establishing the ratio of heavy versus light peaks using mass spectrometry, a turnover rate can be obtained. In fact, this kind of experiment has been performed and there are published databases with abundant information on many

proteins' turnover rate determined using SILAC (Boisvert et al. 2012). It would be a matter of reproducing this kind of experiment while also collecting MHC class I eluted peptides in order to correlate peptide abundance with turnover rates. If a correlation cannot be established, the DRiPs model would be supported, and if there is a correlation, this would point at turnover as the major supplier of peptides for MHC class I presentation.

7.6 The Pioneer Round of Translation

A separate piece was added recently to the DRiPs model: the pioneer round of translation (Dolan et al. 2010; Apcher et al. 2011; Sébastien Apcher et al. 2012). This potential source of MHC class I presented epitopes encompasses the degradation products of a nuclear translation round which is part of the mRNA nonsense-mediated decay (NMD) quality control pathway in the nucleus. It is arguable whether these translation products could be DRiPs, since they are not necessarily defective or shunted by quality control chaperones for degradation. This potential source is nevertheless very different from the one provided by the turnover of mature functional proteins, and it fits other teleological criteria attributed to DRiPs: the products of the pioneer round of translation seem to be degraded rapidly regardless of the half-life of their mature functional counterparts, and

they are separated from the mature proteins at the translation level, thus overriding the putative bias in presentation towards more abundant proteins that the DRiPs hypothesis predicted if the main source of peptides for MHC class I presentation were mature protein turnover.

As described in the introduction chapter, the NMD pathway works in conjunction with the pre-mRNA splicing machinery, and therefore if this were the dominant mechanism for coupling DRiPs to antigen presentation, it would miss so many viral products derived from RNAs that do not contain introns. Although this pathway may contribute to presentation, it is worth noting that with the experimental constructs utilized in the report in question (Apcher et al. 2011), one hundred percent of the mRNAs contained a premature termination codon, whereas in real life situations the frequency of this happening would be much lower. Thus, this overabundance of pre-mRNA substrates that should be recognized and targeted for degradation may have been overwhelming for the system, and a fraction of these RNAs with premature stop codons could have escaped decay and may have been transported out of the nucleus and translated in the cytosol. As a matter of fact, there was a truncated product derived from one of the constructs with an encoded premature termination codon which was clearly detected by western blot, and therefore its mRNA was translated heavily and not just minimally during the pioneer round of translation (Apcher et al. 2011, fig.3).

With regards to the intein constructs described in this dissertation, it is formally possible that intein splicing took place shortly after the pioneer round of translation, and therefore the splice-dependent epitope might derive from this source and not from protein turnover. This is very unlikely for two reasons: one is that the degradation of the products of the pioneer round of translation is believed to occur very quickly, and therefore the fraction of molecules that would have completed their intein splicing before degradation would be very small. Another reason is that the RNAs produced from the expression cassettes in the constructs did not have any introns, and the pioneer round of translation seems to be linked to the nonsense-mediated decay mRNA pathway which requires the pre-mRNA splicing machinery to interact with splicing junctions. A termination codon is recognized as premature as opposed to the *bona fide* termination codon when the exon junction complex is downstream of it. Of course a round of NMD-independent nuclear translation that supplied substrates for protein degradation and MHC class I presentation cannot be ruled out, but there is no evidence yet of its existence. In fact it is not known whether the pioneer round of translation produces any polypeptides at all, it may simply involve scanning

7.7 DRiPs in the Context of the Immune Response

The implications of these results are discordant with the DRiPs hypothesis (Yewdell et al. 1996). Contribution from DRiPs might occur, but they do not seem to be an exclusive, preferential, or even a substantial source of peptides for presentation on MHC class I. According to the hypothesis, DRiPs are preferentially used by the immune system because a source of readily degraded proteins is required to provide peptides for class I presentation, thus allowing swift elimination of virally infected cells before the infection can spread. Let us consider this necessity from the point of view of an *in vivo* immune response.

Immune responses dependent on $CD8^+$ T cell-mediated elimination of infected cells require a priming phase (Bevan 1976), where the appropriate naïve clones are activated by professional antigen presenting cells (Huang et al. 1994)—pAPCs: dendritic cells (Schuler & Steinman 1985; Smith et al. 2003) and macrophages (Pozzi et al. 2005)—before they go on to divide and generate memory and effector $CD8^+$ T cells. Effector $CD8^+$ T cells have cytotoxic activity when they encounter any cell type that displays the cognate MHC class I-peptide complex (Zinkernagel & Doherty 1975). Memory $CD8^+$ T cells can become effectors upon encountering antigen once again.

It is important to distinguish between the initial first encounter with the virus—the induction of the immune response—and subsequent encounters—the recall response. According to the DRiPs model's teleology (Yewdell et al. 1996), the limiting factor for a timely elimination of infected cells is MHC class I antigen presentation. This may be true during a recall response, since the memory $CD8^+$ T cells would be poised to respond to antigens on class I on the surface of infected non-professional antigen presenting cells. In contrast, during the induction of the $CD8^+$ T cell immune response, the potential effector cells would still be naïve, and other time consuming events—known as the priming phase—would have to take place before they can become effectors and respond to presented antigens on infected cells. In the latter type of response the celerity of presentation by non-professional APCs does not seem to be that crucial, since the time required for priming far exceeds the time of a relatively slow acquisition of class I ligands derived from slowly turning over viral proteins in infected cells. In the case of LCMV, $CD8^+$ T cell-mediated interferon gamma production peaks at days four to eight, even after enormous doses are injected intraperitoneally (Merigan et al. 1977). Dendritic cells take one to three days to present antigens derived from herpes simplex virus in the draining lymph node (Smith et al. 2003). In another study, the presentation of antigens derived from influenza A virus inoculated into the mouse airways was first detected in the lymph nodes 1 day after infection, peaking at day three (Belz et al. 2004). In experiments with sheep, the presence of lymphoblasts was detectable eighty hours after a primary infection with vaccinia virus (Issekutz 1984). Therefore an extremely rapid presentation of viral antigens on MHC class I upon first encounter with a virus is

probably not crucial to prevent viral spread, which contradicts a major assumption leading to the DRiPs hypothesis.

The priming phase involves antigen capture and transport to lymphoid organs, where antigens are presented to naïve cells. It has been shown that priming can occur if the pAPC is directly infected by the virus (Norbury et al. 2001). However, often times viruses have a tropism for cells other than pAPCs, and pAPCs acquire and present antigen through a process called cross-presentation (Kovacsovics-Bankowski & Rock 1995; Sigal et al. 1999), in which the antigen is folded functional protein engulfed by phagocytosis (Shen & Rock 2004; Norbury et al. 2004). This process allows the priming of $CD8^+$ T cell responses against viruses that do not infect pAPCs. Therefore, since cross presented antigens come from mature proteins, the teleological argument that DRiPs are needed to initiate a $CD8^+$ T cell response is again flawed.

There are some viral infections, such as the vaccinia virus infection that can be very cytopathic and proceed with great celerity by generating large amounts of viral particles as early as one or two hours after exposure to the virus . In this case the presentation of antigens on class I would need to occur very shortly after viral infection for infected cells to be killed by CTLs before viral particles spread to neighboring cells even in the context of a recall response. It is noteworthy though, that neutralizing antibodies play a major role in the protective immune response against vaccinia (Downie & McCarthy 1958), and

thus containment of the viral progeny does not rely exclusively in the ability of the memory $CD8^+$ T cells to lyse infected cells. This is not the case in the LCMV infection, as it has been shown that the major players in the immunity to LCMV are $CD8^+$ T cells (Asano & Ahmed 1996). However, as discussed above, this infection is not as cytopathic and the primary $CD8^+$ immune response to it proceeds more slowly. Therefore, DRiPs would be more advantageous for the immune response to fast replicating viruses, keeping in mind the caveat that the celerity in class I presentation by non-professional APCs in a primary infection does not warrant a faster generation of effector CTLs.

Another important point comes from considering how many peptide-MHC class I complexes are sufficient to activate $CD8^+$ T cells. In the case of ovalbumin cross-priming, the amount of SIINFEKL-H-$2K^b$ complexes present in pAPCs sufficient to trigger the priming of an immune response is below the limit of detection of the 25-D1.16 antibody used in the studies by Yewdell's group. Cytotoxic $CD8^+$ T cells (CTLs) have a lower activation threshold than naïve cells encountering the antigen for the first time, i.e. even fewer peptide-MHC class I complexes will trigger a cytotoxic response.

There are somewhat diverse estimates in the literature of what the peptide-MHC complex density threshold might be. Villanueva et al. 1994 showed that the number of peptide-MHC complexes on the cell surface was about one for every thirty-five of the source proteins degraded. In a report examining the minimal epitope density necessary

for the lysis of target cells (Sykulev et al. 1996), the known epitope-MHC class I·TCR affinities were plotted against the estimated epitope densities on the cell surface of target cells. A linear trend was obtained, and it was determined that the minimal peptide-MHC class I complexes necessary to promote lysis were between one and ten per cell. However, in the lysis systems used in the experiments discussed above, the epitope-MHC densities were between twenty and one hundred for TCR affinities with a K_D in the μM range, which are similar to the affinities of the TCRs used in the experiments described in this dissertation (Willcox et al. 1999; Alam et al. 1999), except for the HY TCR which has a lower affinity for its peptide-MHC ligand (Ober et al. 2000) and therefore is expected to require a higher peptide-MHC density to trigger lysis. To summarize, most likely the threshold for CD8+ T cell activation is between one hundred and a thousand. The affinity of the OT-I TCR that recognizes S8L on H-2K^b is 6 μM, and therefore the expected threshold in terms of epitope density should be on the lower end.

So if few complexes on the cell surface are enough—certainly below the limit of detection of the 25-D1.16 antibody—there is no need to go above and beyond that limit in the very early phases after infection in order for the CTLs to lyse target cells. It is also important to realize that stable proteins with long half-lives are nevertheless continuously degraded, a process that starts immediately after synthesis. Therefore, the teleological argument behind the DRiPs hypothesis greatly loses strength, since the small amount of

complexes required could be fulfilled by degradation of full-length functional proteins through proteasomal degradation even if their half-lives are long.

The major postulated advantage of DRiPs over mature proteins as a source of MHC class I presented peptides is the quick degradation of the former, which provides a large number of peptides shortly after protein synthesis starts. However, most folding mistakes are not necessarily terminal and there is evidence describing folding and re-folding attempts through the interaction with chaperones (Hartl & Hayer-Hartl 2002; Goldberg 2003; Claessen et al. 2012). These quality control and rescue efforts take time and therefore work against the notion of extremely rapid degradation to build up a large peptide pool. Moreover, when antigens have been made intentionally defective they are most often degraded relatively slowly (Golovina et al. 2005).

7.8 Protein Degradation Kinetics and MHC class I Presentation

Two opposing processes operate to determine the concentration of a protein in the cell: synthesis and degradation. In order to achieve effective concentrations of viral proteins after infection, the balance between synthesis and degradation must be shifted towards synthesis during the period before steady state. At steady state however, both processes

are balanced, i.e. the number of molecules that are degraded equals the number of molecules that are synthesized and this is independent of the degradation rate. Therefore, at steady state the number of peptides generated from a protein will match its synthesis rate and this will be independent of whether it is a short-lived species (including DRiPs) or a long-lived one. For example, a rapidly synthesized viral protein that gets degraded at a very low rate will be abundant at steady state, as long as its likelihood of being degraded remains constant. Such a protein will still yield a high number of peptides per unit of time in spite of its low degradation rate, by virtue of its abundance. On the other hand one should take into account that during viral infection structural proteins are depleted not only by degradation but also due to viral particle egress from the cell. This implies that even at steady state the degradation rate will be slower than the synthesis rate. This might lead to a different scenario where stable long-lived proteins could be rapidly synthesized, incorporated into viral particles and exit the cell at a vigorous rate. In this case there may be an advantage to a DRiPs-based system, but always keeping in mind the caveats that there are typically large pools of unassembled viral proteins in infected cells, that it is probably not necessary to generate a large amount of class I presented epitopes to achieve the desired immune response, and also the aforementioned fact that even long-lived proteins do get degraded at a constant rate albeit slow as soon as they are synthesized.

While much is known about the quality control mechanisms that operate during protein synthesis and folding in the ER (Hartl & Hayer-Hartl 2002; Goldberg 2003; Claessen et al. 2012) and in the cytosol (Hartl & Hayer-Hartl 2002; Goldberg 2003; Komar 2009), the signals that lead to the turnover of mature proteins are still incompletely understood. It has been long speculated that the exposure of a hydrophobic domain might trigger recognition by members of the ubiquitin ligase (E3) family, leading to polyubiquitylation and degradation by the proteasome. Evidence of this has been provided in yeast for the recognition by the ubiquitin ligase San1 (Fredrickson et al. 2011). Oxidation damage is one the best documented causes of mature protein degradation (Berlett & Stadtman 1997). Oxidation of amino acid side chain groups, such as thiols in cysteines can lead to structural changes in proteins, and cellular pathways exist to prevent and even repair such instances (David 2004). These structural changes may expose hydrophobic domains and recognition by the Hsp70/CHIP machinery may target the protein for degradation (Pratt et al. 2010). Remarkably, there is some evidence, albeit *in vitro*, that proteasomes can degrade oxidized proteins independently of ubiquitylation, and again it is speculated that this is due to recognition of exposed hydrophobic domains (Ullrich et al. 1999; Shringarpure et al. 2003). Although it seems plausible for all the reasons stated here that the peptide pool generated by protein turnover is sufficient for the class I system to monitor protein expression in the cell, a system evolved for immune sampling that is not linked to protein synthesis quality control but rather operates at a later stage, cannot be ruled out by the experiments presented in this dissertation. Such a system would reconcile the postulated evolutionary need for quick and uniform sampling of synthesized

polypeptides with the experimental evidence shown in this dissertation that the mature protein pool can contribute peptides to the MHC class I presentation pathway.

7.9 Immune Surveillance and Cancer

Another scenario in which immune-mediated elimination of host cells is beneficial is cancer. $CD8^+$ T cells have been implicated in transformed cell elimination and MHC class I epitopes have been identified (van der Bruggen & Van den Eynde 2006). Cancer antigens that lead to MHC class I presentation encompass those encoded by germline or differentiation genes as well as the products of mutations. Of course some transformation events are the product of tumorigenic virus infection and the expression of viral products by the transformed cells can lead to MHC class I-mediated elimination. The host's tolerance mechanisms generally prevent responses against cells expressing non-mutated self proteins, and therefore other changes must occur in non-virally transduced cancer cells that make them suitable targets for $CD8^+$ T cells and at the same time distinguish them from the normal host's cells. Leaving the tolerance override question aside, it is clear that many class I epitopes in the context of cancer are presented and $CD8^+$ T cell responses are mounted against cells presenting them (for a referenced list see http://www.cancerimmunity.org/peptidedatabase/Tcellepitopes.htm).

With regards to the subject matter of this dissertation, the question is whether the generation of these cancer epitopes preferentially from DRiPs would constitute an advantage for the immune response against cancer. In most cases antigens either start being expressed or their steady state levels greatly increase as a consequence of transformation (van der Bruggen et al. 1991; Gaugler et al. 1994; Boël et al. 1995). This situation would be different than in the context of a viral infection, since the urgency in preventing the spread is not as great. A cancer cell is not like a virally infected cell, where the pathological cell is producing viral progeny that will spread the disease. Therefore, it is not essential to stop the process within hours of onset. The cancer cells will be around for days to years and will have steady state levels of mature proteins. The immune system could be effective in preventing the disease if it eliminated the cell or its progeny even months after transformation. However, it was pointed out a few years ago that peptides derived from alternative reading frames—which can qualify as DRiPs—might become more abundant when overexpression occurs (Ho & Green 2006; Yewdell & Hickman 2007). Therefore, alternative reading frame encoded epitopes appear as an ideal candidate for the $CD8^+$ T cell immune response against cancer and hence cancer would be one situation in which the identification of this kind of DRiPs would be expected. There are a few reports of alternative reading frame derived epitopes in cancer situations. A case has been described where the epitope originated from a non-AUG initiation event that extended the polypeptide length (Ronsin et al. 1999). In other reports (Wang et al. 1996; Rosenberg et al. 2002) epitopes derived from alternative reading

frames elicited T cell clones that could lyse melanoma cells. One should note however, there are cases in which the peptides presented are not necessarily derived from DRiPs, but rather from mutations at the gene level that cause frameshifts (Ripberger et al. 2003; Huang et al. 2004; Oh et al. 2004); in other words, the peptides are not produced due to mistakes in mRNA translation, but rather mutated mRNAs are produced as a result of mutations in transformed cells and likely derived from the transformation causative events, since they are observed in most cancers with similar phenotype. All in all, it seems like the bona fide MHC class I epitopes derived from alternative reading frames identified in the context of cancer are not as numerous as one would expect if DRiPs were a major contributor to the pathway, although the absence of more examples might be due to the difficulty of purifying, expanding and screening $CD8^+$ T cell clones specific for these epitopes.

CONCLUDING REMARKS

I have presented in this dissertation the current model for the generation of presented MHC class I peptides: the DRiPs model. This model has received wide acceptance in the scientific community as reflected by the many publications referring to the issue, none of which have challenged the view that DRiPs are a major contributor to the MHC class I presentation pathway.

This model is based on a teleological argument, and experiments were performed after the hypothesis was postulated. In the discussion chapter of this dissertation I have argued that there is really no need for a rapidly degraded protein pool as a source of peptides for MHC class I presentation for the priming of an immune response, nor for the elimination of infected cells by effector $CD8^+$ T cells.

The experimental data in the literature aimed at providing support for the DRiPs hypothesis were reliant on the use of global protein synthesis inhibition, which as discussed can have collateral effects, and thus the interpretation of the results can be misleading. Nevertheless, there are other pieces of data in the literature that seem to be in accordance with the DRiPs model.

In order to shed light on this issue, I have described an experimental system which allows to quantitatively distinguish the contribution to MHC class I of peptides derived from proteins that have attained enzymatic function and are thus considered mature. The results from my experiments clearly point at an absence of a substantial contribution to MHC class I antigen presentation by DRiPs. This implies that efforts directed at enhancing the immune response for certain $CD8^+$ T cell epitopes by targeting the source antigen to a DRiP compartment are probably futile and should be focused elsewhere, as the importance of such a compartment in the MHC class I presentation pathway has been exaggerated.

REFERENCES

Alam, S.M. et al., 1999. Qualitative and quantitative differences in T cell receptor binding of agonist and antagonist ligands. *Immunity*, 10(2), pp.227–237.

Alarcon, B. et al., 1988. Assembly of the human T cell receptor-CD3 complex takes place in the endoplasmic reticulum and involves intermediary complexes between the CD3-gamma.delta.epsilon core and single T cell receptor alpha or beta chains. *The Journal of Biological Chemistry*, 263(6), pp.2953–2961.

Allen, P.M., Strydom, D.J. & Unanue, E.R., 1984. Processing of lysozyme by macrophages: identification of the determinant recognized by two T-cell hybridomas. *Proceedings of the National Academy of Sciences of the United States of America*, 81(8), pp.2489–2493.

Apcher, S. et al., 2011. Major source of antigenic peptides for the MHC class I pathway is produced during the pioneer round of mRNA translation. *Proceedings of the National Academy of Sciences of the United States of America*, 108(28), pp.11572–11577.

Apcher, S., Manoury, B. & Fåhraeus, R., 2012. The role of mRNA translation in direct MHC class I antigen presentation. *Current Opinion in Immunology*, 24(1), pp.71–76.

Asano, M.S. & Ahmed, R., 1996. CD8 T cell memory in B cell-deficient mice. *The Journal of Experimental Medicine*, 183(5), pp.2165–2174.

Babbitt, B.P. et al., 1985. Binding of immunogenic peptides to Ia histocompatibility molecules. *Nature*, 317(6035), pp.359–361.

Belz, G.T. et al., 2004. Distinct migrating and nonmigrating dendritic cell populations are involved in MHC class I-restricted antigen presentation after lung infection with virus. *Proceedings of the National Academy of Sciences of the United States of America*, 101(23), pp.8670–8675.

Berlett, B.S. & Stadtman, E.R., 1997. Protein oxidation in aging, disease, and oxidative stress. *The Journal of Biological Chemistry*, 272(33), pp.20313–20316.

Bevan, M.J., 1976. Cross-priming for a secondary cytotoxic response to minor H antigens with H-2 congenic cells which do not cross-react in the cytotoxic assay. *The Journal of Experimental Medicine*, 143(5), pp.1283–1288.

Bevan, M.J., 1975. The major histocompatibility complex determines susceptibility to cytotoxic T cells directed against minor histocompatibility antigens. *The Journal of Experimental Medicine*, 142(6), pp.1349–1364.

Bjorkman, P.J. et al., 1987. Structure of the human class I histocompatibility antigen, HLA-A2. *Nature*, 329(6139), pp.506–512.

Van Bleek, G.M. & Nathenson, S.G., 1990. Isolation of an endogenously processed immunodominant viral peptide from the class I H-2Kb molecule. *Nature*, 348(6298), pp.213–216.

Bluestein, H.G., Green, I. & Benacerraf, B., 1971. Specific immune response genes of the guinea pig. I. Dominant genetic control of immune responsiveness to copolymers of L-glutamic acid and L-alanine and L-glutamic acid and L-tyrosine. *The Journal of Experimental Medicine*, 134(2), pp.458–470.

Boël, P. et al., 1995. BAGE: a new gene encoding an antigen recognized on human melanomas by cytolytic T lymphocytes. *Immunity*, 2(2), pp.167–175.

Boisvert, F.-M. et al., 2012. A quantitative spatial proteomics analysis of proteome turnover in human cells. *Molecular & Cellular Proteomics: MCP*, 11(3), p.M111.011429.

Boon, T. & Van Pel, A., 1989. T cell-recognized antigenic peptides derived from the cellular genome are not protein degradation products but can be generated directly by transcription and translation of short subgenic regions. A hypothesis. *Immunogenetics*, 29(2), pp.75–79.

Bremer, M.C. et al., 1992. VDE endonuclease cleaves Saccharomyces cerevisiae genomic DNA at a single site: physical mapping of the VMA1 gene. *Nucleic Acids Research*, 20(20), p.5484.

Van der Bruggen, P et al., 1991. A gene encoding an antigen recognized by cytolytic T lymphocytes on a human melanoma. *Science (New York, N.Y.)*, 254(5038), pp.1643–1647.

Van der Bruggen, P. & Van den Eynde, B.J., 2006. Processing and presentation of tumor antigens and vaccination strategies. *Current Opinion in Immunology*, 18(1), pp.98–104.

Cascio, P., 2001. 26S proteasomes and immunoproteasomes produce mainly N-extended versions of an antigenic peptide. *The EMBO Journal*, 20(10), pp.2357–2366.

Cerundolo, V. et al., 1991. The binding affinity and dissociation rates of peptides for class I major histocompatibility complex molecules. *European Journal of Immunology*, 21(9), pp.2069–2075.

Ciechanover, A. et al., 1980. ATP-dependent conjugation of reticulocyte proteins with the polypeptide required for protein degradation. *Proceedings of the National Academy of Sciences of the United States of America*, 77(3), pp.1365–1368.

Claessen, J.H.L., Kundrat, L. & Ploegh, H.L., 2012. Protein quality control in the ER: balancing the ubiquitin checkbook. *Trends in Cell Biology*, 22(1), pp.22–32.

Corcelette, S., Massé, T. & Madjar, J.J., 2000. Initiation of translation by non-AUG codons in human T-cell lymphotropic virus type I mRNA encoding both Rex and Tax regulatory proteins. *Nucleic Acids Research*, 28(7), pp.1625–1634.

Daskalogianni, C. et al., 2008. Gly-Ala Repeats Induce Position- and Substrate-specific Regulation of 26 S Proteasome-dependent Partial Processing. *Journal of Biological Chemistry*, 283(44), pp.30090 –30100.

David, B., 2004. The role of cysteine residues as redox-sensitive regulatory switches. *Current Opinion in Structural Biology*, 14(6), pp.679–686.

Degen, E. & Williams, D.B., 1991. Participation of a novel 88-kD protein in the biogenesis of murine class I histocompatibility molecules. *The Journal of Cell Biology*, 112(6), pp.1099–1115.

Ding, Y. et al., 2003. Crystal Structure of a Mini-intein Reveals a Conserved Catalytic Module Involved in Side Chain Cyclization of Asparagine during Protein Splicing. *Journal of Biological Chemistry*, 278(40), pp.39133 –39142.

Doherty, P.C. & Zinkernagel, R.M., 1975. H-2 compatibility is required for T-cell-mediated lysis of target cells infected with lymphocytic choriomeningitis virus. *The Journal of Experimental Medicine*, 141(2), pp.502–507.

Dolan, B.P. et al., 2011. Distinct pathways generate peptides from defective ribosomal products for CD8+ T cell immunosurveillance. *Journal of Immunology (Baltimore, Md.: 1950)*, 186(4), pp.2065–2072.

Dolan, B.P. et al., 2010. RNA polymerase II inhibitors dissociate antigenic peptide generation from normal viral protein synthesis: a role for nuclear translation in defective ribosomal product synthesis? *Journal of Immunology (Baltimore, Md.: 1950)*, 185(11), pp.6728–6733.

Dolph, P.J., Huang, J.T. & Schneider, R.J., 1990. Translation by the adenovirus tripartite leader: elements which determine independence from cap-binding protein complex. *Journal of Virology*, 64(6), pp.2669–2677.

Donnelly, M.L. et al., 2001. Analysis of the aphthovirus 2A/2B polyprotein "cleavage" mechanism indicates not a proteolytic reaction, but a novel translational effect: a putative ribosomal "skip." *The Journal of General Virology*, 82(Pt 5), pp.1013–1025.

Donohue, K.B. et al., 2006. Cross-priming utilizes antigen not available to the direct presentation pathway. *Immunology*, 119(1), pp.63–73.

Downie, A.W. & McCarthy, K., 1958. The antibody response in man following infection with viruses of the pox group. III. Antibody response in smallpox. *The Journal of Hygiene*, 56(4), pp.479–487.

Dujon, B. et al., 1986. Mitochondrial introns as mobile genetic elements: the role of intron-encoded proteins. *Basic Life Sciences*, 40, pp.5–27.

Elleuche, S., Döring, K. & Pöggeler, S., 2008. Minimization of a eukaryotic mini-intein. *Biochemical and Biophysical Research Communications*, 366(1), pp.239–243.

Fagan, J.M., Waxman, L. & Goldberg, A L, 1987. Skeletal muscle and liver contain a soluble ATP + ubiquitin-dependent proteolytic system. *Biochemical Journal*, 243(2), pp.335–343.

Falk, K. et al., 1991. Allele-specific motifs revealed by sequencing of self-peptides eluted from MHC molecules. *Nature*, 351(6324), pp.290–296.

Feigenblum, D. & Schneider, R.J., 1993. Modification of eukaryotic initiation factor 4F during infection by influenza virus. *Journal of Virology*, 67(6), pp.3027–3035.

Fernandez, J. et al., 2001. Internal ribosome entry site-mediated translation of a mammalian mRNA is regulated by amino acid availability. *The Journal of Biological Chemistry*, 276(15), pp.12285–12291.

Fredrickson, E.K. et al., 2011. Exposed Hydrophobicity Is a Key Determinant of Nuclear Quality Control Degradation. *Molecular Biology of the Cell*, 22(13), pp.2384–2395.

Gangopadhyay, J.P., Jiang, S.-Q. & Paulus, H., 2003. An in vitro screening system for protein splicing inhibitors based on green fluorescent protein as an indicator. *Analytical Chemistry*, 75(10), pp.2456–2462.

Gaugler, B. et al., 1994. Human gene MAGE-3 codes for an antigen recognized on a melanoma by autologous cytolytic T lymphocytes. *The Journal of Experimental Medicine*, 179(3), pp.921–930.

Georgiadou, D. et al., 2010. Placental leucine aminopeptidase efficiently generates mature antigenic peptides in vitro but in patterns distinct from endoplasmic reticulum aminopeptidase 1. *Journal of Immunology (Baltimore, Md.: 1950)*, 185(3), pp.1584–1592.

Ghosh, I., Sun, L. & Xu, M.-Q., 2001. Zinc Inhibition of Protein trans-Splicing and Identification of Regions Essential for Splicing and Association of a Split Intein*. *Journal of Biological Chemistry*, 276(26), pp.24051 –24058.

Gilden, D.H., Devlin, M. & Wroblewska, Z., 1981. The use of vesicular stomatitis (visna virus) pseudotypes to demonstrate visna virus receptors in cells from different species. *Archives of Virology*, 67(2), pp.181–185.

Gillin, F.D. et al., 1972. 8-Azaguanine resistance in mammalian cells. I. Hypoxanthine-guanine phosphoribosyltransferase. *Genetics*, 72(2), pp.239–252.

Goldberg, A. L, 2003. Protein degradation and protection against misfolded or damaged proteins. *Nature*, 426(6968), pp.895–899.

Golovina, T.N., Morrison, S.E. & Eisenlohr, L.C., 2005. The impact of misfolding versus targeted degradation on the efficiency of the MHC class I-restricted antigen processing. *Journal of Immunology (Baltimore, Md.: 1950)*, 174(5), pp.2763–2769.

Gossen, M. & Bujard, H., 1992. Tight control of gene expression in mammalian cells by tetracycline-responsive promoters. *Proceedings of the National Academy of Sciences*, 89(12), pp.5547–5551.

Grant, E.P. et al., 1995. Rate of antigen degradation by the ubiquitin-proteasome pathway influences MHC class I presentation. *Journal of Immunology (Baltimore, Md.: 1950)*, 155(8), pp.3750–3758.

Grant, E.P. & Rock, K L, 1992. MHC class I-restricted presentation of exogenous antigen by thymic antigen-presenting cells in vitro and in vivo. *Journal of Immunology (Baltimore, Md.: 1950)*, 148(1), pp.13–18.

Grey, H.M. et al., 1973. THE SMALL SUBUNIT OF HL-A ANTIGENS IS β2-MICROGLOBULIN. *The Journal of Experimental Medicine*, 138(6), pp.1608–1612.

Hartl, F.U. & Hayer-Hartl, M., 2002. Molecular chaperones in the cytosol: from nascent chain to folded protein. *Science (New York, N.Y.)*, 295(5561), pp.1852–1858.

Heessen, S. et al., 2002. Functional p53 chimeras containing the Epstein–Barr virus Gly-Ala repeat are protected from Mdm2- and HPV-E6-induced proteolysis. *Proceedings of the National Academy of Sciences*, 99(3), pp.1532 –1537.

Ho, O. & Green, W.R., 2006. Alternative Translational Products and Cryptic T Cell Epitopes: Expecting the Unexpected. *The Journal of Immunology*, 177(12), pp.8283–8289.

Hough, R., Pratt, G. & Rechsteiner, M., 1986. Ubiquitin-lysozyme conjugates. Identification and characterization of an ATP-dependent protease from rabbit reticulocyte lysates. *The Journal of Biological Chemistry*, 261(5), pp.2400–2408.

Hoyt, M.A. et al., 2006. Glycine-alanine repeats impair proper substrate unfolding by the proteasome. *The EMBO Journal*, 25(8), pp.1720–1729.

Huang, A.Y. et al., 1994. Role of bone marrow-derived cells in presenting MHC class I-restricted tumor antigens. *Science (New York, N.Y.)*, 264(5161), pp.961–965.

Huang, J. et al., 2004. T cells associated with tumor regression recognize frameshifted products of the CDKN2A tumor suppressor gene locus and a mutated HLA class I gene product. *Journal of Immunology (Baltimore, Md.: 1950)*, 172(10), pp.6057–6064.

Huang, J.T. & Schneider, R.J., 1990. Adenovirus inhibition of cellular protein synthesis is prevented by the drug 2-aminopurine. *Proceedings of the National Academy of Sciences of the United States of America*, 87(18), pp.7115–7119.

Hurtado, C. et al., 2011. The African swine fever virus lectin EP153R modulates the surface membrane expression of MHC class I antigens. *Archives of Virology*, 156(2), pp.219–234.

Issekutz, T.B., 1984. Kinetics of cytotoxic lymphocytes in efferent lymph from single lymph nodes following immunization with vaccinia virus. *Clinical and Experimental Immunology*, 56(3), pp.515–523.

Johnson, K.A., Simpson, Z.B. & Blom, T., 2009a. FitSpace Explorer: An algorithm to evaluate multidimensional parameter space in fitting kinetic data. *Analytical Biochemistry*, 387(1), pp.30–41.

Johnson, K.A., Simpson, Z.B. & Blom, T., 2009b. Global Kinetic Explorer: A new computer program for dynamic simulation and fitting of kinetic data. *Analytical Biochemistry*, 387(1), pp.20–29.

Kawahara, M. et al., 2009. Analysis of the role of tripeptidyl peptidase II in MHC class I antigen presentation in vivo. *Journal of Immunology (Baltimore, Md.: 1950)*, 183(10), pp.6069–6077.

Khan, S. et al., 2001. Cutting edge: neosynthesis is required for the presentation of a T cell epitope from a long-lived viral protein. *Journal of Immunology (Baltimore, Md.: 1950)*, 167(9), pp.4801–4804.

Kisielow, P. et al., 1988. Tolerance in T-cell-receptor transgenic mice involves deletion of nonmature CD4+8+ thymocytes. *Nature*, 333(6175), pp.742–746.

Klabunde, T. et al., 1998. Crystal structure of GyrA intein from Mycobacterium xenopi reveals structural basis of protein splicing. *Nature Structural Biology*, 5(1), pp.31–36.

Komar, A.A., 2009. A pause for thought along the co-translational folding pathway. *Trends in Biochemical Sciences*, 34(1), pp.16–24.

Kovacsovics-Bankowski, M. & Rock, K L, 1995. A phagosome-to-cytosol pathway for exogenous antigens presented on MHC class I molecules. *Science (New York, N.Y.)*, 267(5195), pp.243–246.

Kukutsch, N.A. et al., 2000. Formation and kinetics of MHC class I-ovalbumin peptide complexes on immature and mature murine dendritic cells. *The Journal of Investigative Dermatology*, 115(3), pp.449–453.

Leaman, D.W. et al., 1998. A mutant cell line defective in response to double-stranded RNA and in regulating basal expression of interferon-stimulated genes. *Proceedings of the National Academy of Sciences of the United States of America*, 95(16), pp.9442–9447.

Leung, C.S. et al., 2010. Nuclear location of an endogenously expressed antigen, EBNA1, restricts access to macroautophagy and the range of CD4 epitope display. *Proceedings of the National Academy of Sciences of the United States of America*, 107(5), pp.2165–2170.

Lev, A. et al., 2010. Compartmentalized MHC class I antigen processing enhances immunosurveillance by circumventing the law of mass action. *Proceedings of the National Academy of Sciences of the United States of America*, 107(15), pp.6964–6969.

Levine, B.B., Stember, R.H. & Fotino, M., 1972. Ragweed hay fever: genetic control and linkage to HL-A haplotypes. *Science (New York, N.Y.)*, 178(4066), pp.1201–1203.

Levitskaya, J. et al., 1997. Inhibition of ubiquitin/proteasome-dependent protein degradation by the Gly-Ala repeat domain of the Epstein–Barr virus nuclear antigen 1. *Proceedings of the National Academy of Sciences*, 94(23), pp.12616 – 12621.

Levkau, B. et al., 2001. xIAP induces cell-cycle arrest and activates nuclear factor-kappaB : new survival pathways disabled by caspase-mediated cleavage during apoptosis of human endothelial cells. *Circulation Research*, 88(3), pp.282–290.

Lévy, F. et al., 1991. ATP is required for in vitro assembly of MHC class I antigens but not for transfer of peptides across the ER membrane. *Cell*, 67(2), pp.265–274.

Lewis, S.M. et al., 2008. The eIF4G homolog DAP5/p97 supports the translation of select mRNAs during endoplasmic reticulum stress. *Nucleic Acids Research*, 36(1), pp.168–178.

Ljunggren, H.G. & Kärre, K., 1985. Host resistance directed selectively against H-2-deficient lymphoma variants. Analysis of the mechanism. *The Journal of Experimental Medicine*, 162(6), pp.1745–1759.

Lurquin, C. et al., 1989. Structure of the gene of tum- transplantation antigen P91A: the mutated exon encodes a peptide recognized with Ld by cytolytic T cells. *Cell*, 58(2), pp.293–303.

Mackay, L.K. et al., 2009. T cell detection of a B-cell tropic virus infection: newly-synthesised versus mature viral proteins as antigen sources for CD4 and CD8 epitope display. *PLoS Pathogens*, 5(12), p.e1000699.

Malarkannan, S. et al., 1999. Presentation of out-of-frame peptide/MHC class I complexes by a novel translation initiation mechanism. *Immunity*, 10(6), pp.681–690.

Markiewicz, M.A. et al., 1998. Long-term T cell memory requires the surface expression of self-peptide/major histocompatibility complex molecules. *Proceedings of the National Academy of Sciences of the United States of America*, 95(6), pp.3065–3070.

McDevitt, H.O. & Tyan, M.L., 1968. Genetic control of the antibody response in inbred mice. Transfer of response by spleen cells and linkage to the major histocompatibility (H-2) locus. *The Journal of Experimental Medicine*, 128(1), pp.1–11.

Merigan, T.C., Oldstone, M.B. & Welsh, R.M., 1977. Interferon production during lymphocytic choriomeningitis virus infection of nude and normal mice. *Nature*, 268(5615), pp.67–68.

Milner, E. et al., 2006. The turnover kinetics of major histocompatibility complex peptides of human cancer cells. *Molecular & Cellular Proteomics: MCP*, 5(2), pp.357–365.

Mo, X.Y. et al., 1999. Distinct proteolytic processes generate the C and N termini of MHC class I-binding peptides. *Journal of Immunology (Baltimore, Md.: 1950)*, 163(11), pp.5851–5859.

Moore, M.W., Carbone, F.R. & Bevan, M.J., 1988. Introduction of soluble protein into the class I pathway of antigen processing and presentation. *Cell*, 54(6), pp.777–785.

Morimoto, T., Tashiro, Y. & Matsuura, S., 1967. Chase of newly synthesized proteins in guinea-pig pancreas with cycloheximide. *Biochimica Et Biophysica Acta*, 138(3), pp.631–633.

Murali-Krishna, K. et al., 1998. Counting antigen-specific CD8 T cells: a reevaluation of bystander activation during viral infection. *Immunity*, 8(2), pp.177–187.

Netzer, N. et al., 2009. Innate immune and chemically triggered oxidative stress modifies translational fidelity. *Nature*, 462(7272), pp.522–526.

Norbury, C.C. et al., 2004. CD8+ T cell cross-priming via transfer of proteasome substrates. *Science (New York, N.Y.)*, 304(5675), pp.1318–1321.

Norbury, C.C. et al., 2001. Multiple Antigen-Specific Processing Pathways for Activating Naive CD8+ T Cells In Vivo. *The Journal of Immunology*, 166(7), pp.4355 – 4362.

Ober, B.T. et al., 2000. Affinity of thymic self-peptides for the TCR determines the selection of CD8(+) T lymphocytes in the thymus. *International Immunology*, 12(9), pp.1353–1363.

Oh, S. et al., 2004. Human CTLs to wild-type and enhanced epitopes of a novel prostate and breast tumor-associated protein, TARP, lyse human breast cancer cells. *Cancer Research*, 64(7), pp.2610–2618.

Okada, C.Y. & Rechsteiner, M., 1982. Introduction of macromolecules into cultured mammalian cells by osmotic lysis of pinocytic vesicles. *Cell*, 29(1), pp.33–41.

Ornstein, L., 1964. DISC ELECTROPHORESIS. I. BACKGROUND AND THEORY. *Annals of the New York Academy of Sciences*, 121, pp.321–349.

Ozawa, T. et al., 2000. A fluorescent indicator for detecting protein-protein interactions in vivo based on protein splicing. *Analytical Chemistry*, 72(21), pp.5151–5157.

Perler, F.B., 2002. InBase: the Intein Database. *Nucleic Acids Research*, 30(1), pp.383–384.

Porgador, A. et al., 1997. Localization, quantitation, and in situ detection of specific peptide-MHC class I complexes using a monoclonal antibody. *Immunity*, 6(6), pp.715–726.

Powis, S.J. et al., 1991. Restoration of antigen presentation to the mutant cell line RMA-S by an MHC-linked transporter. *Nature*, 354(6354), pp.528–531.

Pozzi, L.-A.M., Maciaszek, J.W. & Rock, Kenneth L, 2005. Both dendritic cells and macrophages can stimulate naive CD8 T cells in vivo to proliferate, develop effector function, and differentiate into memory cells. *Journal of Immunology (Baltimore, Md.: 1950)*, 175(4), pp.2071–2081.

Pratt, J.M. et al., 2002. Dynamics of protein turnover, a missing dimension in proteomics. *Molecular & Cellular Proteomics: MCP*, 1(8), pp.579–591.

Pratt, W.B. et al., 2010. Proposal for a role of the Hsp90/Hsp70-based chaperone machinery in making triage decisions when proteins undergo oxidative and toxic damage. *Experimental Biology and Medicine (Maywood, N.J.)*, 235(3), pp.278–289.

Provost, E., Rhee, J. & Leach, S.D., 2007. Viral 2A peptides allow expression of multiple proteins from a single ORF in transgenic zebrafish embryos. *Genesis (New York, N.Y.: 2000)*, 45(10), pp.625–629.

Qian, S.-B. et al., 2006. Tight linkage between translation and MHC class I peptide ligand generation implies specialized antigen processing for defective ribosomal products. *Journal of Immunology (Baltimore, Md.: 1950)*, 177(1), pp.227–233.

Rajagopalan, S. & Brenner, M.B., 1994. Calnexin retains unassembled major histocompatibility complex class I free heavy chains in the endoplasmic reticulum. *The Journal of Experimental Medicine*, 180(1), pp.407–412.

Reits, E.A. et al., 2000. The major substrates for TAP in vivo are derived from newly synthesized proteins. *Nature*, 404(6779), pp.774–778.

Ripberger, E. et al., 2003. Identification of an HLA-A0201-restricted CTL epitope generated by a tumor-specific frameshift mutation in a coding microsatellite of the OGT gene. *Journal of Clinical Immunology*, 23(5), pp.415–423.

Rock, K L et al., 1994. Inhibitors of the proteasome block the degradation of most cell proteins and the generation of peptides presented on MHC class I molecules. *Cell*, 78(5), pp.761–771.

Rock, K L, Rothstein, L. & Gamble, S., 1990. Generation of class I MHC-restricted T-T hybridomas. *Journal of Immunology (Baltimore, Md.: 1950)*, 145(3), pp.804–811.

Roelse, J. et al., 1994. Trimming of TAP-translocated peptides in the endoplasmic reticulum and in the cytosol during recycling. *The Journal of Experimental Medicine*, 180(5), pp.1591–1597.

Van Roey, P. et al., 2007. Crystallographic and Mutational Studies of Mycobacterium tuberculosis recA Mini-inteins Suggest a Pivotal Role for a Highly Conserved Aspartate Residue. *Journal of Molecular Biology*, 367(1), pp.162–173.

Ronsin, C. et al., 1999. A non-AUG-defined alternative open reading frame of the intestinal carboxyl esterase mRNA generates an epitope recognized by renal cell carcinoma-reactive tumor-infiltrating lymphocytes in situ. *Journal of Immunology (Baltimore, Md.: 1950)*, 163(1), pp.483–490.

Rosenberg, S.A. et al., 2002. Identification of BING-4 cancer antigen translated from an alternative open reading frame of a gene in the extended MHC class II region using lymphocytes from a patient with a durable complete regression following immunotherapy. *Journal of Immunology (Baltimore, Md.: 1950)*, 168(5), pp.2402–2407.

Saveanu, L. et al., 2005. Concerted peptide trimming by human ERAP1 and ERAP2 aminopeptidase complexes in the endoplasmic reticulum. *Nature Immunology*, 6(7), pp.689–697.

Schrader, J.W., 1979. Nature of the T-cell receptor. Both the T-cell receptor and antigen-specific T-cell-derived factors are coded for by V genes but express anti-self idiotypes indirectly determined by major histocompatibility complex genes. *Scandinavian Journal of Immunology*, 10(5), pp.387–393.

Schubert, U. et al., 2000. Rapid degradation of a large fraction of newly synthesized proteins by proteasomes. *Nature*, 404(6779), pp.770–774.

Schuler, G. & Steinman, R.M., 1985. Murine epidermal Langerhans cells mature into potent immunostimulatory dendritic cells in vitro. *The Journal of Experimental Medicine*, 161(3), pp.526–546.

Schwab, S.R. et al., 2004. Unanticipated antigens: translation initiation at CUG with leucine. *PLoS Biology*, 2(11), p.e366.

Serwold, T. et al., 2002. ERAAP customizes peptides for MHC class I molecules in the endoplasmic reticulum. *Nature*, 419(6906), pp.480–483.

Sharipo, A. et al., 1998. A minimal glycine-alanine repeat prevents the interaction of ubiquitinated I kappaB alpha with the proteasome: a new mechanism for selective inhibition of proteolysis. *Nature Medicine*, 4(8), pp.939–944.

Shen, L. & Rock, Kenneth L, 2004. Cellular protein is the source of cross-priming antigen in vivo. *Proceedings of the National Academy of Sciences of the United States of America*, 101(9), pp.3035–3040.

Shepherd, J.C. et al., 1993. TAP1-dependent peptide translocation in vitro is ATP dependent and peptide selective. *Cell*, 74(3), pp.577–584.

Shringarpure, R. et al., 2003. Ubiquitin conjugation is not required for the degradation of oxidized proteins by proteasome. *The Journal of Biological Chemistry*, 278(1), pp.311–318.

Sigal, L.J. et al., 1999. Cytotoxic T-cell immunity to virus-infected non-haematopoietic cells requires presentation of exogenous antigen. *Nature*, 398(6722), pp.77–80.

Sigal, L.J. & Wylie, D.E., 1996. Role of non-anchor residues of Db-restricted peptides in class I binding and TCR triggering. *Molecular Immunology*, 33(17-18), pp.1323–1333.

Sin, N. et al., 1999. Total synthesis of the potent proteasome inhibitor epoxomicin: a useful tool for understanding proteasome biology. *Bioorganic & Medicinal Chemistry Letters*, 9(15), pp.2283–2288.

Smith, C.M. et al., 2003. Cutting Edge: Conventional CD8α+ Dendritic Cells Are Preferentially Involved in CTL Priming After Footpad Infection with Herpes Simplex Virus-1. *The Journal of Immunology*, 170(9), pp.4437 –4440.

Sonenberg, N., 2000. *Translational control of gene expression* 2nd ed., Cold Spring Harbor NY: Cold Spring Harbor Laboratory Press.

Spies, T. et al., 1990. A gene in the human major histocompatibility complex class II region controlling the class I antigen presentation pathway. *Nature*, 348(6303), pp.744–747.

Spies, T. & DeMars, R., 1991. Restored expression of major histocompatibility class I molecules by gene transfer of a putative peptide transporter. *Nature*, 351(6324), pp.323–324.

Stark, G.R. et al., 1998. How cells respond to interferons. *Annual Review of Biochemistry*, 67, pp.227–264.

Sugita, M. & Brenner, M.B., 1994. An unstable beta 2-microglobulin: major histocompatibility complex class I heavy chain intermediate dissociates from calnexin and then is stabilized by binding peptide. *The Journal of Experimental Medicine*, 180(6), pp.2163–2171.

Sykulev, Y. et al., 1996. Evidence that a single peptide-MHC complex on a target cell can elicit a cytolytic T cell response. *Immunity*, 4(6), pp.565–571.

Szikora, J.P. et al., 1990. Structure of the gene of tum- transplantation antigen P35B: presence of a point mutation in the antigenic allele. *The EMBO Journal*, 9(4), pp.1041–1050.

Szymczak, A.L. et al., 2004. Correction of multi-gene deficiency in vivo using a single "self-cleaving" 2A peptide-based retroviral vector. *Nature Biotechnology*, 22(5), pp.589–594.

Takei, F., 1985. Inhibition of mixed lymphocyte response by a rat monoclonal antibody to a novel murine lymphocyte activation antigen (MALA-2). *Journal of Immunology (Baltimore, Md.: 1950)*, 134(3), pp.1403–1407.

Thompson, J.D., Higgins, D.G. & Gibson, T.J., 1994. CLUSTAL W: improving the sensitivity of progressive multiple sequence alignment through sequence weighting, position-specific gap penalties and weight matrix choice. *Nucleic Acids Research*, 22(22), pp.4673–4680.

Towne, C.F. et al., 2007. Analysis of the role of bleomycin hydrolase in antigen presentation and the generation of CD8 T cell responses. *Journal of Immunology (Baltimore, Md.: 1950)*, 178(11), pp.6923–6930.

Towne, C.F. et al., 2005. Leucine aminopeptidase is not essential for trimming peptides in the cytosol or generating epitopes for MHC class I antigen presentation. *Journal of Immunology (Baltimore, Md.: 1950)*, 175(10), pp.6605–6614.

Towne, C.F. et al., 2008. Puromycin-sensitive aminopeptidase limits MHC class I presentation in dendritic cells but does not affect CD8 T cell responses during viral infections. *Journal of Immunology (Baltimore, Md.: 1950)*, 180(3), pp.1704–1712.

Townsend, A. et al., 1989. Association of class I major histocompatibility heavy and light chains induced by viral peptides. *Nature*, 340(6233), pp.443–448.

Townsend, A.R., Bastin, J., et al., 1986. Cytotoxic T lymphocytes recognize influenza haemagglutinin that lacks a signal sequence. *Nature*, 324(6097), pp.575–577.

Townsend, A.R., Rothbard, J., et al., 1986. The epitopes of influenza nucleoprotein recognized by cytotoxic T lymphocytes can be defined with short synthetic peptides. *Cell*, 44(6), pp.959–968.

Townsend, A.R., Gotch, F.M. & Davey, J., 1985. Cytotoxic T cells recognize fragments of the influenza nucleoprotein. *Cell*, 42(2), pp.457–467.

Trowsdale, J. et al., 1990. Sequences encoded in the class II region of the MHC related to the “ABC” superfamily of transporters. *Nature*, 348(6303), pp.741–744.

Ullrich, O. et al., 1999. Poly-ADP ribose polymerase activates nuclear proteasome to degrade oxidatively damaged histones. *Proceedings of the National Academy of Sciences of the United States of America*, 96(11), pp.6223–6228.

Vabulas, R.M. & Hartl, F.U., 2005. Protein synthesis upon acute nutrient restriction relies on proteasome function. *Science (New York, N.Y.)*, 310(5756), pp.1960–1963.

Villanueva, M.S. et al., 1994. Efficiency of MHC class I antigen processing: A quantitative analysis. *Immunity*, 1(6), pp.479–489.

Vitiello, A., Heath, W.R. & Sherman, L.A., 1989. Consequences of self-presentation of peptide antigen by cytolytic T lymphocytes. *Journal of Immunology (Baltimore, Md.: 1950)*, 143(5), pp.1512–1517.

Voo, K.S. et al., 2004. Evidence for the presentation of major histocompatibility complex class I-restricted Epstein-Barr virus nuclear antigen 1 peptides to CD8+ T lymphocytes. *The Journal of Experimental Medicine*, 199(4), pp.459–470.

Wallny, H.-J. & Rammensee, H.-G., 1990. Identification of classical minor histocompatibility antigen as cell-derived peptide. *Nature*, 343(6255), pp.275–278.

Wang, R.F. et al., 1996. Utilization of an alternative open reading frame of a normal gene in generating a novel human cancer antigen. *The Journal of Experimental Medicine*, 183(3), pp.1131–1140.

Willcox, B.E. et al., 1999. TCR binding to peptide-MHC stabilizes a flexible recognition interface. *Immunity*, 10(3), pp.357–365.

Yewdell, J W, Antón, L.C. & Bennink, J.R., 1996. Defective ribosomal products (DRiPs): a major source of antigenic peptides for MHC class I molecules? *Journal of Immunology (Baltimore, Md.: 1950)*, 157(5), pp.1823–1826.

Yewdell, J. W. & Hickman, H.D., 2007. New lane in the information highway: alternative reading frame peptides elicit T cells with potent antiretrovirus activity. *The Journal of Experimental Medicine*, 204(11), pp.2501–2504.

Yewdell, J. W. & Nicchitta, C.V., 2006. The DRiP hypothesis decennial: support, controversy, refinement and extension. *Trends in Immunology*, 27(8), pp.368–373.

York, I.A. et al., 2002. The ER aminopeptidase ERAP1 enhances or limits antigen presentation by trimming epitopes to 8-9 residues. *Nat Immunol*, 3(12), pp.1177–1184.

Zhang, W. et al., 2011. A role for UDP-glucose glycoprotein glucosyltransferase in expression and quality control of MHC class I molecules. *Proceedings of the National Academy of Sciences of the United States of America*, 108(12), pp.4956–4961.

Ziegler, K. & Unanue, E.R., 1981. Identification of a macrophage antigen-processing event required for I-region-restricted antigen presentation to T lymphocytes. *Journal of Immunology (Baltimore, Md.: 1950)*, 127(5), pp.1869–1875.

Zinkernagel, R.M. & Doherty, P.C., 1975. H-2 compatability requirement for T-cell-mediated lysis of target cells infected with lymphocytic choriomeningitis virus. Different cytotoxic T-cell specificities are associated with structures coded for in H-2K or H-2D; *The Journal of Experimental Medicine*, 141(6), pp.1427–1436.